ISSN 1173-5996

Mixing in Fire Induced Doorway Flows

J M Clements

Supervised by

Dr Charley Fleischmann

Fire Engineering Research Report 96/2
December 1996

This report was presented as a project report
as part of the M.E.(Fire) degree at the University of Canterbury

School of Engineering
University of Canterbury
Private Bag 4800
Christchurch, New Zealand

Phone 643 366-7001
Fax 643 364-2758

ABSTRACT

This report is a review of the mixing that occurs in fire induced gas flows through a doorway. The purpose of the report to provide a basis from which launch future experimental investigations.

A detailed review is presented of the past research concerned with mixing in doorway flows. A number of fluid dynamic aspects associated with doorway flows are examined. The current zone model approximations, used to account for the mass transfer associated with vent flow mixing, are discussed. Theory for salt water modelling of fire induced gas flows through a compartment doorway is presented, and a relationship for the correct modelling of the volumetric flux is derived.

This document concludes by detailing a number of specific aspects associated with doorway flows that require further research. An outline for future experimental work to be undertaken by the author is also presented.

Acknowledgments

Financial support for the Master of Fire Engineering course has been provided by the New Zealand Fire Service Commission to whom I am extremely grateful. Without their support and contact this course would not be as valuable nor as practical as it has been.

To my supervisor and good friend Dr. Charlie Fleischmann, thanks for the huge effort. Your enthusiasm and dedication has been inspirational.

To Assoc. Prof. Andrew Buchanan, thanks for your perseverance and effort in creating the Masters in Fire Engineering course. The demand for the course graduates is a credit to your insight and to the practical nature of the program.

I would like to express my gratitude to Prof. David Wilkinson for his enthusiasm and for his open door policy. Thanks David for making the time to discuss this project with me and for your insight into some of the problems I encountered.

Thanks to my fellow classmates, Mike Radford, Tony Parkes, Tom Kardos and Michael Belsham for the support and the laughs.

A special thanks to my family for their endless support, encouragement and love.

Last but definitely not least, thanks to my partner Ruth Cowell for her love, understanding and patience.

Table of Contents

Title		i
Abstract		iii
Acknowledgments		v
Table of Contents		vi
List of Figures		ix
List of Tables		
Nomenclature		
Chapter One	INTRODUCTION	1
1.1	Impetus for Research	1
1.2	Research Purpose	2
1.3	Outline of Research	2
Chapter Two	PREVIOUS RESEARCH	5
2.1	Introduction	5
2.2	Quintiere, J.G. and DenBraven, K., (1978)	6
	2.2.1 Experimental Setup	6
	2.2.2 Experimental Method	7
	2.2.3 Data Analysis	8
	2.2.4 Results	12
2.3	Lim, C.S., (1984)	15
	2.3.1 Experimental Setup	15
	2.3.2 Data Analysis	16
	2.3.3 Results	20
	2.3.4 Entrainment Model	24
2.4	Zukoski and Kubota, (1980)	26
2.5	Summary	30

Chapter Three FLUID DYNAMIC ASPECTS 31

3.1 Introduction 31

3.2 Flow Development in the Fire Situation 31

3.3 The Concept of Entrainment 32

3.4 The Richardson Number 33

3.5 Stratified Shear Flow 34

3.6 Kelvin-Helmholtz Shear Instability 35

3.7 The Drop Structure Analogy 37

3.8 Forced Plumes 38

3.9 The Effect of Boundaries on Entrainment 42

3.10 The Surface Spreading Plume 43

3.11 The Density Jump 44

3.12 The Prandtl and Schmidt Numbers 46

Chapter Four ZONE MODELLING 49

4.1 Zone Models 49

4.2 Vent Flow 50

4.3 Entrainment into the Hot Upper Door Jet 54

4.4 Entrainment into the Lower Door Jet 58

4.5 Vent Flow Mixing in Zone Models 65

4.5.1 The HARVARD Zone Model 65

4.5.2 The CCFM Zone Model 66

4.5.3 The CFAST Zone Model 68

4.5.4 The BRI Zone Model 72

4.6 Conclusion 73

Chapter Five SALT WATER MODELLING 75

5.1 Salt Water Modelling Analogy 75

5.2 Governing Theory 76

5.3 Limitations of Salt Water Modelling 81

5.3.1 Boussinesq Approximation 81

5.3.2 Heat Transfer Deficiency 82

	5.3.3 Initial Plume Momentum	82
	5.3.4 Exact Reynolds Number Matching	83
	5.3.5 Salt Water Source Geometry	83
	5.3.6 Plume Mass Flux	83
5.4	Correct Modelling of the Volumetric Flux	84
5.5	Conclusion	87
Chapter Six	CONCLUSIONS & FUTURE RESEARCH	89
6.1	Conclusion	89
6.2	Areas Requiring Research	89
6.3	Useful Techniques for Researching Mixing in Doorway Flows	92
	6.3.1 Species Concentration Profiles	92
	6.3.2 Salt Water Modelling	92
6.4	Outline for Further Research	93
	6.4.1 The Salt Water Model	94
	6.4.2 Experimental Technique	96
	6.4.3 Research Methodology	99
List of References		103
Bibliography		111
Appendix 1		113
Appendix 2		119
Appendix 3		123

List of Figures & Tables

Figure 2.1	Oblique sketch of the 1/7th Scale Model used by Quintiere and DenBraven
Figure 2.2	Location of the thermocouples and pitot static tubes in the 1/7th scale model
Figure 2.3	Determination of the homogeneous zone properties for use in the calculation of the theoretical velocities
Figure 2.4	Results plot of mass flow through the model doorways as a function of the corridor exit doorway width
Figure 2.5	Schematic of the four zones used in the mass transfer calculations and the associated notation
Figure 2.6	Diagram of the half scale model used by Lim, (1984), to simulate the fire conditions in a single compartment
Figure 2.7	Experimental Results of Lim, (1984)
Figure 2.8	Schematic of the mixing layers observed by Lim in the model
Figure 2.9	Schematic of two doorway flow situations in which strong entrainment has been observed
Figure 2.10	Schematic showing the two possible flow configurations for the upper door jet after the hydraulic jump structure has been drowned out
Figure 3.1	Development of the mixing layer between the hot upper layer and the cool lower layer within a compartment
Figure 3.2	A schematic for the development of the Kelvin-Helmholtz instability
Figure 3.3	Typical flow situation at the base of a free overfall in an open channel drop structure
Figure 3.4	Schematic for the zone of flow establishment in a horizontal jet
Figure 3.5	Dilution as a function of the distance along the axis of a round turbulent jet
Figure 3.6	Schematic for the wall attachment of a two dimensional jet
Figure 3.7	Schematic for an effluent plume from an ocean outfall
Figure 3.8	Schematic showing the roller region and the entrainment region of a density jump

Figure 4.1 Schematic representation of the concept of using two homogeneous zones to represent the compartment atmosphere

Figure 4.2 Schematic showing the compartment conditions and assumed pressure distributions for the calculation of vent flows in zone modelling

Figure 4.3 Different flow phases for the upper door jet will cause different entrainment characteristics

Figure 4.4 Schematic of a door plume spilling into an atrium or sports stadium

Figure 4.5 Schematic of the inverse plume analogy used for the lower door jet

Figure 4.6 Schematic defining the mass flow notation and the compartment zones

Figure 4.7 Flow apportioned according to relative densities

Figure 4.8 Schematic diagram showing the virtual source concept for the upper door jet

Figure 5.1 Schematic of the variables used in salt water modelling calculations

Figure 5.2 Schematic showing the mass flux notation for a simple compartment fire situation

Figure 5.3 Schematic showing the mass flux notation for the salt water modelling situation

Figure 6.1 Diagram of the salt water model to be used in future research of the mixing that occurs in fire induced doorway flows

Figure 6.2 Schematic of the pump system to be used in the salt water modelling

Figure 6.3 Fictitious plot of the fractional interface height versus the ratio of flow rates through the compartment doorway

Table 6.1 Full scale and salt water model dimensions for room size, *Height* × *Width* × *Length*

Table 6.2 The range of soffit depths for the corridor exit doorway

Nomenclature

English Symbols

A - Empirical Constant for Entrainment Model, Equation (2.25)

A - Area

A_1 - Empirical Constant, Equation (2.25)

A_2 - Empirical Constant, Equation (2.25)

b_2 - Empirical Constant, Equation (3.11)

b_3 - Empirical Constant, Equation (3.10)

B_o - Specific Buoyancy Flux

C - Mole Fraction of Carbon Dioxide

C_{in} - Inflow Coefficient for Lower Layer = 0.68

C_J - Empirical Constant for Door Jet Entrainment Equation

C_l - Constant in Buoyant Axisymmetric Plume Representation

C_{out} - Outflow Coefficient for Upper Layer = 0.73

C_p - Specific Heat of Gas

C_v - Constant in Buoyant Axisymmetric Plume Representation

d_p - Diameter of Plume Source

D - Fractional Density Interface Height D = Z_D/H_d

E_o - Empirical Constant, Equation (2.26)

F - Scaled Froude Number, defined by Equation (2.27), or, Ratio of Initial Momentum Flux to Buoyancy Flux, Equation (5.16)

Fr - Froude Number

g - Gravitational Acceleration

g' - Effective Gravity = $\frac{g\Delta\rho}{\rho}$

G - Ratio of Length Scales Cubed, Equation (5.15)

h - Height of Salt Water Model Compartment

H - Height of Compartment

H_d - Height of Doorway

k - Thermal Diffusivity

k_c - Concentration Diffusivity

l - Characteristic Length of Salt water Source

l_m - Characteristic Length Scale for Forced Plumes

l_Q - Characteristic Length Scale for Forced Plumes

L - Characteristic Length for Overall Richardson Number, Equation (4.11), or Characteristic Length of heat Source

k_m - Entrainment Constant

m - Specific Momentum Flux

$\dot{m}$ - Mass Flux

M_o - Specific Momentum Flux at the Forced Plume Source

n - Empirical Constant, Equation (2.26)

N - Fractional Neutral Layer Height $N = Z_N/H_d$

$\tilde{p}$ - Pressure Perturbation about Hydrostatic

Pr - Prandtl Number

ΔP - Pressure Difference

q_H^* - Dimensionless Buoyancy Flux Parameter

$\dot{Q}$ - Heat Release Rate

Q_d^* - Dimensionless Heat Input Parameter for Doorway

Q_Z^* - Dimensionless Heat Input Parameter for Axisymmetric Plume

$\dot{Q}_{eq}$ - Equivalent Heat Release Rate ≡ Convective Heat Loss

Re - Reynolds Number

Ri - Gradient Richardson Number

Ri_o - Overall Richardson Number

$(Ri_x)_{cr}$ - Critical Gradient Richardson Number

R_o - Jet Richardson Number, defined by Equation (3.8)

R_p - Plume Richardson Number, defined by Equation (3.9)

Sc - Schmidt Number

t - Time

T - Temperature

ΔT - Temperature Difference

$\overline{u}$ - Mean Velocity

U - Velocity

U_o - Velocity at the Source

ΔU - Velocity Difference across the Layer

V - Volume Flux

V_o - Volumetric Flow Rate at the Source

$\dot{V}_o$ - Volumetric Flow Rate at the Source

W - Width

$\overline{x}$ - Position Vector in Salt Fire Situation

Y - Mass Fraction of Carbon Dioxide or Salt

z - Elevation

Z_d - Door Plume Entrainment Length

Z_D - Elevation of the Density Interface in Burn Room

Z_{D3} - Elevation of the Density Interface in Adjacent Room

z_f - Elevation above the Fuel Surface

Z_N - Elevation of the Neutral Plane

Z_P - Length of Entrainment for Plume Above the Visible Flame Region

Z_{Sill} - Elevation of the Vent Sill

Z_{Soffit} - Elevation of the Vent Soffit

Z_{TP} - Total Length of Entrainment for the Plume

Z_{vs} - Virtual Source Length for Plume

Greek Symbols

α - Expansion Factor

μ - Specific Volume Flux or Dynamic Viscosity

$\overline{\mu}$ - Dimensionless Dilution

ν - Kinematic Viscosity

ρ - Density

$\Delta\rho$ - Density Difference

δ - Thickness of the Mixing Layer

ζ - Elevation Parameter or Perturbation Scale

Subscripts

c - Compartment

d - Doorway

e - Entrained into

E - Corridor Exit Doorway

fresh - Fresh Water Entering the Compartment through the Doorway

fire - Given off by the Combustion Reaction

fuel - Methane to Furnace

F - Leaving the Furnace

g - Fire Situation

in - Entering the Compartment

LL - Lower Layer

o - Ambient or Source

out - Exiting the Compartment

p - Plume

s - Salt Water Situation

saline - Saline Solution Leaving the Compartment through the Doorway

salt - Salt Water Injected into the Compartment

UL - Upper Layer

∞ - Ambient

Superscripts

* - Non-Dimensional

Zone Definition

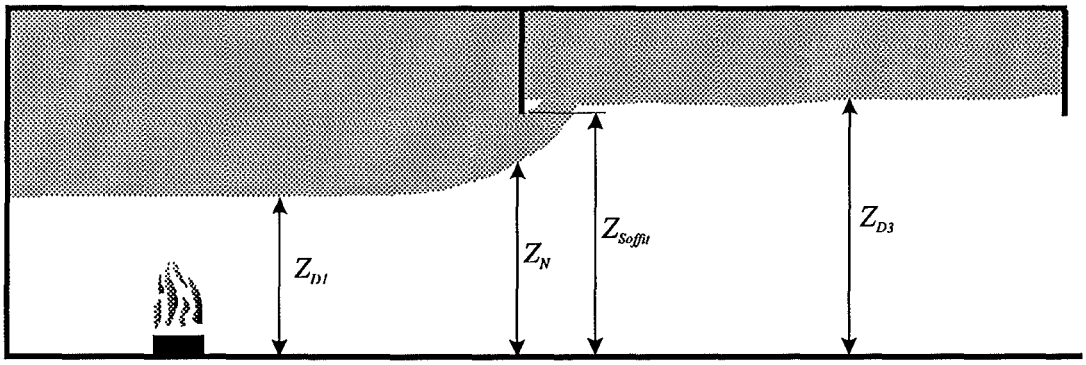

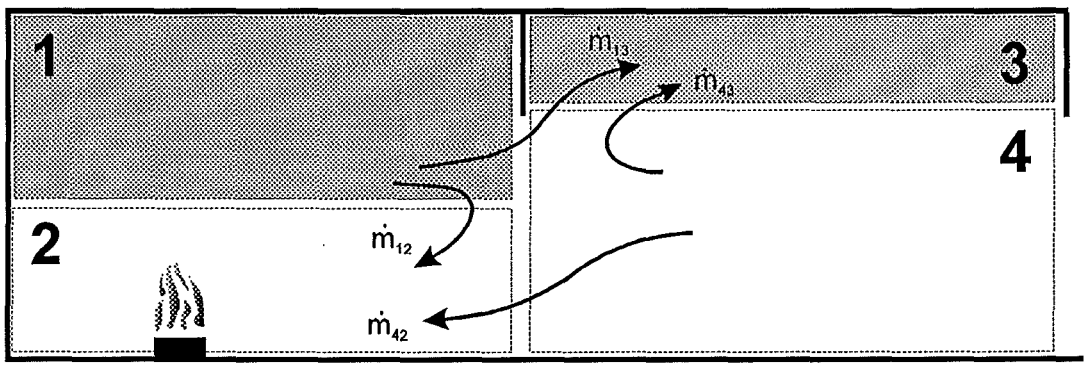

Chapter 1
INTRODUCTION

1.1 Impetus for Research

It is widely accepted that smoke inhalation is the major cause of fatalities in building fires, (Berl and Halpin, 1980). When a fire engineer is required to make a life safety assessment of a fire scenario, his or her main concern is therefore the movement and characteristics of the smoke layer within the building. To assist engineers with the analysis of the smoke migration, computer fire models are often employed. One particular type of computer fire model that is commonly used by engineers is the zone model. The zone model uses our existing knowledge of certain fire phenomena to discretely simulate the processes involved in compartment fires. The models consider the interaction of the processes and predict the compartment atmosphere as a function of time.

Consider the development of a fire within a small room of a multicompartment building. The combustion reaction heats the surrounding air which rises toward the ceiling. The hot buoyant gases, rise in a plume and form a mixture of products from the combustion reaction and the air that is entrained from the compartment atmosphere. Once the gases in the buoyant plume impinge upon the ceiling, they spread out radially in a thin layer. When the gases in the ceiling layer reach the bounding walls of the compartment, the hot upper layer starts to deepen. The rate of decent of the upper layer and the temperature of the gases in it, is governed by the entrainment that occurs in the fire plume. The cool air that is entrained into the plume, lowers the average temperature and reduces the concentration of the combustion products.

When the ceiling layer is deep enough, the hot gases start to spill out under the soffit of the doorway. In the lower portion of the doorway, cooler air is drawn into the compartment to feed the combustion reaction and the demand of the plume. At a

certain elevation in the doorway, the out-flowing hot gases shear over the in-flowing cooler gases. Mixing occurs between the gases along this shear interface. Hot combustion products are entrained into the cooler gas layer that enters the room, while cooler gases are entrained into the hot upper door jet that exits the room. The amount of mixing that occurs in the doorway affects the characteristics of the smoke layer in the adjacent room, and the characteristics of the lower layer in the burn room.

Presently very little is known about the mixing that occurs in doorway flows. As a consequence, multicompartment zone models are required to estimate the mass exchange between the gas streams with crude estimates. Since entrainment is the governing process in determining the characteristics of the smoke layer, inaccuracies in the estimate increase the uncertainty associated with the models predictions of the smoke layer movement and properties. To further complicate the problem, the inaccuracies of the estimate are compounded each time the smoke moves on through another doorway into a new compartment. A number of zone model packages have cited the need for research in this area, however, this need has not yet been adequately addressed.

1.2 Research Purpose

The purpose of this research report is to provide a basis from which further research can be launched into the mixing that occurs in doorway flows. The author hopes that by clearly outlining the phenomena, the report will stimulate thought and consideration of some of the aspects involved in the problem, identify areas where further research is required, and provide a reference source for future research work.

11.3 Outline of Research

Since the purpose of this research report is to provide a basis from which to launch future research, the report has attempted to cover a broad spectrum of topics associated with mixing in doorway flows.

Chapter 2 is a topical review of the previous research that has investigated the mixing associated with doorway flows. The purpose of this chapter is to introduce the reader to the problem and bring the reader quickly up to the present state of understanding.

Chapter 3 provides an introduction to some of the fluid dynamic aspects that are present in doorway flows. A great deal of specialised research has been carried out under the fluid dynamics title; much of this research is applicable to fire induced flow problems.

Chapter 4 is a review of the present way that mixing in doorway flows is treated in zone models. The purpose of this chapter is to review the approximations that zone models make in light of the previous research that has been carried out, and to familiarise the reader with the possible future application of their research work results.

Chapter 5 is an introduction to salt water modelling of fire induced gas flows. The governing equations are presented, and the limitations and necessary considerations of the modelling technique are discussed.

Chapter 6 suggests direction for future research work and illuminates some experimental techniques and methods that may be useful in studying the topic. In addition, this chapter outlines a plan for future experimental research that will be undertaken using salt water modelling.

Chapter 2
PREVIOUS RESEARCH

2.1 Introduction

The development of fire behaviour zone models over the past 30 years has meant a move from single compartment models to more advanced multi-compartment models. This has introduced new incentives for research in the areas associated with the movement of combustion products within buildings. Although the basic theory has been developed to quantify the mass flux through the vents between compartments, (see Rocket, 1976), there is still a large amount of refinement work to be done in the mass transport area. The mixing that occurs in vent flows is one area that has been identified as requiring further research. A number of research projects have observed the phenomenon while researching associated topics, however, very few researchers have set out to specifically investigate the problem.

This chapter is a topical review of the work that has been done on the mixing that occurs in fire induced doorway flows. The aim of this chapter is to quickly bring the reader up to speed with the state of the understanding of vent flow mixing. Since very little work has been done in this area, and because the work that has been done by each researcher has concentrated on a different aspect of the problem, a detailed review of each researchers methods, results and conclusions is presented rather than a historical development of the subject.

Three pieces of research work have been reviewed in this section.

- Quintiere and DenBraven, (1976), on some of the observed aspects of doorway flow in a multi-compartment model;
- Lim, (1984), on the entrainment of hot gases into the cooler lower layer in doorway flow; and

- Zukoski and Kubota, (1980), on two-layer modelling of smoke movement in buildings.

The work of each researcher has been presented separately.

2.2 Quintiere, J.G. and DenBraven, K., (1978)

Some Theoretical Aspects of Fire Induced Flows through Doorways in a Room-Corridor Scale Model

James Quintiere and Karen DenBraven studied the fire induced gas flow in a $1/7^{th}$ scale model of a room and adjoining corridor. They investigated the effect that varying the width of the corridor exit doorway had on the mass flow and the value of the flow coefficient for each gas stream. They also compared the measured mass flow through a doorway with the mass flow predicted by the two zone orifice flow theory used in zone models. Quintiere and DenBraven's results revealed some interesting mass flow behaviour for flow through doorways in multi-compartment buildings.

2.2.1 Experimental Setup

Quintiere and DenBraven used a $1/7^{th}$ scale model of a room and adjoining corridor. The scale model had been used previously to study the flow patterns in a corridor adjoining a burn room; (see McCaffrey and Quintiere (1975), McCaffrey and Quintiere (1976), and Quintiere *et. al.* (1978)). Data from this previous research was used by Quintiere and DenBraven in their analysis. An oblique sketch of the $1/7^{th}$ scale model and the principle dimensions of the model is presented in Figure 2.1.

A porous plate, diffusion flame gas burner was used to simulate a fire. The burner was placed in the centre of the burn room against the back wall. Velocities in each doorway were measured along a vertical traverse using small pitot-static tubes. Temperatures were recorded in the doorways and rooms using 5mm chromel-alumel

wire thermocouples. Figure 2.2 shows the positioning of the burner and the data collection equipment within the model.

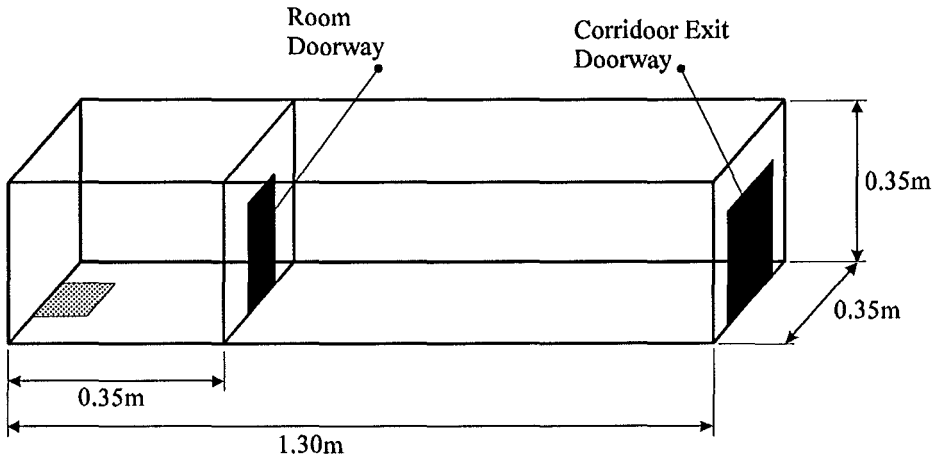

Figure 2.1 ***Oblique sketch of the 1/7th Scale Model used by Quintiere and DenBraven***

A point to note about the velocity profiles, is that there was only one pitot-static tube in each doorway. Velocity measurements taken at different positions in the doorway were therefore not taken simultaneously. Another point to note, is the position of the thermocouples in the rooms, the temperature profiles may have been influenced by recirculating flows in the corners.

2.2.2 Experimental Method

In each experiment, the diffusion gas burner was lit and the model was preheated until the ceiling layer in the room reached a stable temperature of 330 ± 30°C. Once this had been achieved, experimental measurements were taken.

Data for the lower inflowing gas stream was recorded at 0.013m vertical intervals on the center-line of the doorway below the neutral plane. Data for the outflowing gas stream was recorded on a grid like structure across the entire width of the doorway above the neutral plane. The grid spacing was 0.025m in the vertical and horizontal

directions. Quintiere and DenBraven gave no reason for recording the data in different positions for the upper and lower gas streams.

The width of the corridor exit doorway was varied between 0.034m and 0.35m during the experiments. The doorway between the burn room and the corridor was kept at a constant width of 0.113m. The height of both doorways were constant at 0.293m.

2.2.3 Data Analysis

Quintiere and DenBraven examined the mass flow and the value of the flow coefficient for the upper and lower gas streams in each doorway. The flow coefficient was calculated as the ratio of the measured to theoretical mass flow. The theoretical mass flow rate was calculated based upon Bernoulli's equation. The measured mass flow was taken as the product of the measured velocity profile and the actual gas density, (as given by the measured temperature profile and the ideal gas law).

By combining the ideal gas law with Bernoulli's equation, and assuming that the pressure varies hydrostatically within the rooms, the theoretical velocity of the gases was calculated based upon Rockett's two zone vent flow theory , (see Rockett, 1976).

$$U(z)_{THEORY-In} = \sqrt{2gT_d(z)\int_{z}^{Z_N}\left(\frac{1}{T_d(z)}-\frac{1}{T_c(z)}\right)dz} \qquad (2.1)$$

$$U(z)_{THEORY-Out} = \sqrt{2gT_c(z)\int_{Z_N}^{Z_S}\left(\frac{1}{T_d(z)}-\frac{1}{T_c(z)}\right)dz} \qquad (2.2)$$

where

z is the height above the compartment floor

Z_N is the height of the neutral plane

T_d is the temperature in the doorway, and

T_c is the temperature in the compartment atmosphere.

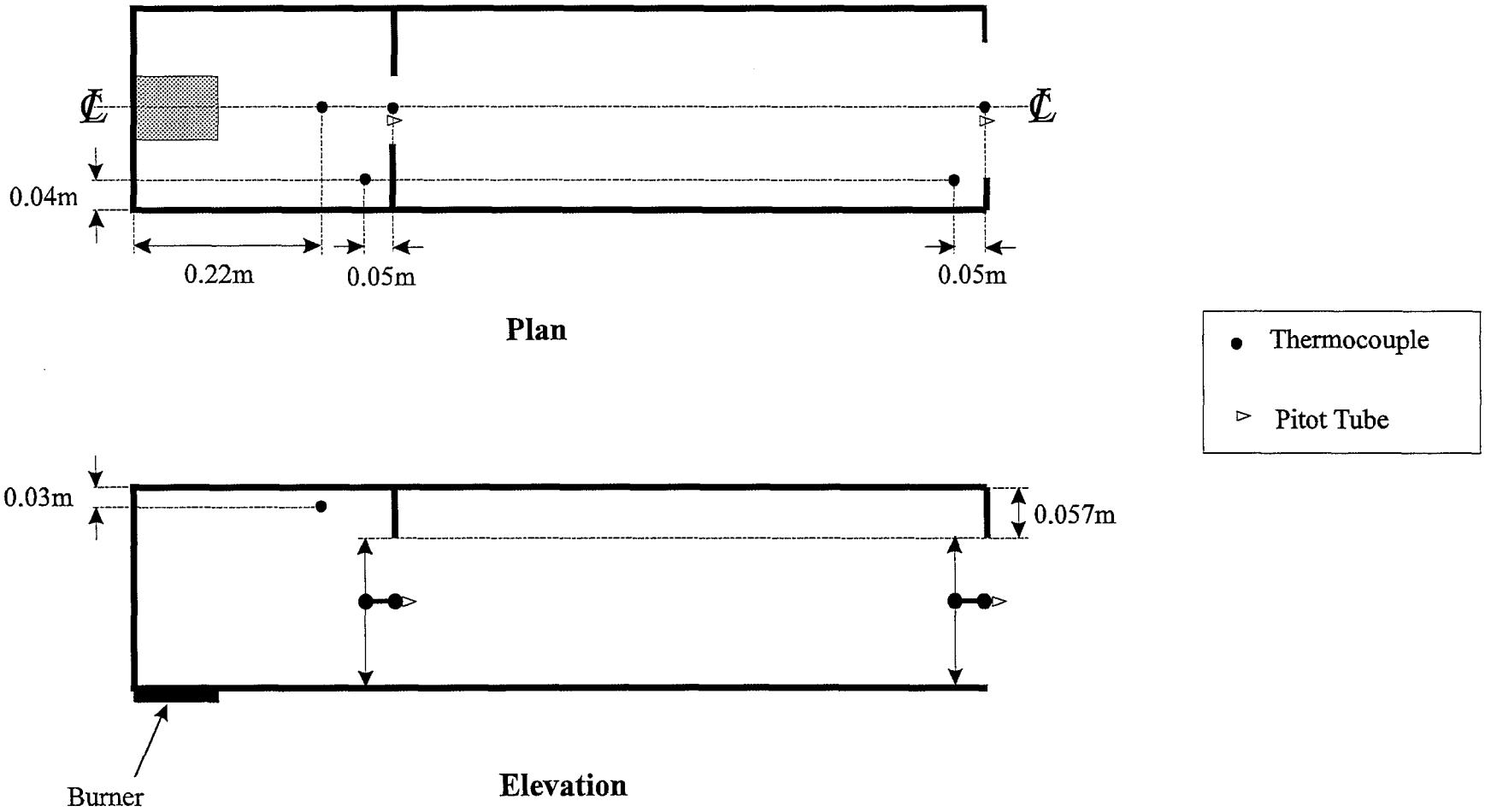

Figure 2.2 Location of the thermocouples and pitot static tubes in the 1/7th scale model.

The numerical integration of the temperature profiles required by Equations (2.1) and (2.2) was carried out using Simpson's 1/3 rule.

The theoretical mass flow was calculated as

$$\dot{m}_{THEORY} = W_d \int \rho(z)_{EXP} U(z)_{THEORY} \, dz \, . \tag{2.3}$$

The experimental mass flow was calculated as

$$\dot{m}_{EXP} = W_d \int \rho(z)_{EXP} U(z)_{EXP} \, dz \, . \tag{2.4}$$

The flow coefficient, C, was calculated as the ratio of the experimental mass flow to the theoretical mass flow.

$$C = \frac{\dot{m}_{EXP}}{\dot{m}_{THEORY}} \tag{2.5}$$

In addition to the calculation of the flow coefficient values, Quintiere and DenBraven also made a comparison between the mass flow measured in the experiments and the mass flow predicted by zone model theory. The comparison only considered the mass flow in the lower layer through the corridor exit doorway. No reason was given for why only this gas stream was considered in the comparison. It may, however, have been due to the fact that the lower layer of the corridor exit doorway receives ambient uncontaminated air, whereas the lower layer entering the burn room doorway has been contaminated by mixing that occurred upstream in the corridor.

A basic description of the technique used to calculate the mass flux through a vent in zone models is provided latter in Section 4.2; it will not be covered here. A description of the method used by Quintiere and DenBraven to determine the homogeneous properties of the lower layer zone from the experimental data is presented.

For the zone model predictions, the temperature of the lower layer, T_c, was approximated from the experimental data as the maximum temperature of the gas below the neutral plane. The height of the effective interface between the layers, Z_D, was calculated using what has been referred to as the tangent-intercept method, (see Figure 2.3). The height of the neutral plane, Z_N, was determined by the position of zero velocity. Figure 2.3 graphically illustrates the determination of these parameters.

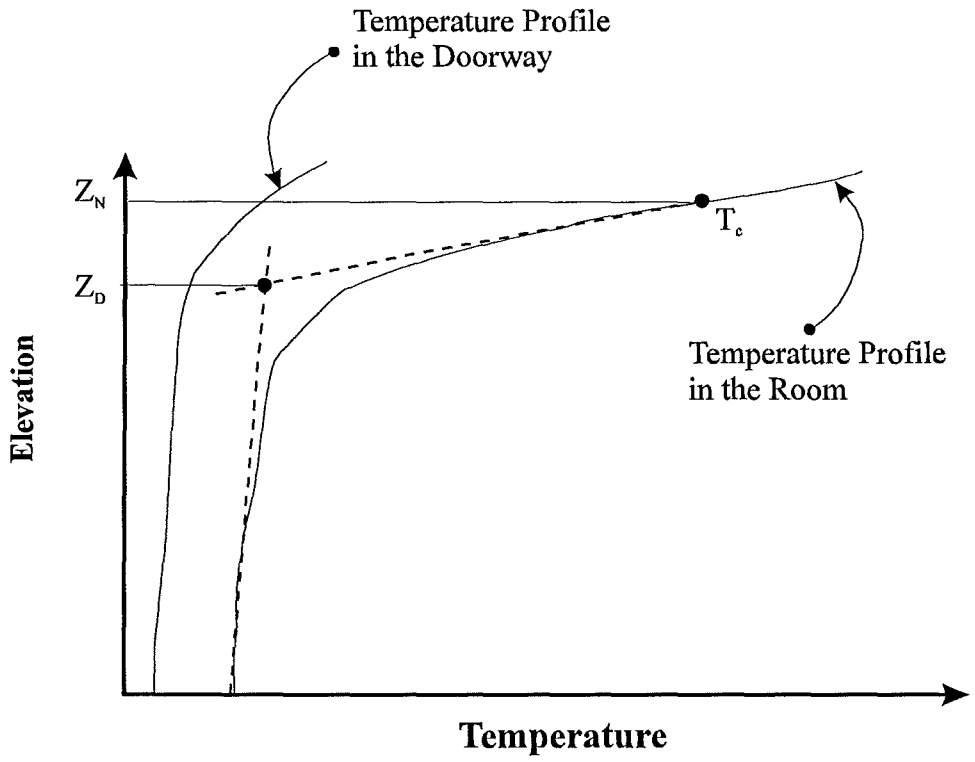

Figure 2.3 ***Determination of the homogeneous zone properties for use in the calculation of the theoretical velocities.***

From zone model theory, the mass flux into the compartment in the lower layer can be calculated from the following expression,

$$\dot{m}_{in} = \frac{2}{3} C_{in} W_d \rho_o \sqrt{2g\left(1-\frac{T_d}{T_c}\right)} \left(Z_N - Z_D\right)^{\frac{1}{2}} \left(Z_N + \frac{Z_D}{2}\right) \qquad (2.6)$$

Quintiere and DenBraven compared the mass flux predicted by this zone model equation to the mass flux measured in the experiments.

2.2.4 Results

Quintiere and DenBraven presented the mass flux through both doorways as a function of the ratio of corridor exit doorway width to the burn room doorway width, (W_E/W_d). This plot has been reconstructed in Figure 2.4 from Quintiere and DenBraven's report.

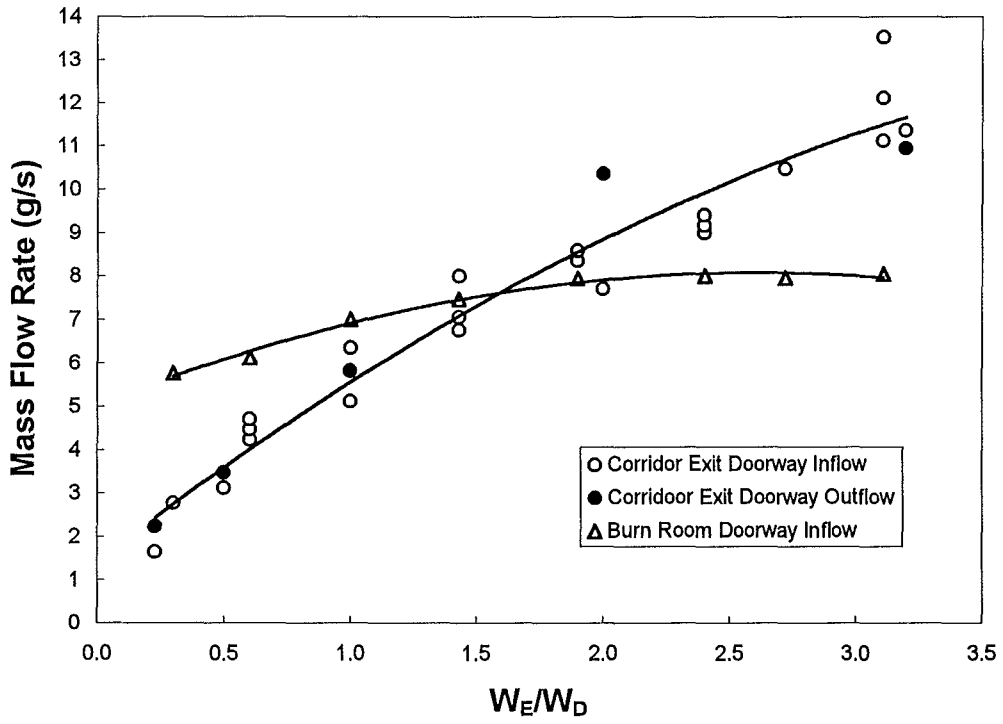

Figure 2.4 ***Results plot of mass flow through the model doorways as a function of the corridor exit doorway width.***

Figure 2.4 shows that as the width of the corridor exit doorway increases, the mass flux through the corridor exit doorway increases almost directly. The mass flux through the room doorway increases also, however it is not influenced as directly as the corridor exit doorway has been. The difference between the two lines represents

the net entrainment or recirculation that is occurring in the corridor between the two doorways.

For $W_E/W_d < 1.6$ the mass flux entering the burn room is far greater than the mass flux entering the corridor. This implies that there is a net entrainment of upper layer mass into the lower layer occurring in the corridor.

For $W_E/W_d > 1.6$ the mass flux entering the corridor exit doorway is greater than the mass flux entering the burn room. This implies that there is a net entrainment of lower layer mass into the hot upper layer occurring in the corridor.

It is difficult to draw any further conclusions from Figure 2.4 as we are unable to precisely say whereabouts in the corridor the entrainment is occurring, and how it is distributed.

Quintiere and DenBraven showed the calculated value of the flow coefficient for the inflowing and outflowing gas streams as a function of the Reynolds number and as a function of the doorway width ratio (W_E/ W_d). Their results showed that the flow coefficient values for each gas stream varied with doorway width and that the value of the coefficient for the outflow was consistently higher than it was for the inflow. This is in agreement with the findings of Steckler *et. al.* (1984) who estimated that the value of the inflow coefficient was 0.68, and the value of the outflow coefficient was 0.71.

Quintiere and DenBraven presented the temperature and velocity profiles from inside each room and doorway for four experiments in which the corridor exit doorway width was varied. The profiles extend from the floor to the height of the neutral plane, and are therefore only directly relevant to the inflowing cool air. Quintiere and DenBraven's plots showed that as the width of the corridor exit doorway was reduced, the velocity of the gases in the lower layer of the corridor exit doorway increased. The shape of the temperature profile in the corridor exit doorway did not change significantly; however, the shape of the temperature profile in the corridor

became more curved rather than being divided into two relatively straight sections. This implies that as the width of the corridor exit doorway was reduced, the mixing that occurs along the shear interface, downstream of the doorway, increased. This is reinforced by the fact that the temperature of the gases in the lower layer of the corridor increased as the doorway width was reduced.

With respect to the burn room, the reduction in the width of the corridor exit doorway did not significantly change the velocity of the gases in the burn room doorway, (although they did increase slightly). The shape of the temperature profile in the burn room doorway became more curved and the temperature of the gases increased. This is likely to be accountable to the increased mixing that is occurring upstream in the corridor. An interesting point to note, is that although the shape of the temperature profile in the burn room doorway changed, the shape of the temperature profile inside the burn room itself did not change significantly. The temperature profile within the burn room maintained its shape while the gases in the room increased in temperature.

Quintiere and DenBraven's comparison of the mass flux from the zone model theory and the mass flux from the experiments revealed that in general there was a good agreement between the two. The zone model theory did tend to underestimate the experimental flow rate; at times by as much as 30%. What must be noted here, is that the mass flux from the zone model theory depends upon the definition of the layer properties. The method for determining the temperature of the layers and the height of the effective interface from experimental data effects the mass flux predictions generated by the model theory. A different method to the tangent-intercept method could have resulted in a better, (or worse), comparison with the experimental results.

2.3 Lim, C.S., (1984)

Mixing in Doorway Flows and Entrainment in Fire Plumes

In a two part report, Christopher Lim studied the mixing that occurs in fire induced doorway flows and the entrainment that occurs in the fire plume. This review only considers the first part of his report; that is, the section concerned with the mixing that occurs in doorway flows. Although the title of his section is "mixing in doorway flows", Lim only considers the amount of hot gas entrained into the cool lower layer of fresh air that enters the compartment through a doorway. No consideration is given to the entrainment of cool gas into the hot upper door jet.

In addition to presenting the results of his experimental work, Lim developed a model for estimating the entrainment of hot gases into the lower layer. Lim's model is presented in this section, however, the derivation of the model is in Appendix 1.

2.3.1 Experimental Setup

Lim investigated the mixing phenomenon in a 1/2 scale model of a rectangular room with a single doorway opening. No actual fire was used in the model, rather, a pump and methane fuelled furnace were used to simulate the entrainment and heating that would occur in a fire plume. Figure 2.6 shows the layout of the 1/2 scale model.

A moveable arm equipped with probes was used to collect a series of gas samples and temperatures from the compartment atmosphere. The arm was able to swing 180° in the horizontal plane and could be shifted vertically to sample at different elevations. The gas samples were analysed using a Beckman Model 864 Non-Dispersive Infrared Analyser. The gas analysis provided vertical profiles of the carbon dioxide concentrations. Iron-Constantan thermocouples were used to construct vertical temperature profiles of the atmosphere. No velocity measurements were made. Figure 2.6 shows the approximate locations of the data collecting probes.

A comparison of both the temperature and carbon dioxide concentration profiles from different locations in the room revealed that a single temperature and carbon dioxide concentration profile could adequately predict the general atmosphere in the compartment. All data analysis was therefore carried out using profiles taken from the centre of the compartment.

2.3.2 Data Analysis

To analysis the mass transfer associated with mixing, Lim assumed that the atmosphere could be separated into four distinct gaseous zones, each with uniform thermodynamic properties. The four zones that Lim considered were the hot layer, the cold layer, the furnace, and the ambient or outside air. By applying a series of mass balance relations to each zone, the mass transfer between zones could be quantified.

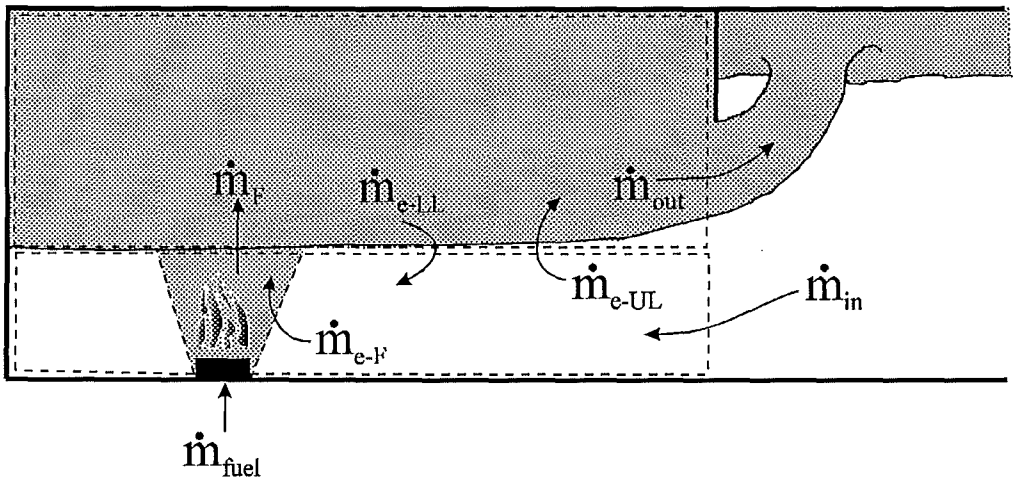

Figure 2.5 ***Schematic of the four zones used in the mass transfer calculations and the associated notation.***

Consider both the total and the carbon dioxide mass flow in each zone at steady state, refer Figure 2.5.

Y_i is the mass fraction of carbon dioxide in the flow stream i.

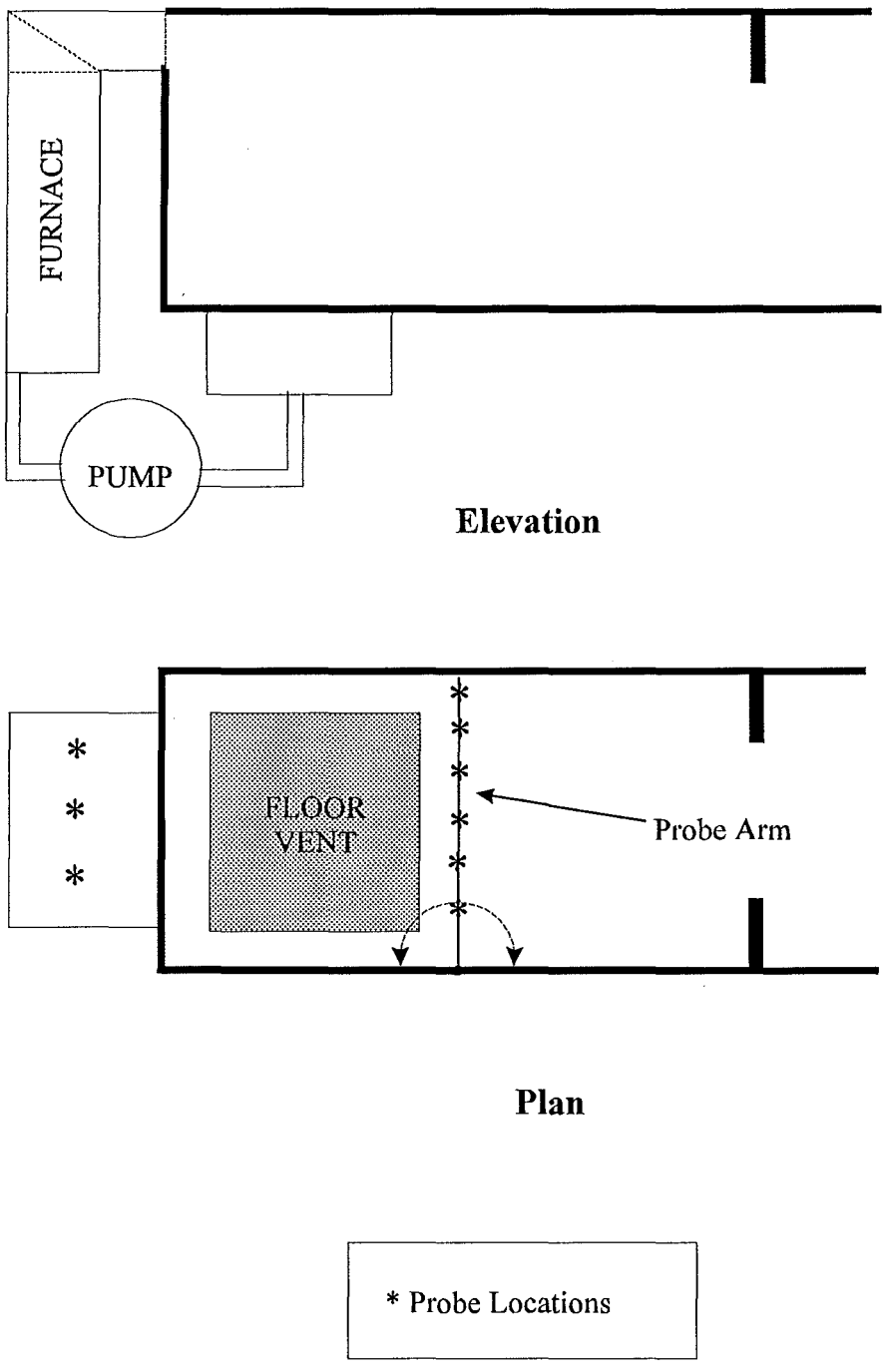

Figure 2.6 ***Diagram of the half scale model used by Lim, (1984), to simulate the fire conditions in a single compartment.***

Cold Layer:

$$\dot{m}_{in} + \dot{m}_{e-LL} - \dot{m}_{e-UL} - \dot{m}_{e-F} = 0 \tag{2.7}$$

$$Y_{\infty}\dot{m}_{in} + Y_{UL}\dot{m}_{e-LL} - Y_{LL}\dot{m}_{e-UL} - Y_{LL}\dot{m}_{e-F} = 0 \tag{2.8}$$

Hot Layer:

$$\dot{m}_{F} + \dot{m}_{e-UL} - \dot{m}_{out} - \dot{m}_{e-LL} = 0 \tag{2.9}$$

$$Y_{F}\dot{m}_{F} + Y_{LL}\dot{m}_{e-UL} - Y_{UL}\dot{m}_{out} - Y_{UL}\dot{m}_{e-LL} = 0 \tag{2.10}$$

Furnace:

$$\dot{m}_{F} = \dot{m}_{e-F} + \dot{m}_{fuel} \tag{2.11}$$

The fuel mass flow rate, $\dot{m}_{fuel}$, was considered to be negligible when compared to the mass flow rate entrained into the furnace, $\dot{m}_{e-F}$; ($\dot{m}_{e-F}$ simulates the mass flow rate in the plume).

$$\dot{m}_{F} \approx \dot{m}_{e-F} \tag{2.12}$$

Manipulation of Equations (2.7)-(2.12) results in the following relationships.

$$\dot{m}_{out} = \frac{(Y_{\infty} - Y_{LL})\dot{m}_{e-F} + (Y_{F} - Y_{\infty})\dot{m}_{F}}{(Y_{UL} - Y_{\infty})} \tag{2.13}$$

$$\dot{m}_{in} = \dot{m}_{e-F} - \dot{m}_{F} + \dot{m}_{out} \tag{2.14}$$

$$\dot{m}_{e-UL} = \frac{\dot{m}_{F}(Y_{F} - Y_{UL})}{(Y_{UL} - Y_{LL})} \tag{2.15}$$

$$\dot{m}_{e-LL} = \dot{m}_{e-F}\left[\frac{(Y_F - Y_{LL})(Y_{LL} - Y_\infty)}{(Y_{UL} - Y_{LL})(Y_{UL} - Y_\infty)}\right] \tag{2.16}$$

Lim measured the following mass flow rates and carbon dioxide concentrations in his experiments: $\dot{m}_{e-p}$, $\dot{m}_{fuel}$, C_F, C_{LL}, C_{UL}, and C_∞.

If it is assumed that the molecular weight of the gas in the room is approximately equal to the molecular weight of the ambient air; the mass fractions of carbon dioxide, Y_i, can be replaced with mole fractions, C_i. This assumption results in the following four relationships that can be solved with the available experimental data to find the mass transfer.

$$\dot{m}_{out} = \frac{(C_\infty - C_{LL})\dot{m}_{e-F} + (C_F - C_\infty)\dot{m}_F}{(C_{UL} - C_\infty)} \tag{2.17}$$

$$\dot{m}_{in} = \dot{m}_{e-F} - \dot{m}_F + \dot{m}_{out} \tag{2.18}$$

$$\dot{m}_{e-UL} = \frac{\dot{m}_F(C_F - C_{UL})}{(C_{UL} - C_{LL})} \tag{2.19}$$

$$\dot{m}_{e-LL} = \dot{m}_{e-F}\left[\frac{(C_F - C_{LL})(C_{LL} - C_\infty)}{(C_{UL} - C_{LL})(C_{UL} - C_\infty)}\right] \tag{2.20}$$

In considering the mass transfer between zones, it was necessary for Lim to define a distinct interface between the hot and cold layer. Lim defined the effective interface height based upon both the temperature and carbon dioxide concentration profiles. The effective interface height, Z_D, is defined as the height where,

$$\frac{T(Z_D) - T_\infty}{T_F - T_\infty} \quad and \quad \frac{C(Z_D) - C_\infty}{C_F - C_\infty} \quad equals \quad \frac{1}{2} \tag{2.21}$$

In cases where the heights given by the temperature and carbon dioxide concentration ratios did not coincide, the average value was used.

2.3.3 Results

Lim's experimental investigation considered the effect of the floor suction rate and the furnace temperature on the mixing that occurred in the doorway.

Effect of Floor Suction Rate

To study the effect of the floor suction rate, the furnace temperature was set at approximately 160°C while the floor suction rate was varied from 0.03 kg/s to 0.20 kg/s. For relatively low floor suction rates, the effective interface was observed to be well above the floor and the carbon dioxide concentrations in the hot and cold layers were sharply separated by a thin layer. For high floor suction rates, the effective interface was drawn very close to the floor and it became difficult to distinguish the cold layer from the separating mixing layer.

Lim noted that the carbon dioxide concentration profiles gave a better reflection of the mixing that was occurring than the temperature profiles did. This was attributed to the fact that mass transfer and heat transfer processes are not similar. Heat transfer can occur by radiation, conduction and convection; mass transfer, however, is entirely due to mixing.

Lim found that for a given floor suction rate, the effect of decreasing the door area was to lower the effective interface, and increase the average velocity of the inflowing air. This resulted in increased mixing. The door height was found to be a stronger influence on the mixing than the door width was. This is not unexpected; Rockett (1976) showed that in a two layer atmosphere, (such as used in zone models), the velocity is directly proportional to the door width, and also proportional to the door height to the power of 1.5; see Equation (2.22).

$$U_d \propto f\left(W_d, H_d^{\frac{3}{2}}\right) \tag{2.22}$$

Assuming that the exchange of mass between the layers is enhanced by a larger velocity gradient, Rockett's relationship shows that the door height will have a stronger influence than the door width on mixing.

Lim found from his experiments that the exchange of mass between layers correlated well with a form of the overall Richardson number. The form of the overall Richardson number, R_o, used in Lim's correlations used the effective interface height, Z_D, as the characteristic length and the average inflow velocity, U_{in}, as the characteristic velocity.

$$Ri_o = \frac{\Delta\rho\, g\, Z_D}{\rho_\infty U_{in}^2} \tag{2.23}$$

where

$$U_{in} = \frac{\dot{m}_{in}}{\rho_\infty W_d Z_D} \tag{2.24}$$

Lim calculated the average velocity of the lower layer gas in the doorway using the effective interface height, Z_D, as the depth. This should in fact be the neutral layer height, Z_N. The effect of this approximation is to slightly raise the value of the average velocity. Another point to note about this form of the overall Richardson number, is that the characteristic velocity, U_{in}, is taken from the doorway, while the characteristic depth, Z_D, is from a downstream location in the compartment. Lim did state that a number of different forms for the overall Richardson number were trialed; it was found, however, (by trial and error), that this form of the Richardson number provided the best correlation with the experimental data.

Using this form of the Richardson number, Lim showed the ratio of the cold layer entrainment rate to the floor suction rate, ($\dot{m}_{e-LL}/\dot{m}_{e-F}$), as a function of $Ri_o^{-\frac{1}{2}}$. This plot been copied from Lim, (1984), into Figure 2.7.

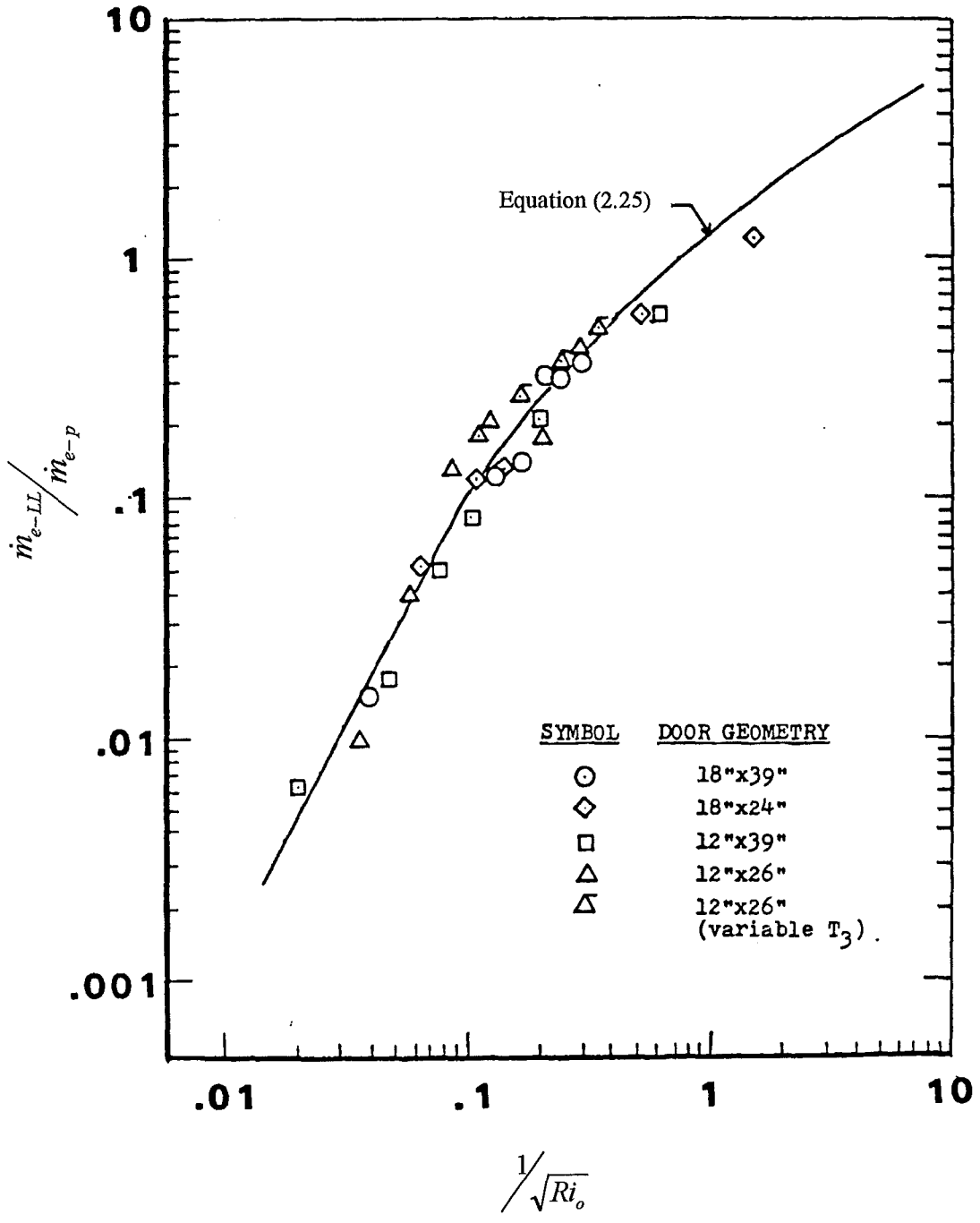

Figure 2.7 Experimental Results of Lim, (1984)

Effect of Furnace Temperature

To study the effect of the furnace temperature, Lim held the floor suction rate constant while he varied the temperature in the furnace. He found from the temperature profiles, that when the hot layer temperature was lowered from 150°C to 65°C, the temperature of the cold layer did not change significantly. The carbon dioxide concentration profiles exhibited similar behaviour. Lim proposed that this could be explained by the fact that a reduction in hot layer temperature reduced the buoyancy energy in upper layer, and therefore the rate of mixing between the layers increased. According to Lim's data, the change in the mixing rate is just sufficient to maintain the temperature and carbon dioxide concentration of the lower layer at a constant level.

Mixing Layers

Lim identified two regions in which mixing layers formed within the 1/2 scale model. The first was a mixing layer in the vertical plane between the hot and cold layers; the second, was a mixing layer that formed between the cool jet of air entering the room and the recirculating flows in the room corners, refer Figure 2.8.

Lim observed that the mixing layer between upper and lower layers grew in thickness along the shear interface from the plane of the doorway to some critical point downstream in the compartment. The growth of the layer is due to turbulent entrainment. Beyond the critical point, the mixing layer maintained a constant thickness due to the suppression of mixing by buoyancy forces.

Within the recirculation regions, (in the corners of the room adjacent to the doorway), mass was transported in the vertical direction. Mixing that occurred along the shear layer between the cool jet and the recirculating flows, therefore acted as an indirect exchange of mass between the hot upper layer and the cool lower layer.

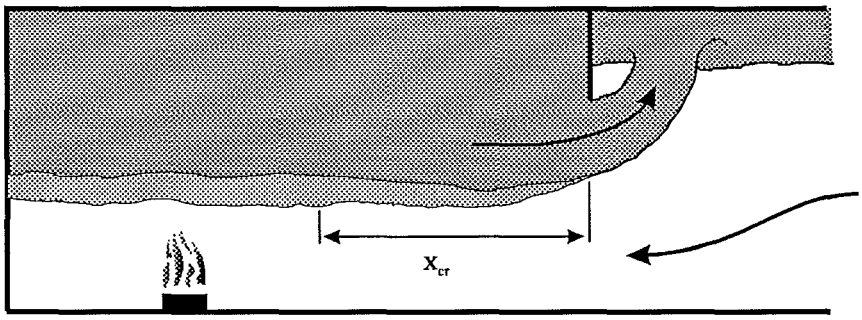

Elevation

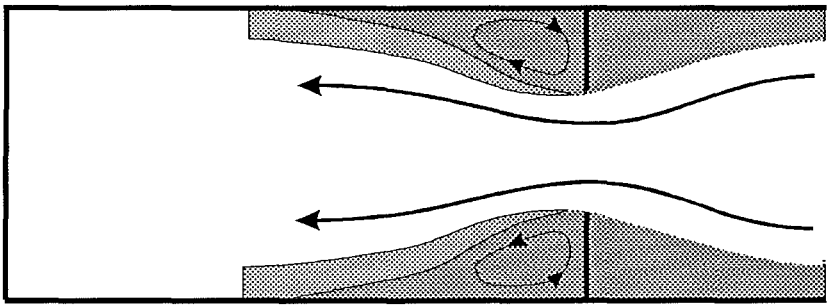

Plan

Figure 2.8 Schematic of the mixing layers observed by Lim in the model.

2.3.4 Entrainment Model

Lim derived a theoretical model for estimating the entrainment rate of hot gases into the lower layer. The derivation of Lim's model involves combining an array of fluid dynamics principles. A number of the principles used in Lim's derivation are not valid in the manner that he has applied them, and little or no explanation, (graphical or theoretical), was provided to justify his assumptions. The derivation of Lim's model is reproduced in Appendix 1.

The entrainment model derived by Lim for estimating the entrainment of mass into the lower door jet is given by Equation (2.25).

$$\left[\frac{1}{2}\left[\frac{\dot{m}_{e-LL}}{\dot{m}_{in}}\right]^2 + \frac{\dot{m}_{e-LL}}{\dot{m}_{in}}\right]\left[1+\frac{\dot{m}_{e-LL}}{\dot{m}_{in}}\right]^2 = AF^2 \qquad (2.25)$$

where

$$A = \frac{A_1^3}{A_2}\frac{E_o}{n+1}(Ri_x)_{cr} \qquad (2.26)$$

$$F = \frac{\rho_{UL}}{\rho_\infty}\frac{W_d}{W_c}\frac{1}{\sqrt{Ri_o}} \qquad (2.27)$$

Figure 2.7 shows a comparison of the experimental data with the theoretical predictions of Lim's entrainment model. Lim found from his experimental data that the empirical constant A defined by Equation (2.26) had a mean value of 11.7 ± 5.3.

Using numerical values obtained from fluid dynamics literature, and the empirically determined value for A, Lim estimated the value of the constant A_1, used in Equation (2.26), as 9.46 ± 1.37.

The numerical values used by Lim from the fluid dynamics literature are listed below.

$\Rightarrow (Ri_x)_{cr} \approx 0.25$	- Scotti and Corcos, (1972)
$\Rightarrow E_o \approx 0.036$ and $n \approx 2$	- Chu and Vanvari, (1976)
$\Rightarrow A_2 \approx 0.23$	- Abramovich, (1963)

Lim stated that the analysis involved in the derivation of his entrainment model did not account for the following:

1. Three dimensional effects, that impact upon the maximum velocity decay, U_{max}, the entrainment coefficient, E_o, and the rate of growth of the mixing layer. Lim notes that all these aspects may in fact be functions of the door geometry.

2. The presence of the back wall of the compartment, (normal to the direction of flow), has not been accounted for. The analysis ignores the effect of the door jet impinging on this wall.
3. The losses due to the presence of wall friction and pressure gradients within the room. These aspects will have a greater influence the further downstream the flow is considered.
4. The effects of a counter flowing hot layer.

From Figure 2.7 the comparison of the experimental data and the entrainment model predictions seems to give good agreement. This seems surprising given the methodology used in the derivation of the model.

2.4 Zukoski and Kubota, (1980)

Two-Layer Modelling of Smoke Movement in Building Fires

Zukoski and Kubota, (1980), describe the equations used in the development of a simple two room zone model. As part of the model description they discuss the correlations used to simulate the entrainment in vent flows. The correlations used in the model come from experimental salt water modelling work done by Zukoski and Peterka (1979). The author has been unable to review the Zukoski and Peterka, (1979) reference, and therefore this section is only able to present the final form of the correlations presented in Zukoski and Kubota (1980).

Zukoski and Kubota presented two situations where strong entrainment occurs in a compartment vent; these situations are illustrated in Figure 2.9. In Figure 2.9 (a), the jet of hot gases flows under the soffit of the vent, then rises to the ceiling of the adjacent room. In Figure 2.9 (b), the cool gases that flow into the compartment, are drawn over the sill of the vent and then plunge downward through a section of the hot upper layer.

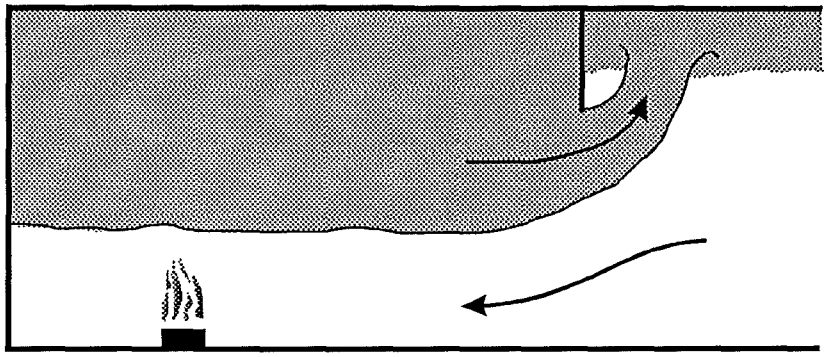

(a)

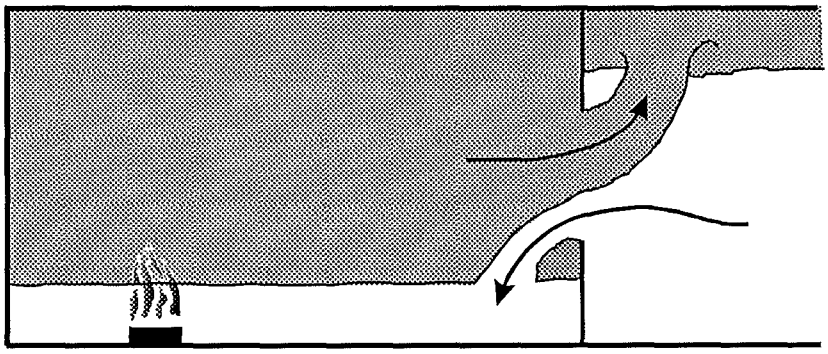

(b)

Figure 2.9 ***Schematic of two doorway flow situations in which strong entrainment has been observed.***

Zukoski and Kubota, (1980), noted that the hot upper door jet would not always separate from the door soffit. Initially the jet would remain attached to the soffit and then separate from it as the depth of the source layer increased below the soffit of the doorway, refer Figure 2.10. The exact point of transition between these two flow cases has not yet been identified, Figure 2.10 illustrates two possible flow regimes for the upper door jet.

A third possible flow regime for the hot upper door jet was also referred to by Zukoski and Kubota when the depth of the upper layer in the receiving compartment was thin. The hot door jet would rise to the ceiling of the receiving room and splash

energetically through the thin ceiling layer. This caused very rapid mixing in the layer in a process similar to a hydraulic jump structure.

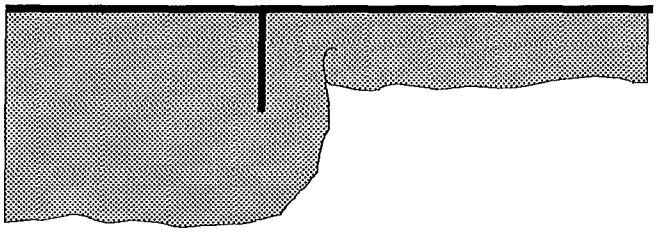

(a) Attached Flow Case

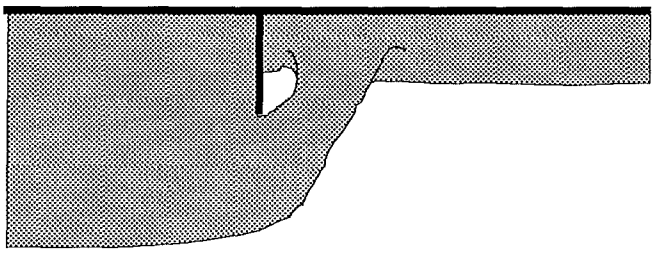

(b) Separated Flow Case

Figure 2.10 ***Schematic showing the two possible flow configurations for the upper door jet after the hydraulic jump structure has been drowned out.***

Zukoski and Kubota presented a formula, based upon the experimental work of Zukoski and Peterka, (1979), to estimate the entrainment into the hot upper door jet after the hydraulic jump structure had been drowned out.

Zukoski proposed that the entrainment of lower layer material into the upper door jet could be approximated by;

$$\dot{m}_{43} = (C_J)\rho_4\sqrt{g\,Z_d}\,Z_d^2\left(Q_d^*\right)^{\frac{1}{3}} \qquad (2.28)$$

where

$$Q_d^* = \frac{\dot{m}_{13} C_p (T_1 - T_4)}{\rho_4 C_p T_4 \sqrt{g Z_d} Z_d^2} \tag{2.29}$$

$$Z_d = Z_{D3} - Z_N \tag{2.30}$$

and

$C_J = 0.30$ for the separated door jet, and

$C_J = 0.18$ for the attached door jet.

This formula results in the following relationship between the mass flux exiting the vent and the mass entrained into the door jet.

$$\frac{\dot{m}_{43}}{\dot{m}_{13}} = C_J \left(\frac{\rho_1 - \rho_4}{\rho_4} \right) \left(Q_d^* \right)^{-\frac{2}{3}} \tag{2.31}$$

It should be noted that the mass entrainment formula for the door jet is very similar to Zukoski's mass flux formula for an axisymmetric buoyant plume.

$$\dot{m}_p = \left(\pi C_v C_l^2 \right) \rho_\infty \sqrt{g Z_p} Z_p^2 \left(Q_Z^* \right)^{\frac{1}{3}} \tag{2.32}$$

where

$$Q_Z^* = \frac{\dot{Q}}{\rho_\infty C_p T_\infty \sqrt{g Z_p} Z_p^2} \tag{2.33}$$

The relative size of the entrainment coefficients, (C_J), for the separated and attached flow cases can be compared to the relative magnitude of entrainment between a normal fire plume and a fire plume next to a wall. Zukoski and Kubota estimate that an attached door jet will entrain approximately 60% of the mass that a separated door jet will. Zukoski *et. al.*, (1980a), found that a plume attached to a wall entrained approximately 57% of the mass that a normal, free standing plume will.

In Zukoski and Kubota's relationship, (Equation 2.28), the entrainment into the door jet is assumed to occur over a length equal to the distance between the neutral plane and the zone interface in the adjacent compartment, (Z_{D3} - Z_N). It is unclear if the proposed equation considers the possible contribution of mass transported from the lower layer to the upper layer in recirculation regions that may form adjacent to the vent.

Zukoski and Kubota proposed that the same relationship, (Equation 2.28), could be used to model the entrainment into the lower layer. The applicability of this equation is based on the assumption that the lower layer gas stream behaves somewhat like an inverted plume plunging through a section of the hot upper layer, refer Figure 2.9 (b).

2.5 Summary

Two researchers have attempted to quantify the mass exchange between the two gas streams present in fire induced doorway flow; the work of neither researcher has been verified. Each researcher has concentrated on a different aspect of the vent flow mixing problem. Lim, (1984), dubiously derived a model for estimating the entrainment of hot layer mass into the lower door jet of cool gases. His work was carried out in a half scale model that mechanically simulated the characteristics of a fire plume. Zukoski and Kubota, (1980), presented a relationship for estimating the amount of lower layer mass entrained into the hot upper door jet. Their work was based upon salt water modelling work carried out by Zukoski and Peterka, (1979). Further research is required in this area, and the verification of previous research work would be a good place to start.

Chapter 3
FLUID DYNAMIC ASPECTS

3.1 Introduction

The fluid dynamic structures included in this chapter are only covered with a very simple introduction. In most cases there has been extensive research carried out on the individual topics that goes well beyond the scope of the brief coverage provided within this chapter. The purpose of this chapter is to introduce the reader to some of the fluid dynamic aspects present in doorway flow that may contribute to the mixing between the upper and lower door jets. It is intended that this chapter will spur thought on some of the considerations needed in tackling the problem and also provide a reference source for further detailed material.

3.2 Flow Development in the Fire Situation

In a pre-flashover room fire, it is generally accepted that the atmosphere in the burn room can be approximated as two stratified layers. The fire plume above the combustion zone, entrains air from the cooler lower layer, heats it, and pushes it into the upper layer. When the upper layer of hot gases is sufficiently deep, the gases start to spill out under the soffit of any windows or doorways that are open in the room. In the lower portion of the open vents, cool air is drawn into the compartment to feed the combustion reaction and the entrainment demand of the fire plume. The upper layer in the burn room will continue to drop until its starts to choke the supply of oxygen rich air to the fire. Eventually, if left long enough, an equilibrium will be established between the air supply entering the room and the hot gases exiting the room.

The cool air that is drawn into the burn room along the floor of an open doorway, accelerates due to the reduction in height of the lower layer and the width contraction of the doorway. Once the flow passes through the doorway, it is able spread out

laterally again until it is restrained by the bounding walls of the room and the density interface with the hot upper layer.

The hot gases exiting the room through the upper portion of the doorway rise and impinge upon the ceiling of the adjacent room. Near the impingement point on the ceiling, a hydraulic jump-like structure temporarily exists where the hot gases turbulently entrain cooler gases from the lower layer. The jump structure is quickly drowned out by a returning wave of hot gases that has been reflected off the walls of the compartment. The upper layer in the room then continues to deepen until it is also able to spill out through an open doorway or window.

3.3 The Concept of Entrainment

When a turbulent fluid flow is injected or induced in a stationary ambient fluid, the turbulent fluid region expands as it moves downstream and entrains ambient fluid. The ambient fluid is entrained into the turbulent region through instabilities along the shear boundary between the fluids. The shear induced flow of ambient fluid into the turbulent region gives the impression that there is a small mean velocity component perpendicular to the main turbulent flow. This velocity is referred to as the entrainment velocity. Morton, Taylor and Turner (1956) proposed that the entrainment velocity is proportional to the velocity scale of the turbulent region. The constant of proportionality is referred to as the entrainment constant, E, and this was the basis for their original plume theories.

In a two layer stratified fluid system the boundary between the fluids will be near horizontal. In this case, the mixing that occurs between the fluids is inhibited by the stable density gradient across the boundary. Stabile stratification implies that the density decreases with height. Vertical motions, therefore tend to carry heavier fluid upwards and draw lighter fluid downward and are inhibited by gravity forces. This is in stark contrast to what happens in buoyant plumes, where the boundary of the turbulent region is almost vertical and buoyancy is the driving force for the shear induced entrainment. Ellison and Turner, (1959), investigated the turbulent

entrainment that occurs in stratified shear flows. To account for the inhibiting effect of the stable density gradient, they proposed that provided the Reynold's number is sufficiently large, and the density differences are sufficiently small, the entrainment is proportional to the velocity scale of the moving layer multiplied by an empirical function of the overall Richardson number, $E(Ri_o)$.

3.4 The Richardson Number

The Richardson number is a dimensionless parameter that describes the stability of a stratified shear layer. There are primarily two different forms of the Richardson number; the overall Richardson number, Ri_o, and the gradient Richardson number, Ri. It is important to make a clear distinction between the two different forms.

The overall Richardson number, Ri_o, is given by Equation (3.1). The form of the dimensionless number reflects the destabilising influence of the velocity and the stabilising influence of the density gradient. It is the ratio of the buoyancy and inertia terms;

$$Ri_o = \frac{g'L}{U^2} = \frac{g(\rho_\infty - \rho)L}{\rho U^2} \tag{3.1}$$

The inverse square root of the overall Richardson number is equal to the densimetric or internal Froude number.

The gradient Richardson number is a localised stability parameter based upon the vertical density and velocity gradients at a given position in the flow. It is described by Equation (3.2).

$$Ri = \frac{-g\frac{\partial \rho}{\partial z}}{\rho\left(\frac{\partial u}{\partial z}\right)^2} \tag{3.2}$$

The Gradient Richardson number may be approximated as

$$Ri = \frac{g(\Delta\rho)\delta}{(\Delta U)^2} \tag{3.3}$$

where

δ is the thickness of the layer,

$\Delta\rho$ is the density difference across the layer, and

ΔU is the velocity difference across the layer.

As the Richardson number decreases in value, the layer becomes more unstable.

3.5 Stratified Shear Flow

A large amount of work has been done on stratified shear flows. The very basic introduction below is an injustice to the existing knowledge on the topic, however, the subject is far to vast and complex to present here in any substantial detail. Turner (1973), is an excellent reference for further detail on this topic.

In fire induced doorway flow, the interface between the hot gases exiting the compartment and the cool gases entering the compartment is a density interface. The opposite direction of flow for each of the two gas streams travelling through the doorway causes a shear across the density interface. If the shear is sufficiently large, such that the Gradient Richardson number is less than 0.25, Kelvin-Helmholtz instabilities grow along the interface and collapse creating an intermediate density mixing layer. The mixing layer grows in thickness as it entrains fluid until it reaches an overall Richardson number equal to approximately 0.25. At this point, the mixing layer stops entraining fluid from the bounding layers due to the suppression of turbulent mixing by buoyancy forces, see Figure 3.1. Classical theory stipulates that the mixing layer will cease to grow in depth at an overall Richardson number value of 0.25, however in reality, the value may range anywhere from 0.25 through to about unity.

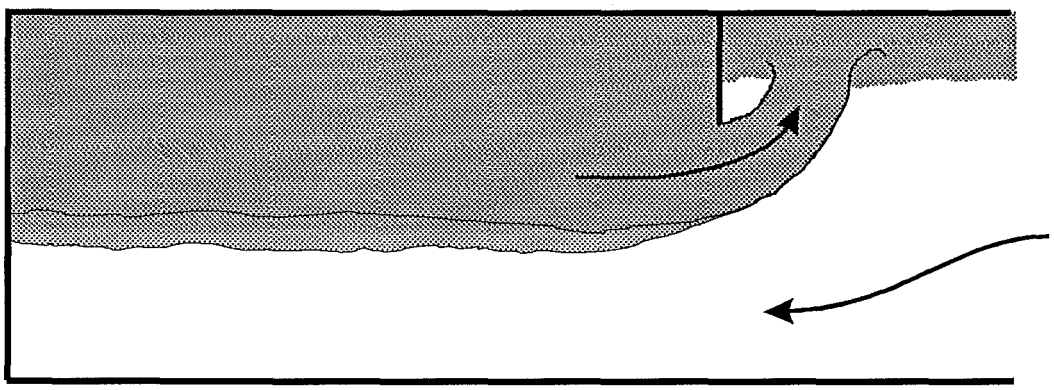

Figure 3.1 ***Development of the mixing layer between the hot upper layer and the cool lower layer within a compartment.***

The term "mixing" is used in the description of the mass exchange that takes place between two layers in stratified shear flows. One might ask therefore, what is the difference between entrainment and mixing? Entrainment is associated with the movement of one turbulent fluid in an essentially stationary ambient fluid. The turbulent fluid region draws ambient fluid into its structure through the instabilities along the interface between them. Mixing is generally associated with two fluids that are turbulent. The turbulence causes the two fluids to exchange mass which results in an intermediate density mixing layer forming between them.

3.6 Kelvin-Helmholtz Shear Instability

The Kelvin-Helmholtz instability is a shear induced instability that occurs on the density interface in a stratified fluid. The instability can grow to form "billows" that collapse and cause turbulent mixing, (Thorpe, 1973), the mixing develops an intermediate density layer discussed above in Section 3.5. The disturbances caused by the Kelvin-Helmholtz instability begin when the gradient Richardson number falls below about 0.25.

Benjamin (1963) identified three types of instability that can occur on a density interface across which there is a velocity difference. The instabilities were classified as followed:

Class A instability: - waves of the same kind as Tollmien-Schlichting (T-S) waves. The presence of viscosity is essential for the growth of these waves.

Class B instability: - waves similar to those on a free surface. Shear is an essential factor for the growth of these waves.

Class C instability: - Kelvin-Helmholtz instability. These waves occur when the Class A and B waves above, coincide in both speed and wavelength.

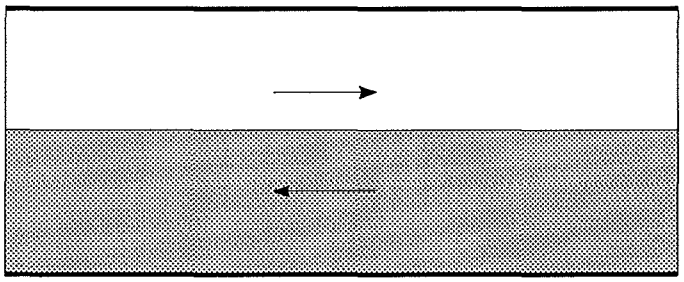

(a)

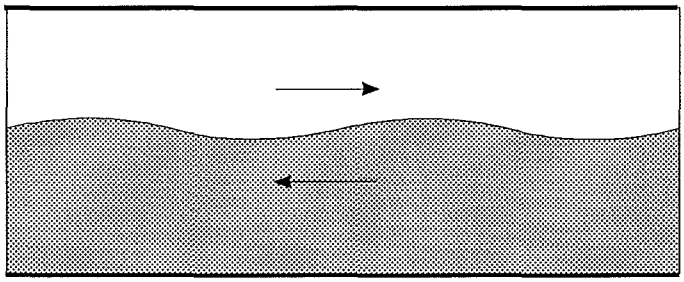

(b)

(c)

Figure 3.2 A schematic for the development of Kelvin-Helmholtz instability

The development of the Kelvin-Helmholtz instability can be illustrated by simplistically considering a two layered system in which the flow in each layer is equal but opposite in direction, (such that the disturbance will not travel with the flow), see Figure 3.2(a). Consider now that the interface between the two fluid layers becomes slightly wavy in profile, refer Figure 3.2 (b). The fluid above the crests and beneath the troughs of the interface will accelerate; from Bernoulli's equation the pressure at these positions will drop. Similarly, the fluid above the troughs and beneath the crests will slow slightly and the pressure will rise in these regions; see Figure 3.2 (c). The resulting pressure gradients cause the disturbance to amplify.

3.7 The Drop Structure Analogy

Drop structures are used in open channel flow to dissipate energy, (Moore, 1943). In fire engineering they may be considered analogous to the jet of hot gases leaving a compartment through a doorway and impinging upon the ceiling of the adjacent room. Figure (3.3) shows the typical flow situation at the base of a free overfall in a drop structure.

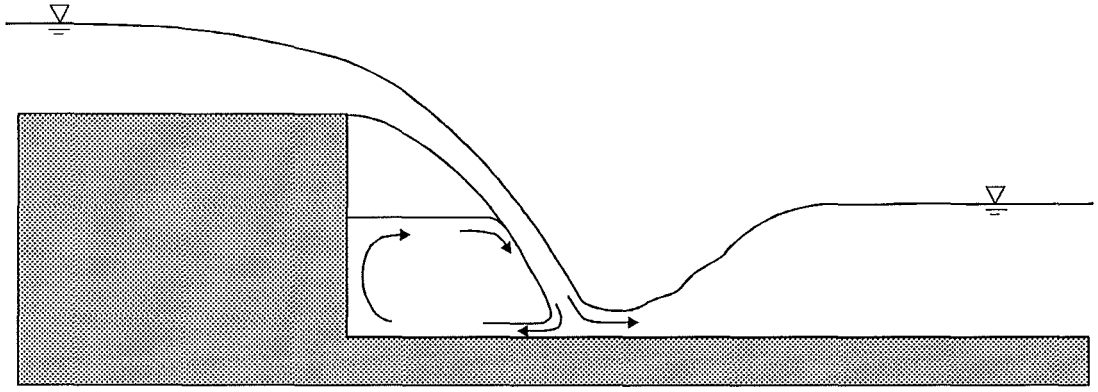

Figure 3.3 [†] ***Typical flow situation at the base of a free overfall in a open channel drop structure.***

The jet of water from the free overfall strikes the horizontal surface at an angle; the majority of the discharge flows to the right, the remainder flows back to the left. The velocity in each stream changes in direction only, not in magnitude. The water in the

[†] Figure copied from Henderson, (1966).

flow travelling left, (according to Figure 3.3), flows into the standing pool beneath the nappe of the jet. This causes a clockwise rotation in the pool. At steady state, the flow into the standing pool must be equal to the flow drawn from the standing pool into the jet. The entrainment of this flow into the jet, reduces the average velocity and thickens the width of the jet below the level of the standing pool.

3.8 Forced Plumes

The upper door jet of hot gases exiting a compartment beneath the soffit of a doorway has been likened to a forced plume, (or equivalently, a buoyant jet), discharged horizontally. A forced plume differs from a pure plume in that it has an initial momentum at the source. The flow within a forced plume can be divided into two separate sections based upon the initial momentum and buoyancy of the flow. Near the source the initial momentum dominates and the flow can be characterised by the properties of a pure jet. At some distance downstream, the buoyancy becomes the dominant driving force and the flow becomes indistinguishable from a plume.

The transition from a jet-like flow to a plume-like flow is defined in terms of a characteristic length scale, l_m. The length scale l_m is derived from the initial specific momentum flux, M_o, and the initial specific buoyancy flux, B_o, of the flow at the source.

$$l_m = \frac{M_o^{\frac{3}{4}}}{B_o^{\frac{1}{2}}} \tag{3.4}$$

where

$$M_o = \frac{\pi}{4} d_p^2 U_o \tag{3.5}$$

$$B_o = \frac{\Delta\rho}{\rho_\infty} g V_o \tag{3.6}$$

V_o is the volumetric discharge at the source, and

U_o is the average velocity of the jet at the source.

Another characteristic length scale, l_Q, is often discussed when considering forced plumes. The length scale l_Q is used to account for the initial zone of flow establishment near the source. Consider a forced plume of saline solution being injected into an ambient freshwater fluid. When the saline solution exits the pipe at the source, the velocity distribution of the flow is approximately uniform, (if the pipe is long enough). The velocity at the centerline of the injected flow remains uninfluenced by the turbulence of the shear for some distance downstream from the source, see Figure (3.4). This distance is called the zone of flow establishment.

$$l_Q = \frac{V_o}{M_o^{\frac{1}{2}}} \tag{3.7}$$

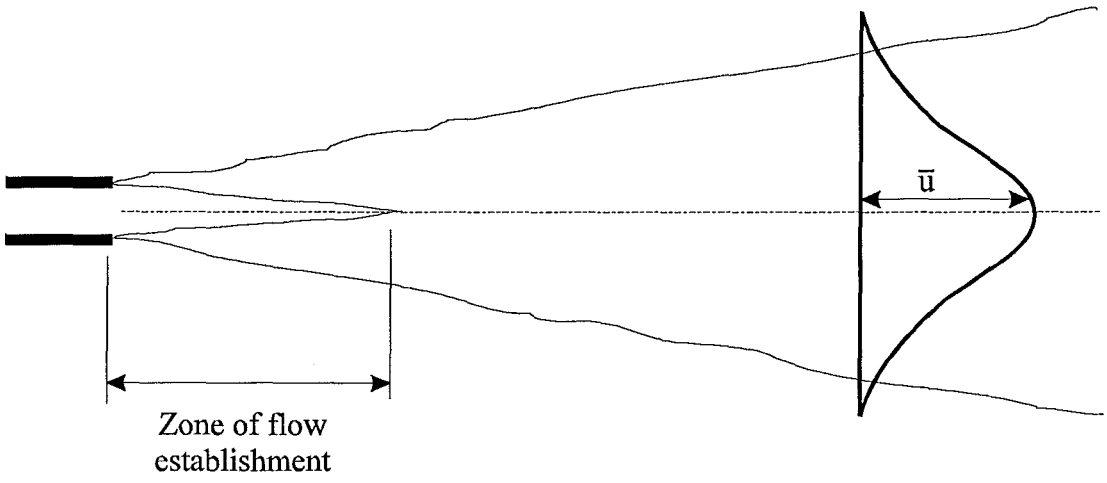

Figure 3.4 Schematic for the zone of flow establishment in a horizontal jet

The theory for the calculation of the volumetric flow rate within a forced plume is presented below as it requires consideration in the salt water modelling of fire induced doorway flows.

The ratio of the characteristic lengths, l_Q/l_M, is called the jet Richardson number, R_o; it can be defined as,

$$R_o = \frac{l_Q}{l_M} = \frac{V_o B_o^{\frac{1}{2}}}{M_o^{\frac{5}{4}}} \tag{3.8}$$

The plume Richardson number, R_p, can be defined as

$$R_p = \frac{\mu B_o^{\frac{1}{2}}}{m^{\frac{5}{4}}} \tag{3.9}$$

where

$$\mu = b_3 B_o^{\frac{1}{3}} z^{\frac{5}{3}} \tag{3.10}$$

and

$$m = b_2 B_o^{\frac{2}{3}} z^{\frac{4}{3}} \tag{3.11}$$

and where b_2 and b_3 have experimentally determined values of 0.35 and 0.15 respectively for round plumes.

The dependence of the Plume Richardson number on z, (distance along the axis of the plume), is eliminated when Equations (3.10) and (3.11) are substituted into Equation (3.9). This results in the following expression

$$R_p = b_3 b_2^{-\frac{5}{4}} = 0.557 \tag{3.12}$$

Dimensionless values for the volume flux and the distance from the jet orifice are given by Equations (3.13) and (3.14) respectively

$$\overline{\mu} = \frac{\mu B_o^{\frac{1}{2}}}{R_p M_o^{\frac{5}{4}}} = \frac{\mu}{V}\left(\frac{R_o}{R_p}\right) \tag{3.13}$$

$$\zeta = \frac{c_p z}{R_p l_M} = c_p \left(\frac{z}{l_Q}\right)\left(\frac{R_o}{R_p}\right) \tag{3.14}$$

where

$\overline{\mu}$ is referred to as the dimensionless dilution, and

ζ is the elevation parameter.

$c_p = b_3 / b_2^{\frac{1}{2}}$ has the experimentally determined value of approximately 0.254.

The volume flux within the jet-like region is then given by;

$$\overline{\mu} = \zeta, \quad \text{for} \quad \zeta << 1. \tag{3.15}$$

The volume flux within the plume-like region is given by;

$$\overline{\mu} = \zeta^{\frac{5}{3}}, \quad \text{for} \quad \zeta >> 1. \tag{3.16}$$

The flow in a jet becomes fully developed at a distance of approximately 5-15l_Q from the orifice. Inside this region of flow establishment, the jet does not entrain fluid as quickly as it does in the fully developed region. This is shown in Figure 3.5, reproduced from Fischer *et. al.*, (1979).

The volume flux relationships for a forced plume, (Equations 3.15 and 3..16), do not account for the low entrainment rate over the zone of flow establishment in the jet-like region near the source.

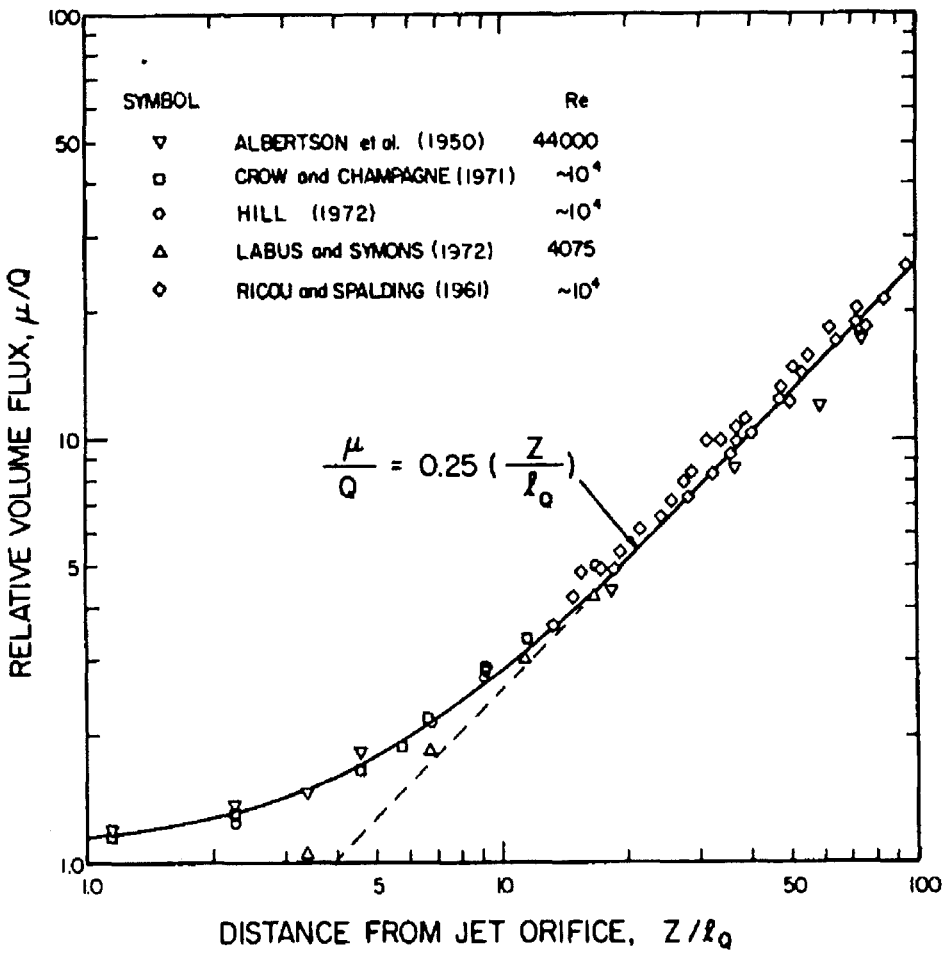

Figure 3.5[†] ***Dilution as a function of the distance along the axis of a round turbulent jet.***

3.9 The Effect of Boundaries on Entrainment

The behaviour of a plume or jet may be strongly influenced by the nearby presence of a solid boundary. If there is a shallow depth of fluid between the boundary and the turbulent flow, then the entrainment demand of the turbulent region may not be met and the plume or jet is drawn onto the solid surface. This behaviour is known as wall attachment; it is an example of what is called the conda effect. The conda effect occurs much more strongly where the flow is turbulent, due to the higher entrainment rate. Two dimensional flows will also be more prone to this effect than three

[†] Figure copied form Fischer *et. al.* (1979).

dimensional flows because fluid can not be supplied from the sides to satisfy the entrainment demand. Wall attachment has the effect of restricting entrainment into the turbulent flow wherever the boundary is and imposing frictional effects on the jet. Figure 3.6 shows schematically the wall attachment of a two dimensional jet discharged near a horizontal boundary.

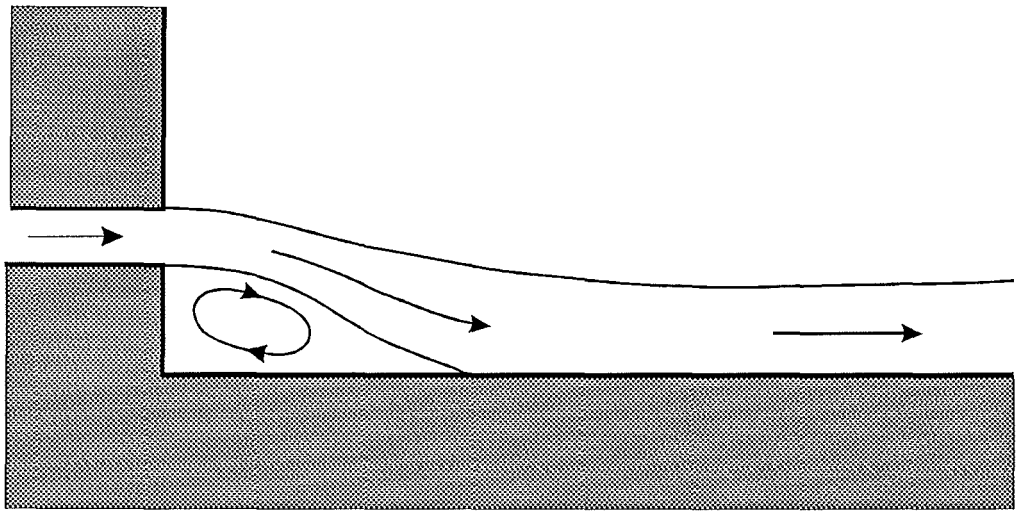

Figure 3.6[†] *Schematic for the wall attachment of a two dimensional jet*

References: Wood and Knudsen, (1990), and Sharp and Vyas, (1977).

3.10 The Surface Spreading Plume

In the ocean disposal of wastewater, the effluent rises to the ocean surface and is then redirected to flow horizontally. This can be likened to the flow of hot gases from the upper door jet, rising and impinging upon the ceiling of an adjacent room. One obvious difference with the ocean outfall analogy, is that in the fire situation, the geometrical layout of the receiving room will limit the direction in which the horizontal flow can travel.

Wood *et. al.*, (1993), discusses the creation of an effluent field at the ocean surface and some of the previous research that has been done on this topic. The effluent

[†] Figure copied from Tritton, (1977).

plume from an ocean outfall rises to the ocean surface with some density deficit remaining. On the ocean surface a small boil is created; the change in surface elevation at the boil provides the necessary pressure gradient required to redirect the flow from vertical to horizontal. The impingement region may be followed by a short jet like region in which fluid is entrained, and then a jump like region. The jump like structure transforms the flow into sub-critical flow downstream, refer Figure 3.7.

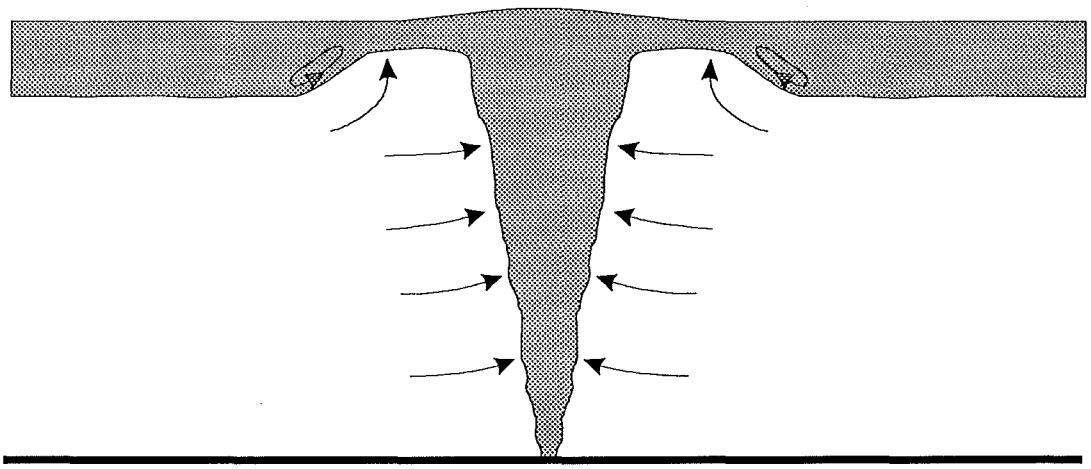

Figure 3.7 Schematic for an effluent plume from an ocean outfall.

The jump like region consists of a slowly recirculating eddy which effectively blocks off entrainment over its length. The majority of the entrainment occurs in the jet-like region prior to the jump; downstream of the jump there is little entrainment, refer Fisher, T., (1995).

3.11 The Density Jump

In density stratified flows the abrupt transition between supercritical flow and subcritical flow is referred to as a density jump. The density jump is very similar to the hydraulic jump that occurs in open channel flow. The principle difference between the two, is that the density jump may entrain ambient fluid, thereby changing its downstream flow rate and density profile.

The density jump can be divided into two distinct regions; an entrainment region and a roller region, refer Figure 3.8. The entrainment region occurs on the upstream end of the jump and is responsible for nearly all the entrainment that occurs at the jump. The roller region occurs on the downstream end of the jump and is characterised by the flow at the interface of the two fluids being in the reverse direction. The relative length of the entrainment region to the roller region, and therefore the amount of entrainment that occurs at the jump, is determined by the downstream control.

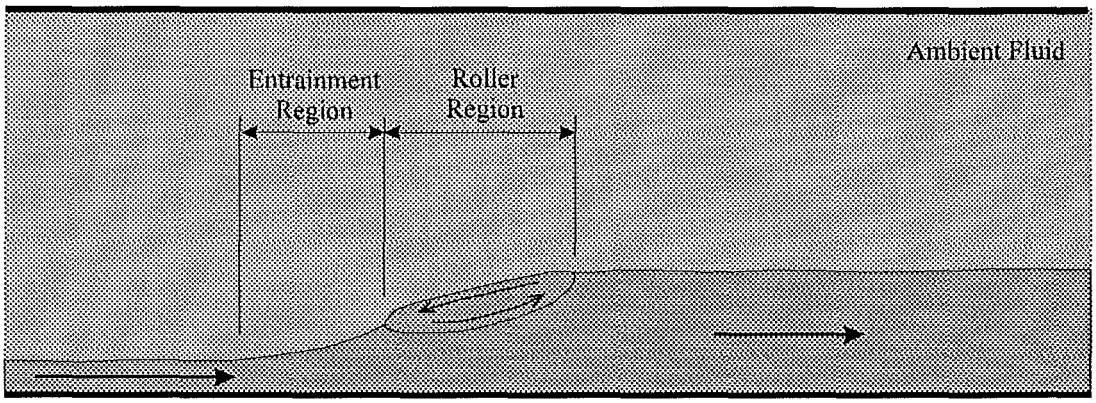

Figure 3.8 ***Schamatic showing the roller region and the entrainment region of a density jump.***

In the case of the hydraulic jump, the jump will only form between two controls if the upstream and downstream depths are conjugate to each other. If the downstream depth increases above its conjugate depth, the jump will move upstream until it drowns out the upstream control. If the downstream depth decreases below its conjugate depth, the jump will move downstream until the supercritical flow above the jump strikes the downstream control. The case is not as simple with the density jump as changing the downstream control changes the entrainment, and therefore the flow rate downstream of the jump.

In the case of the density jump, if the downstream control forces an increase in the downstream depth, the interface between the roller region and the entrainment region moves further upstream. This reduces the length of the entrainment region, thereby reducing the amount entrained and consequently lowering the downstream flow rate. In the limiting case, a point can be reached where the roller region extends over the

entire length of the jump, thereby eliminating any entrainment. Increasing the downstream depth beyond this point causes the jump to be flooded out so that the upstream end is totally submerged in its own fluid. There is no entrainment at a flooded density jump.

Considering the other case, where the downstream control reduces the downstream depth of the density jump, the interface between the roller region and the entrainment region moves downstream. This increases the length of the entrainment region and therefore the amount of ambient fluid entrained into the flow. Wood and Wilkinson (1971), showed that as the interface between the roller region and the entrainment region moves downstream, the Froude number of flow downstream of the jump increases in value. At the limit, the entrainment region extends over the entire length of the jump and the jump entrains a maximum amount of ambient fluid. In this case, the downstream Froude number has a value of unity.

3.12 The Prandtl and Schmidt Numbers

Both the Prandtl number and the Schmidt number are non-dimensional variables. The Prandtl number is used in convective motion problems. It is the ratio of two diffusivities; ν, being the diffusion of momentum, and k being the diffusion of heat.

$$\mathrm{Pr} = \frac{\nu}{k}$$

The Schmidt number is used in mass transfer problems. Again, it is also the ratio of two diffusivities, ν being the diffusion of momentum, and k_c being the diffusion of concentration.

$$Sc = \frac{\nu}{k_c}$$

The Schmidt number and the Prandtl number describe the relative diffusion of mass and heat respectively, by its advection by moving particles and by its diffusion between fluid particles.

The similarity between the equations for flows containing concentration variations and the equations for convection in the Boussinesq approximation allows ideas and results to be transferred between the two systems. This is a concept that is utilised in the salt water modelling theory described latter in Chapter 5.

Chapter 4
ZONE MODELLING

4.1 Zone Models

The zone model is a computer fire model used to approximate the conditions generated in a compartment fire. It is a deterministic model that solves a set of equations based upon the conservation equations of mass, momentum and energy to predict compartment conditions as a function of time. Zone models provide a practical and relatively simple method for estimating compartment fire conditions without the requirement of considerable computer resources needed for field models.

In reality, compartment fires involve a multitude of complicated and highly interactive processes; zone models discretely simulate each of these processes with fundamental laws or empirical correlations. Each compartment is assumed to be divided into two distinct gaseous layers, a hot upper layer and a cool lower layer, see Figure 4.1.

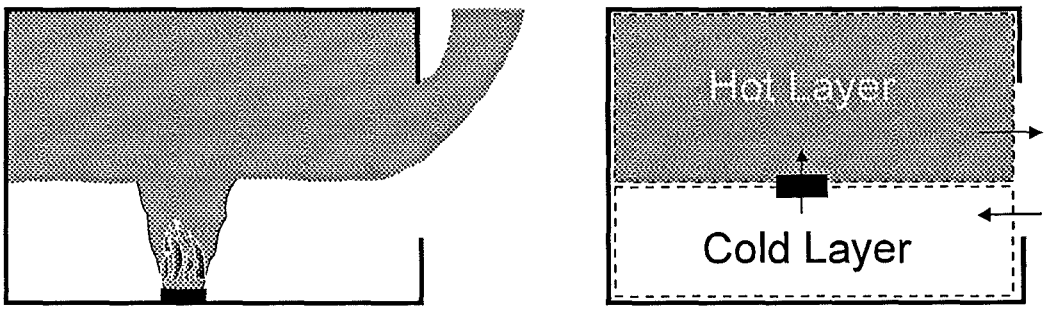

Figure 4.1 ***Schematic representation of the concept of using two homogeneous zones to represent the compartment atmosphere.***

Each layer, or zone, is considered as a control volume and assumed to be internally homogeneous. The conservation equations are applied to each control volume, and used to determine it's average macroscopic properties as a function of time. The subject of zone models has been well documented and will not be recovered in great detail here. A more complete and detailed description of the fundamentals involved in

zone modelling can be found in the following references; Quintiere (1989), Mitler (1991), Quintiere (1993), and Peacock *et. al.* (1993).

Exchange of mass between zones is assumed to only occur through the buoyant effect of the fire plume and by the shear mixing associated with the flow of gases through a vertical vent in the compartment wall. The shear mixing that occurs in fire induced vent flows has not been adequately studied by any researchers; zone models approximate the process with a crude estimate. This chapter reviews the approximations made by zone models in estimating the vent flow mixing, specifically the approximation used in CFAST, and discusses the ramifications of the assumptions with respect to door flows.

4.2 Vent Flow

There are two categories of vent flow used in zone models. Horizontal flow through a vertical vent, and vertical flow through a horizontal vent. The shear mixing associated with doorway flow relates to the first category of the two; horizontal flow through a vertical vent. This vent flow regime is the only one considered in this chapter.

The early work of Kawagoe (1958) and Thomas *et. al.* (1967) addressed the problem of fire induced vent flows for fully developed fires. They approximated the post-flashover compartment atmosphere as a single uniform temperature zone. The buoyancy driven flow through the vent was treated as an orifice flow problem, incorporating an empirically determined flow coefficient.

Prahl and Emmons (1975) developed a theory for calculating the vent flow from a two zone compartment model that would be applicable in the early stages of an enclosure fire. They considered the problem as a analogy to the flow of water over a sharp crested weir. Bernoulli's equation was used to obtain the velocity in the vent between a reservoir of stationary fluid and the vena contracta of a separated door jet.

From a series of kerosene/water analog experiments they determined an average flow coefficient of 0.68 for both the out-flowing and in-flowing door jets.

Rockett (1976) expanded the two zone vent flow work to prove the functional dependence of the incoming mass flow on the ventilation parameter.

$$\dot{m}_{in} \propto A_d \sqrt{H_d} \tag{4.1}$$

The fundamental theory of the two zone static pressure flow model is represented simplistically here; further detail can be found in Rockett (1976).

Consider a small fire in a compartment with a single doorway as a vent. The atmosphere in the compartment is sharply stratified and can be approximated by two homogeneous gaseous layers separated by a thermal discontinuity, refer Figure 4.2, (a) and (d). Hot gases leaving the compartment spill out under the soffit of the doorway while the cooler gases entering the compartment are drawn in along the floor. The cool air entering the compartment is entrained into the fire plume, heated, and then driven by buoyancy into the hot upper layer. The driving buoyancy force arises because the cooler air expands as it is heated in the fire plume.

The gaseous layers are assumed to be motionless and the pressure is assumed to vary hydrostatically, see Figure 4.2, (b) and (e). In reality there is some internal motion within the layers, for simplicity however, it is considered to be negligible, refer Zukoski (1985) and Steckler (1989).

At a certain height in the plane of the doorway the out-flowing hot gases shear over the in-flowing cooler gases. The two flows are in opposite directions, therefore there is a point at the interface separating the flows where the velocity is zero. This point/elevation in the doorway is called the neutral plane; it is the level at which the pressure both outside and inside the compartment are assumed to be the same.

From Bernoulli's equation and the assumption that the gases in the compartment have no initial momentum, it is possible to calculate the door flow velocity as a function of elevation, refer Figure 4.2, (c) and (f).

$$U = \sqrt{\frac{2\,\Delta P}{\rho}} \tag{4.2}$$

Considering the flows above and below the neutral plane separately, it is possible to calculate the mass flux entering and exiting the compartment by integrating over the vent area available to each.

$$\dot{m}_{in} = C_{in} \int_{width} \int_{0}^{Z_N} \sqrt{2\rho\,\Delta P}\; dz \tag{4.3}$$

$$\dot{m}_{out} = C_{out} \int_{width} \int_{Z_N}^{Z_{soffit}} \sqrt{2\rho\,\Delta P}\; dz + \dot{m}_{fire} \tag{4.4}$$

The mass flux derived from Bernoulli's equation is idealised. It is multiplied by a flow coefficient, C, to primarily account for the difference between the cross sectional flow area at the vent and the flow area at the vena contracta where the pressure is assumed to match ambient. Steckler, Baum and Quintiere, (1984), investigated the value of the flow coefficients for fire induced vent flows. Using the results from the 55 full scale steady state experiments, they computed an average value of 0.73 for the outflow coefficient and 0.68 for the inflow coefficient. They also noted that theory predicted a systematic variation in the value of the orifice coefficient with the ratio of vent width to the room of origin width. In the extreme case, where both widths are equal, the problem becomes that of a uniform channel flow where the orifice coefficient has a value of unity.

Steckler, Quintiere and Rinkinen, (1982), compared the two zone static pressure flow model predictions with the experimental data from 55 full scale compartment fires. The experiments investigated the variation in vent flow as a function of the vent

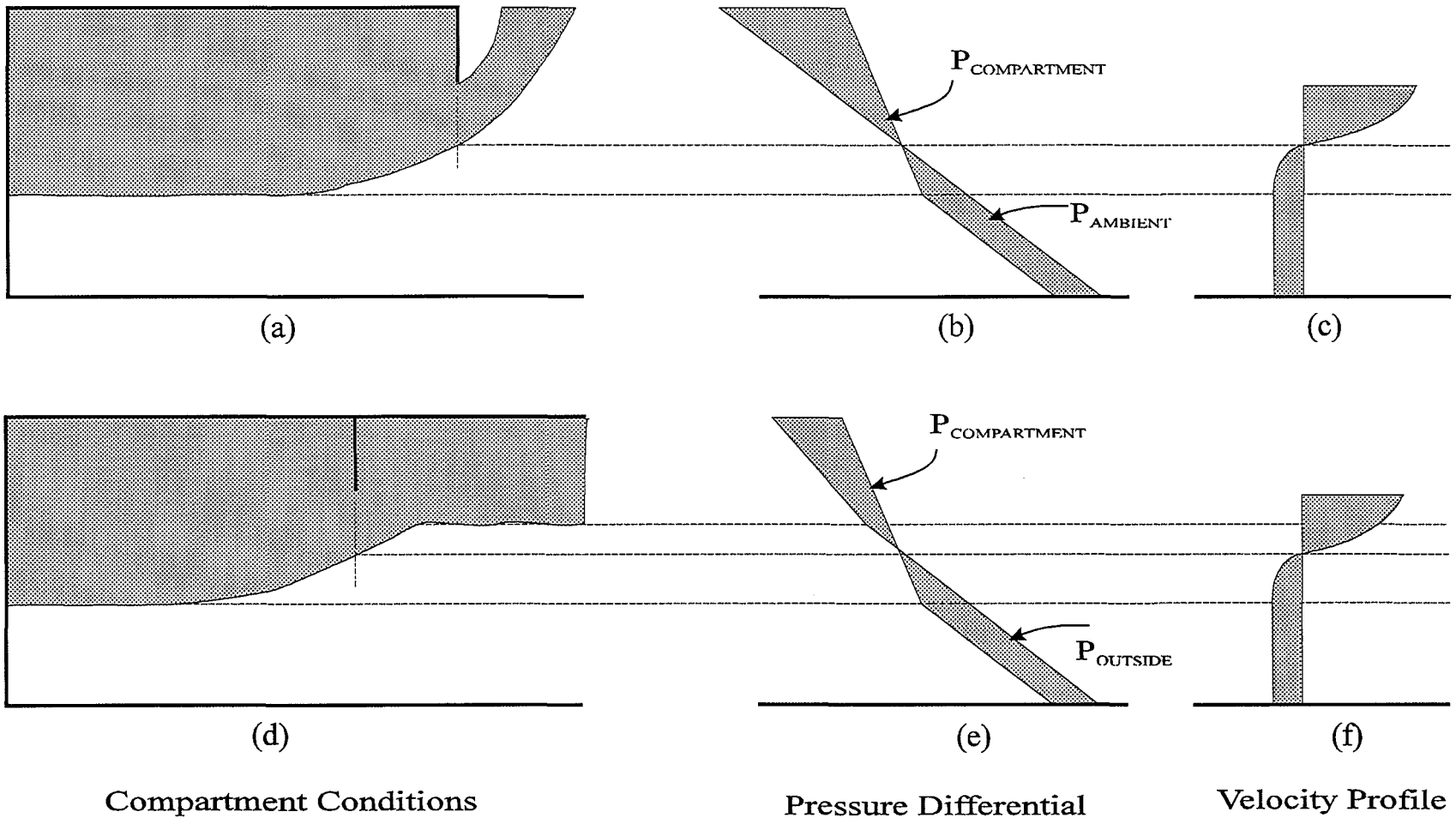

Figure 4.2 ***Schematic showing the compartment conditions and assumed pressure distributions for the calculation of vent flows in zone modelling.***

geometry, the fire size and the fire location. A good correlation was found between the actual mass flows and those predicted by the static pressure flow model.

4.3 Entrainment into the Hot Upper Door Jet

Entrainment into the hot upper door jet is probably the more complex of the two door jet problems to simulate with a zone model. The primary problem is the changing flow phases that develop as the compartment fire progresses, refer Figure 4.3. Each different flow phase has different entrainment characteristics.

Initially as the smoke spills under the soffit of a door way, it rises and impinges on the ceiling of the adjacent room where it starts to spread out, see Figure 4.3 (b). Near the point where the door jet impinges on the ceiling, a turbulent hydraulic jump structure has been observed where the jet entrains cooler mass from the lower layer. The hot gases from the jet spread out in a thin layer across the ceiling until they hit the bounding walls. The gravity current is then reflected off the walls and travels back, below the existing layer of hot gases, to the impingement point where it drowns out the hydraulic jump, Figure 4.3 (c). The upper layer then continues to increase in depth until it is also able to spill out through a doorway or window, Figure 4.3 (d). Steckler (1989), discusses the key features of the corridor filling process and the best methods for modelling them.

The entrainment of lower layer mass into the upper layer door jet will change as the upper layer in the adjacent room develops. Initially there will be a large amount of entrainment due to the hydraulic jump, however, after the jump is drowned out by the returning gravity current, the entrainment will be reduced. As the depth of the upper layer in the adjacent room increases, the length over which the door plume itself can entrain will also be reduced. Eventually, downstream conditions will control the fire size and layer depth such that the effect of the door soffit on entrainment may become negligible.

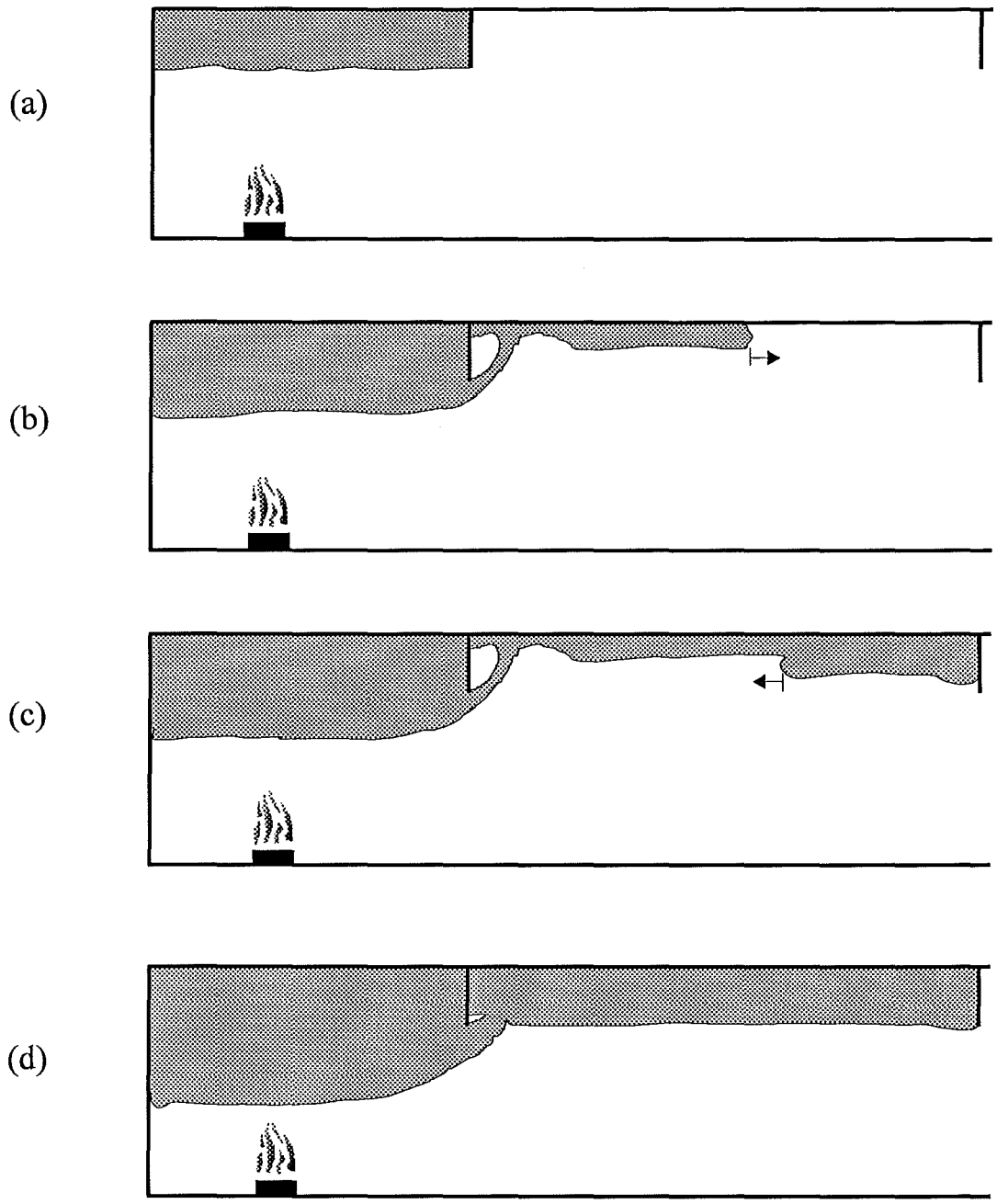

Figure 4.3[†] ***Different flow phases for the upper door jet will cause different entrainment characteristics.***

[†] Figure copied from Zukoski (1985).

Zukoski and Kubota, (1980), proposed that the entrainment of lower layer mass into the upper door jet could be approximated by,

$$\dot{m}_{43} = (C_J)\rho_4\sqrt{g Z_d}\, Z_d^2 \left(Q_d^*\right)^{\frac{1}{3}} \tag{4.5}$$

where

$$Q_d^* = \frac{\dot{m}_{13} C_p \left(T_1 - T_4\right)}{\rho_4 C_p T_4 \sqrt{g Z_d} Z_d^2} \tag{4.6}$$

$$Z_d = Z_{D3} - Z_N \tag{4.7}$$

C_J is an experimentally determined constant that has the value of 0.30 for a door jet that has separated from the door soffit and 0.18 for a door jet that remains attached to the soffit; refer Section 2.4.

This formula results in the following relationship between the mass flux exiting the vent and the mass entrained into the door jet.

$$\frac{\dot{m}_{43}}{\dot{m}_{13}} = C_J \left(\frac{\rho_1 - \rho_4}{\rho_4}\right)\left(Q_d^*\right)^{-\frac{2}{3}} \tag{4.8}$$

The height of the connected compartment and the proximity of the door to compartment walls will influence whether or not the plume attaches to a boundary. For example, a door jet of hot smoke exiting a small room into a large space with a high ceiling, (say an atrium), may initially separate from the soffit of the door and then reattach at a higher elevation, see Figure 4.4. Then again, the door jet may not separate at all from the soffit/wall. The applicability of a normal plume correlation versus a correlation for a plume attached to a wall may be questioned in this case.

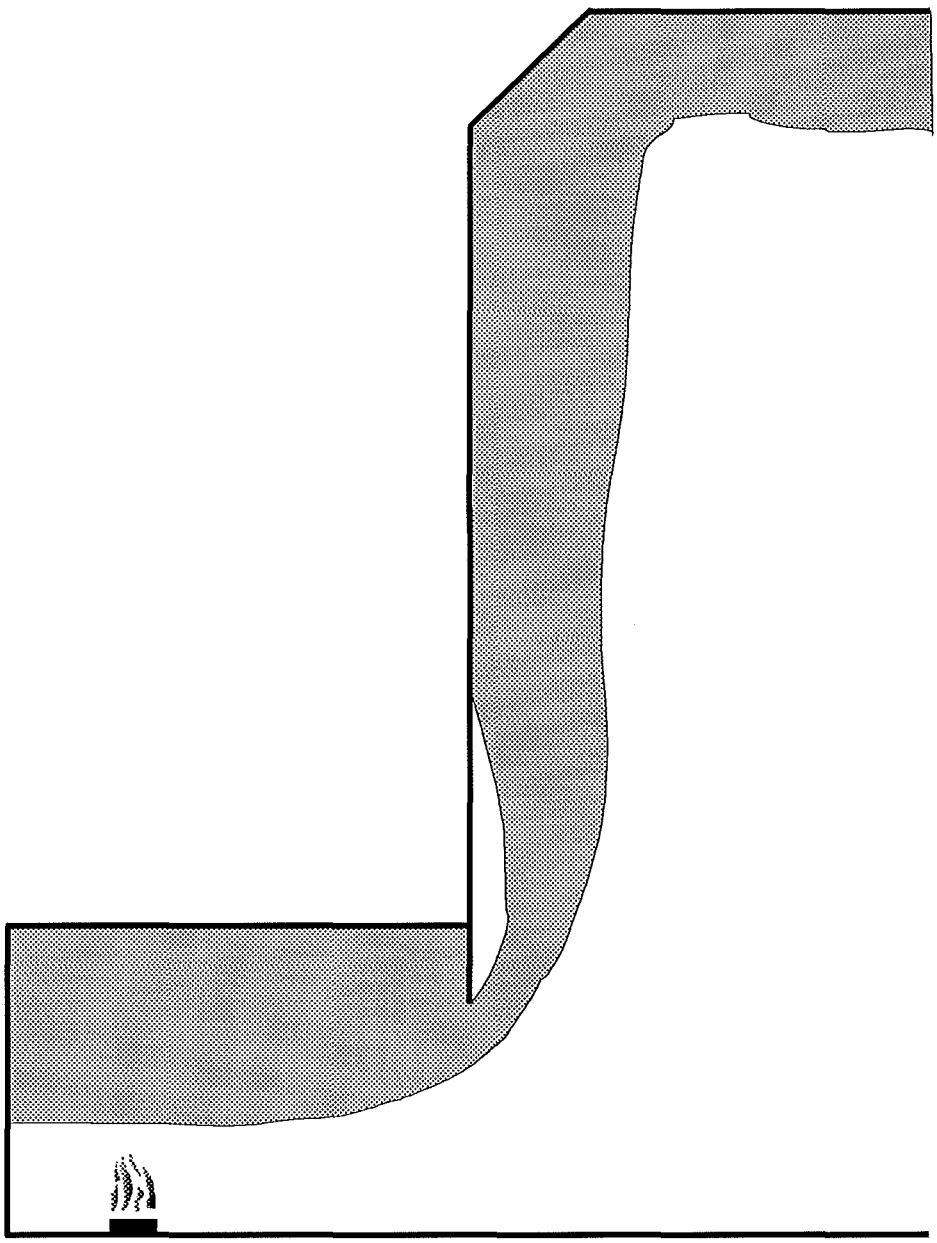

Figure 4.4 ***Schematic of a door plume spilling into an atrium or sports stadium.***

The proximity of the doorway to compartment walls will also influence the formation of any recirculation regions. Lim (1984), observed recirculation regions adjacent to the doorway and noted that they also transport mass between the upper and lower layers. This phenomenon may require attention in zone modelling of vent flow mixing.

The external burning of unburnt fuel in the hot upper door jet is another factor that will also influence the entrainment that takes place outside a doorway. In this situation, the height of the adjacent compartment ceiling will have some impact on the mixing that occurs. If the ceiling is high enough, then the burning door jet may generate a plume similar to that generated by a fire adjacent to a wall. On the other hand, if the adjacent ceiling is relatively low, then the flames may impinge on ceiling and spread out, causing a lot of turbulent mixing. Very little is known about the entrainment associated with the burning of exhaust gases and further research is needed in this area.

4.4 Entrainment into the Lower Door Jet

An open vent in a compartment provides the supply of air necessary for a combustion reaction to take place in an enclosure. The supply air is drawn into the compartment through the lower portion of the vent and the hot smoke exits the compartment through the upper portion of the vent. When the vent is a doorway, the air is drawn in along the floor. When the vent is a window however, the air must flow over a sill. Therein lies the primary difference between general vent flow and doorway flow; a sill. The obvious question now is, does the presence of a sill influence the mixing that takes place in a vent? If so, is there a minimum sill height, relative to the height of the vent and layer interface, beneath which the presence of a sill can be ignored and the mixing can be modelled as would occur in a door?

Quintiere, Steckler and McCaffrey, (1981), were the first to attempt to model the entrainment of hot gas into the lower door jet with a zone model. They conducted a number of crib fire experiments in a compartment with the aim of comparing the

experimental data with an early zone model. A model for the turbulent shear mixing that occurs in the doorway was proposed and resulted in the following relationship:

$$\frac{\dot{m}_{12}}{\dot{m}_{42}} = 0.5\left(\frac{T_4}{T_1}\right)\left(\frac{Z_N - Z_D}{Z_N}\right)\left(\frac{W_C}{W_d}\right)^{\frac{1}{4}} \tag{4.9}$$

The derivation of this relationship in represented in Appendix 2.

Zukoski and Kubota ,(1980), also proposed an equation that could be used to model the entrainment into the lower layer. The equation is identical to that they proposed for modeling the entrainment into the hot upper door jet, (Equation 4.5). The applicability of this equation is based on the assumption that the lower layer vent flow behaves somewhat like an inverted plume plunging over the vent sill and through a section of the hot upper layer, refer Figure 4.5. Zukoski's equation is probably more suitable in situations were the vent has a significant sill rather than in situations where the vent flow is through an unobstructed doorway.

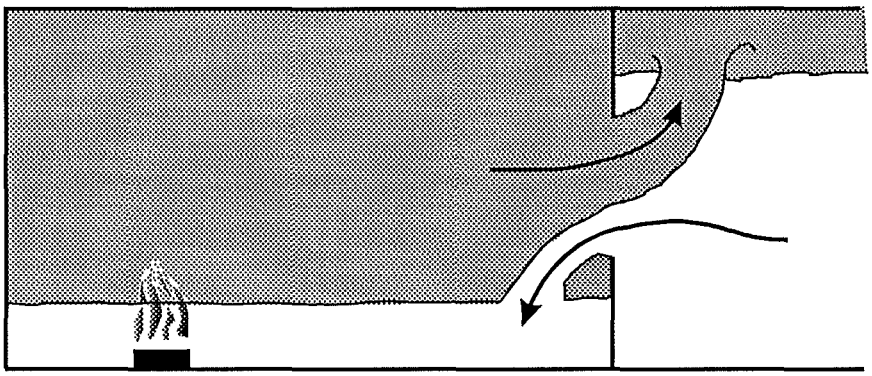

Figure 4.5 Schematic of the inverse plume analogy used for the lower door jet.

Lim (1984) showed the ratio of the cold layer entrainment rate to the plume entrainment rate as a function of the inverse square root of the overall Richardson number.

$$\frac{\dot{m}_{12}}{\dot{m}_{42}} = f\left(\frac{1}{\sqrt{Ri_o}}\right) \tag{4.10}$$

(The inverse square root of the overall Richardson number is equivalent to the internal or densimetric Froude number).

Lim's form for the overall Richardson number seems incorrect in theory. In his form of the Richardson number, the characteristic length and velocity used are taken from two different positions in the flow. The characteristic velocity is the mean velocity of the flow through the doorway, while the characteristic length is the downstream depth of the layer in the compartment.

A derivation of the overall Richardson number is shown below for two positions in the lower layer, it assumes that the two zone static pressure flow model can be used to approximate the average inflow velocity of the lower layer. This seems a reasonable approximation given the comparison of the model predictions with experimental data from 55 full scale fire tests carried out by Steckler *et al.* (1982).

The overall Richardson Number, Ri_o, is defined by

$$Ri_o = \frac{g'L}{(\Delta U)^2} = \frac{g\Delta\rho L}{\rho(\Delta U)^2} \tag{4.11}$$

If we consider the lower layer of in-flowing cool air in the compartment, (such that the door jet had spread out sufficiently to be in contact with the compartment walls), the average velocity of the layer can be expressed as,

$$U = \frac{\dot{m}_{42}}{\rho_2(Z_D W_C)} \tag{4.12}$$

The overall Richardson for the layer then becomes

$$Ri_o = \frac{g\rho_2(\rho_1 - \rho_2)Z_D^3 W_C^2}{\dot{m}_{42}^2} \tag{4.13}$$

From the theory of vent flow in zone models, Rockett (1976), the mass flux of the cool air entering the compartment through a single doorway can be expressed as

$$\dot{m}_{42} = \rho_2 A_d \left(2gH_d\left(\frac{T_2 - T_1}{T_2}\right)\right)^{\frac{1}{2}} \times \frac{2}{3}C_{in}\left(\frac{Z_N - Z_D}{H_d}\right)^{\frac{1}{2}} \times \left(\left(\frac{Z_N - Z_D}{H_d}\right) + \frac{3}{2}\frac{Z_D}{H_d}\right) \tag{4.14}$$

Such that

$$\dot{m}_{42}^2 = \rho_2^2 A_d^2 2gH_d\left(\frac{T_2 - T_1}{T_2}\right)\left(\frac{2}{3}C_{in}\right)^2 \times \left(\frac{Z_N - Z_D}{H_d}\right) \times \left(\left(\frac{Z_N - Z_D}{H_d}\right) + \frac{3}{2}\frac{Z_D}{H_d}\right)^2 \tag{4.15}$$

This form can be simplified to

$$\dot{m}_{42}^2 = 2\left(\frac{2}{3}C_{in}\right)^2 \rho_2^2 W_d^2 g\left(\frac{\rho_1 - \rho_2}{\rho_1}\right)(Z_N - Z_D)\left(Z_N + \frac{Z_D}{2}\right)^2 \tag{4.16}$$

$$\dot{m}_{42}^2 = k_{in}\rho_2^2 W_d^2 g\left(\frac{\rho_1 - \rho_2}{\rho_1}\right)(Z_N - Z_D)\left(Z_N + \frac{Z_D}{2}\right)^2 \tag{4.17}$$

Substituting this result into Equation (4.15) gives,

$$Ri_o = \frac{g\rho_2(\rho_1 - \rho_2)Z_D^3 W_C^2}{k_{in}\rho_2^2 W_d^2 g(Z_N - Z_D)\left(Z_N + \frac{Z_D}{2}\right)^2(\rho_1 - \rho_2)}\frac{\rho_1}{} \tag{4.18}$$

and again simplifying, this can be expressed as

$$Ri_o = \frac{1}{k_{in}}\left(\frac{W_C}{W_d}\right)^2\left(\frac{Z_D^3}{Z_N - Z_D}\right)\left(\frac{T_2}{T_1}\right)\left(Z_N + \frac{Z_D}{2}\right)^{-2} \tag{4.19}$$

From Rockett (1976) we know that at steady state, the neutral plane in the doorway and the density interface in the compartment can be related by

$$\left(\frac{1-N}{N}\right)^3 = \left[\left(1-\frac{D}{N}\right)\left(1+\frac{D}{2N}\right)^2\right]\left(1+\frac{\dot{m}_{fire}}{\dot{m}_{42}}\right)\frac{T_1}{T_2} \tag{4.20}$$

This is equivalent to,

$$\left(\frac{H_d - Z_N}{Z_N}\right)^3 = \left[\left(1-\frac{Z_D}{Z_N}\right)\left(1+\frac{Z_D}{2Z_N}\right)^2\right]\left(1+\frac{\dot{m}_{fire}}{\dot{m}_{42}}\right)\frac{T_1}{T_2} \tag{4.21}$$

Multiplying this expression through by Z_N^2 gives

$$Z_N^2\left(\frac{H_d - Z_N}{Z_N}\right)^3 = \left[\left(1-\frac{Z_D}{Z_N}\right)\left(Z_N+\frac{Z_D}{2}\right)^2\right]\left(1+\frac{\dot{m}_{fire}}{\dot{m}_{42}}\right)\frac{T_1}{T_2} \tag{4.22}$$

This relationship can be re-arranged to give

$$\left(Z_N+\frac{Z_D}{2}\right)^2 = \frac{Z_N^2\left(\frac{H_d - Z_N}{Z_N}\right)^3}{\left(1+\frac{\dot{m}_{fire}}{\dot{m}_{42}}\right)\frac{T_1}{T_2}\times\left(1-\frac{Z_D}{Z_N}\right)} \tag{4.23}$$

If we assume that $\dot{m}_{fire}$ is negligible, then

$$\left(Z_N+\frac{Z_D}{2}\right)^2 = Z_N^2\left(\frac{H_d - Z_N}{Z_N}\right)^3\left(\frac{T_2}{T_1}\right)\left(\frac{Z_N}{Z_N - Z_D}\right) \tag{4.24}$$

such that

$$\left(Z_N + \frac{Z_D}{2}\right)^{-2} = \frac{1}{Z_N^2}\frac{Z_N^3}{(H_d - Z_N)^3}\left(\frac{T_1}{T_2}\right)\left(\frac{Z_N - Z_D}{Z_N}\right) \tag{4.25}$$

The above expression can be substituted into the overall Richardson number expression derived earlier, (Equation 4.19),

$$Ri_o = \frac{1}{k_{in}}\left(\frac{W_C}{W_d}\right)^2\left(\frac{Z_D^3}{Z_N - Z_D}\right)\left(\frac{T_2}{T_1}\right)\left(Z_N + \frac{Z_D}{2}\right)^{-2} \tag{4.26}$$

This substitution results in the following expression for the overall Richardson number of the lower layer in the compartment.

$$Ri_o = \frac{1}{k_{in}}\left(\frac{W_C}{W_d}\right)^2\left(\frac{Z_D}{H_d - Z_N}\right)^3 \tag{4.27}$$

where,

$$k_{in} = 2\left(\frac{2}{3}C_{in}\right)^2 = 2\left(\frac{2}{3}0.68\right)^2 = 0.411 \tag{4.28}$$

so that

$$\boxed{Ri_{o,C} = 2.43\left(\frac{W_C}{W_d}\right)^2\left(\frac{D}{1-N}\right)^3} \tag{4.29}$$

Now if we consider the overall Richardson number for the lower layer <u>in the plane of the doorway</u>.

$$U = \frac{\dot{m}_{42}}{\rho_2 (Z_N W_d)} \tag{4.30}$$

The overall Richardson for the layer becomes

$$Ri_o = \frac{g\rho_2(\rho_1 - \rho_2) Z_N^3 W_d^2}{\dot{m}_{42}^2} \tag{4.31}$$

and by the same substitution and manipulation as carried out in the previous derivation, this can be expressed as,

$$\boxed{Ri_{o,d} = 2.43 \left(\frac{N}{1-N}\right)^3} \tag{4.32}$$

The most surprising aspect of the two equations for the Richardson number shown above, is the non-appearance of terms such as the density difference or the layer velocity. The influence these parameters is incorporated in the equations used in the derivation of the above expressions.

If Equations (4.29), and (4.32) are each substituted separately into Equation (4.10) as a form of the overall Richardson number, the following relationships are obtained.

$$\frac{\dot{m}_{12}}{\dot{m}_{42}} = f\left(\frac{1}{\sqrt{Ri_{o,C}}}\right) = 0.64 \left(\frac{W_d}{W_C}\right)\left(\frac{D}{1-N}\right)^{-\frac{3}{2}} \tag{4.33}$$

or,

$$\frac{\dot{m}_{12}}{\dot{m}_{42}} = f\left(\frac{1}{\sqrt{Ri_{o,d}}}\right) = 0.64 \left(\frac{N}{1-N}\right)^{-\frac{3}{2}} \tag{4.34}$$

4.5 Vent Flow Mixing in Zone Models

The shearing that occurs along the density interface in vent flows results in entrainment of mass into both the hot upper layer and the cool lower layer. Figure 4.6 shows the notation that will be used to describe the mass transfer between zones in the following section.

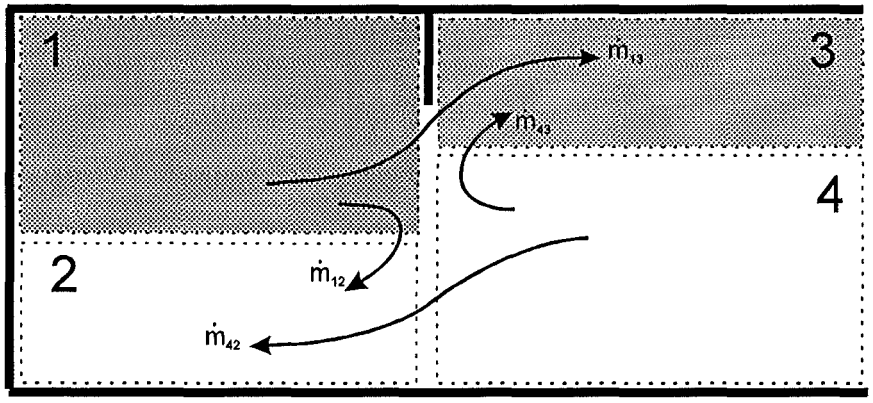

Figure 4.6 ***Schematic defining the mass flow notation and the compartment zones.***

Presently there is insufficient knowledge concerning shear mixing in fire induced vent flows to model the phenomena with any established theory or empirical correlations. Zone models therefore approximate the situation. This section documents and discusses how a number of different zone models approximate the vent flow mixing problem.

4.5.1 The HARVARD Zone Model

The HARVARD zone model was originally developed by Professor Howard Emmons and Dr Henri Mitler at Harvard University; see Mitler, (1978), and Mitler & Emmons, (1981). In 1983, with the retirement of Prof. Emmons, the HARVARD model was handed over to the National Bureau of Standards for further development. At no stage has the HARVARD zone model officially incorporated any vent flow mixing in the modelling routines. An enhanced version of the HARVARD Mark V model, (see

Rockett, 1982) did at one stage incorporate a mixing algorithm, however this was never officially incorporated into the NBS/HARVARD or HARVARD/NIST zone model, (see Mitler, (1985), Rockett and Morita, (1986), Rockett *et. al.*, (1987), and Rockett, (1990)).

Rockett (1982), enhanced the HARVARD Mark V version to unofficially incorporate a vent flow mixing algorithm. The mixing algorithm only considered the entrainment of hot gases from the upper layer into the lower door jet. Two possible vent flow mixing formulas were investigated for implementation in the model. One of the formula was proposed by Zukoski and Kubota, (1980); the other was proposed by Quintiere *et. al.* (1981). A comparison was made of the enhanced model predictions with data collected from seven full scale mattress fires. The fires were all conducted in a compartment with a single open doorway as the only vent. Comparison of the model predictions with the experimental mattress fire data, revealed that Zukoski's formula appeared to underestimate the amount of mixing that occurred while Quintiere's formula seemed to give satisfactory results.

4.5.2 The CCFM Zone Model

The CCFM, (Consolidated Compartment Fire Model), was first developed by the National Institute of Standards and Technology, (NIST), as a prototype called CCFM.VENTS, refer Forney *et. al.*, (1990). The model was a consolidation of the past progress that had made in zone-type compartment fire models at the time of its development.

The zone model package CCFM.VENTS did account for the exchange of mass between the upper and lower layers in vent flow, however, the derivation of the mass exchange algorithm was not based upon the vent flow mixing phenomenon. The mass flux in each gas stream in the doorway was distributed between the upper and lower layer of the receiving compartment. The rule for apportioning the fractions of each gas stream into either the upper or lower layer was based upon an idea proposed in Mitler, (1984). Mitler was working on a forced ventilation algorithm for use in the

HARVARD zone model and proposed a means of distributing material that was pumped into a stratified compartment atmosphere between the upper and lower layers.

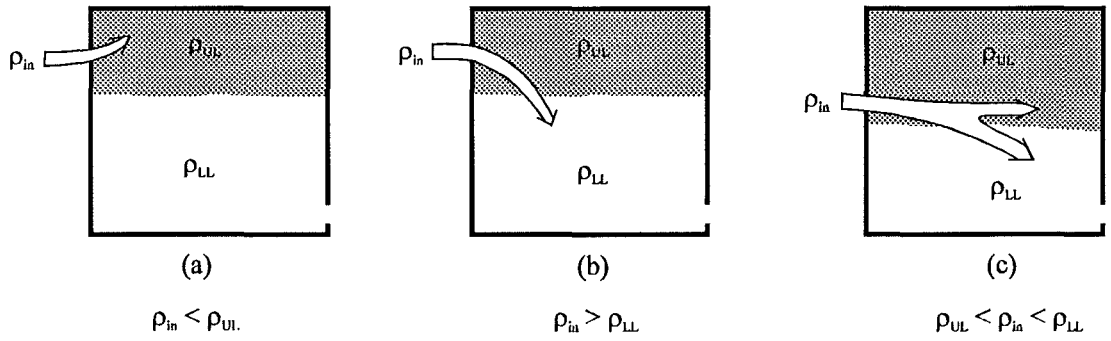

Figure 4.7 [†] ***Flow apportioned according to relative densities***

Mitler proposed that the inflowing material was distributed between the two layers in the receiving room based upon the relative densities of the gases in the door jet and the gases in each layer. If the gases in the door jet were less dense than the gases in the upper layer of the receiving room, then all the material in the door jet would be deposited into the upper layer. If the gases in the door jet were heavier than the gases in the lower layer, then all the material in the door jet would be deposited into the lower layer. In cases where the gases in the door jet were of a density intermediate to the densities of the gases in the two layers, then Mitler proposed that the material in the door jet would be apportioned between the layers as follows:

$$\dot{m}_{UL} = \dot{m}_{in}\left(\frac{\rho_{LL} - \rho_{in}}{\rho_{LL} - \rho_{UL}}\right) = \dot{m}_{in}\left(\frac{T_{in} - T_{LL}}{T_{UL} - T_{LL}}\right)\left(\frac{T_{UL}}{T_{in}}\right) \tag{4.35}$$

$$\dot{m}_{LL} = \dot{m}_{in}\left(\frac{\rho_{in} - \rho_{UL}}{\rho_{LL} - \rho_{UL}}\right) = \dot{m}_{in}\left(\frac{T_{UL} - T_{in}}{T_{UL} - T_{LL}}\right)\left(\frac{T_{LL}}{T_{in}}\right) \tag{4.36}$$

The CCFM.VENTS zone model apportions the mass flux in a doorway gas stream according to the temperature differences as given by the following relationships:

[†] Figure copied from Mitler (1984)

$$\dot{m}_{UL} = \dot{m}_{in}\left(\frac{T_{in} - T_{LL}}{T_{UL} - T_{LL}}\right) \tag{4.37}$$

$$\dot{m}_{LL} = \dot{m}_{in}\left(\frac{T_{UL} - T_{in}}{T_{UL} - T_{LL}}\right) \tag{4.38}$$

4.5.3 The CFAST Zone Model

The CFAST zone model is a combination of the FAST and the CCFM.VENTS zone models. It is a multicompartment zone model that has been developed by the National Bureau of Standards since approximately 1984, refer Jones (1984), Jones and Peacock (1989) and Cooper and Forney (1990).

CFAST postulates that the entrainment associated with vent flow mixing, (in either layer), can be approximated with a normal plume correlation. The basis for this assumption is the observation that the door jet of hot gases leaving a compartment is comparable to the far field of a normal fire plume. With respect to entrainment in the lower layer, the assumption is defended on the basis that lower door jet behaves like an inverted plume plunging over the sill of the vent and through the hot gases of the upper layer, refer Figure 4.5 and Section 4.4. Based on this assumption, CFAST uses the mass flux correlations of McCaffrey (1983) to approximate the entrainment associated with mixing in vent flows.

$$\frac{\dot{m}}{\dot{Q}_{eq}} = 0.011\left(\frac{Z_{TP}}{\dot{Q}_{eq}^{\frac{2}{5}}}\right)^{0.566} \quad \text{if} \quad 0.00 < \frac{Z_{TP}}{\dot{Q}_{eq}^{\frac{2}{5}}} \leq 0.08 \tag{4.39}$$

$$\frac{\dot{m}}{\dot{Q}_{eq}} = 0.011\left(\frac{Z_{TP}}{\dot{Q}_{eq}^{\frac{2}{5}}}\right)^{0.566} \quad \text{if} \quad 0.08 < \frac{Z_{TP}}{\dot{Q}_{eq}^{\frac{2}{5}}} \leq 0.20 \tag{4.40}$$

$$\frac{\dot{m}}{\dot{Q}_{eq}} = 0.011\left(\frac{Z_{TP}}{\dot{Q}_{eq}^{\frac{2}{5}}}\right)^{0.566} \quad \text{if} \quad 0.20 < \frac{Z_{TP}}{\dot{Q}_{eq}^{\frac{2}{5}}} \tag{4.41}$$

In the vent flow mixing algorithm, the plume correlations are applied with an entrainment length that incorporates a virtual source length extension. The virtual source is a distance Z_{vs} back from the door such that the mass flux in the plume, m_p, (induced by an equivalent heat release rate), matches the actual mass flux, m_{13}, exiting the room at the doorway, (see Figure 4.8). The total length of entrainment for the plume is

$$Z_{TP} = Z_{vs} + Z_{13} \tag{4.42}$$

where

Z_{13} is the difference in elevation between the upper layers, ($Z_{13} = Z_{D3}$-Z_{D1}).

The matching of the mass flux at the doorway means that the entrainment due to vent flow mixing effectively occurs over the distance Z_{13}.

The virtual source length extension, Z_{vs}, is calculated from a rearrangement of McCaffrey's correlations; Equations (4.44), (4.45) and (4.46). The equivalent heat release rate, Q_{eq}, is the convective heat loss from the compartment through the vent.

$$\dot{Q}_{eq} = \dot{m}_{13} C_p (T_1 - T_4) \tag{4.43}$$

A discussion of the virtual source theory is given by Cetegen *et al.* (1984).

$$\frac{Z_{vs}}{\dot{Q}_{eq}^{\frac{2}{5}}} = \left(\frac{90.9\,\dot{m}_{13}}{\dot{Q}_{eq}}\right)^{1.76} \quad \text{if} \quad 0.00 < \frac{Z_{vs}}{\dot{Q}_{eq}^{\frac{2}{5}}} \leq 0.08 \tag{4.44}$$

$$\frac{Z_{vs}}{\dot{Q}_{eq}^{\frac{2}{5}}} = \left(\frac{38.5\,\dot{m}_{13}}{\dot{Q}_{eq}}\right)^{1.001} \quad \text{if} \quad 0.08 < \frac{Z_{vs}}{\dot{Q}_{eq}^{\frac{2}{5}}} \leq 0.20 \tag{4.45}$$

$$\frac{Z_{vs}}{\dot{Q}_{eq}^{\frac{2}{5}}} = \left(\frac{8.10\,\dot{m}_{13}}{\dot{Q}_{eq}}\right)^{0.528} \quad \text{if} \quad 0.20 < \frac{Z_{vs}}{\dot{Q}_{eq}^{\frac{2}{5}}} \tag{4.46}$$

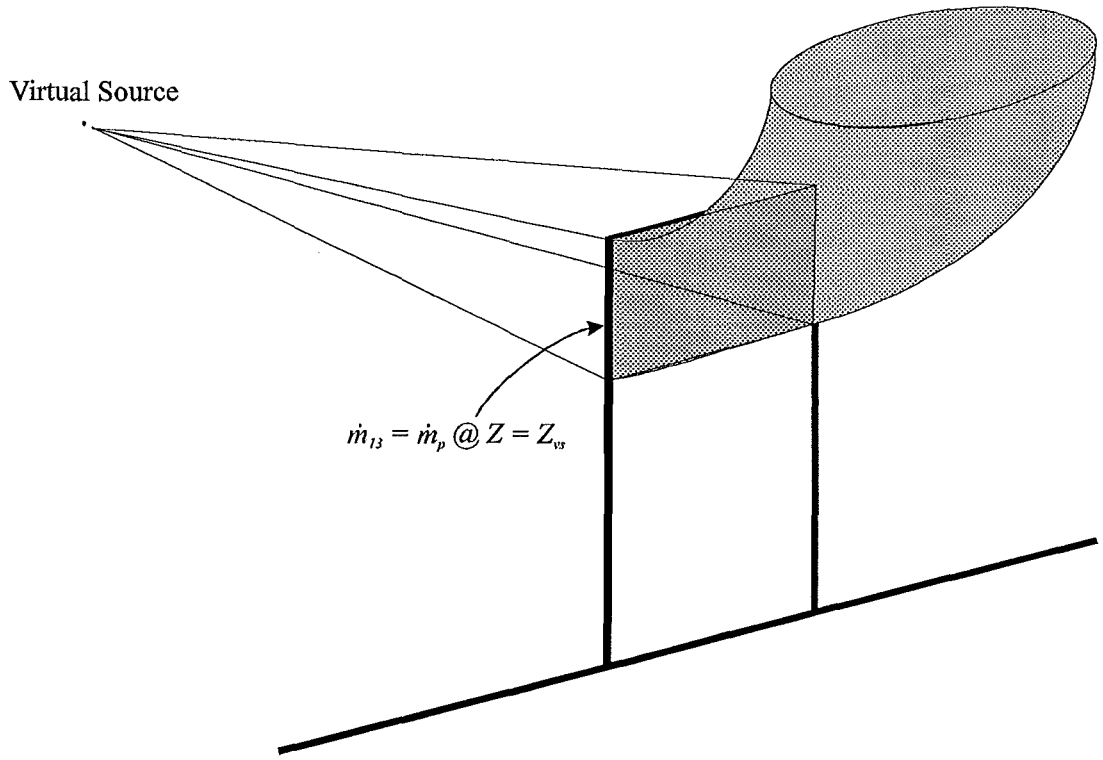

Figure 4.8 ***Schematic diagram showing the virtual source concept for the upper door jet***

Zukoski and Kubota, (1980), proposed a formula for calculating the mass entrained into the upper door jet. The form of Zukoski's relation is very similar to that of an axisymmetric buoyant plume and may be rearranged into a form similar to that of McCaffrey's for a comparison with the CFAST assumption.

By substituting Equation (4.6) into Equation (4.5), and using the equivalent heat release rate described by Equation (4.43), Zukoski's correlation can be re-written as

$$\frac{\dot{m}_p}{\dot{Q}_{eq}} = (C_J)\left(\frac{\rho_\infty^2 g}{C_p T_\infty}\right)^{\frac{1}{3}} \cdot \left(\frac{Z_p}{\dot{Q}_{eq}^{\frac{2}{5}}}\right)^{\frac{5}{3}} \tag{4.47}$$

where

$C_J = 0.30$ for the separated door jet, and
$C_J = 0.18$ for the attached door jet.

The following values for ambient conditions can be used to complete the necessary transformation of Zukoski's correlation

$$\begin{aligned} T_\infty &= 293\ K \\ \rho_\infty &= 1.20\ kg/m^3 \\ C_p &= 1.05 \\ g &= 9.81\ m/s^2 \end{aligned}$$

such that,

For the attached flow case;

$$\frac{\dot{m}_{43}}{Q_{eq}} = 0.065 \cdot \left(\frac{(Z_{D3} - Z_N)}{Q_{eq}^{\frac{2}{5}}}\right)^{1.667} \tag{4.48}$$

and, for the separated flow case;

$$\frac{\dot{m}_{43}}{Q_{eq}} = 0.108 \cdot \left(\frac{(Z_{D3} - Z_N)}{Q_{eq}^{\frac{2}{5}}}\right)^{1.667} \tag{4.49}$$

A direct comparison of McCaffrey's correlations with Zukoski's relationship is not possible due to the different length variables used in the equations. McCaffrey's

correlations apply to all three regions of the fire plume; continuous flaming, intermittent flaming and the plume. The correlations use the height above the burner, or virtual source, as the entrainment length. Zukoski's correlation, uses the distance between the neutral plane and the zone interface, (Z_{D3} - Z_N), as the entrainment length, (this is equivalent to the height above the interface separating the flaming region and the fire plume).

Verification of the CFAST Model

A possible means of assessing the accuracy of an assumption is to compare the model predictions with full scale experimental data. This has been done for the CFAST zone model with data collected in five separate full-scale fire tests.. The results from the model and the data collected from the full scale fire tests are presented in the CFAST manual, refer Peacock *et al.* (1993).

A comparison of the mass flux through a vent has been presented for two of the five fire tests. The two comparisons were a single room in which individual furniture items were burnt, and a three room configuration, incorporating a corridor, in which a gas burner was used. The comparisons show that CFAST typically underestimates the mass flow through a vent. A comparison of the zone temperatures revealed that the model slightly over predicted the upper layer temperature and somewhat under predicted the lower layer temperature. One possible contributing factor to this error is the incorrect modelling of the exchange of mass between zones. Entrained mass carries with it enthalpy that will alter the average temperature of the layer. Vent flow mixing will cause the lower layer to rise in temperature and the upper layer to cool slightly.

4.5.4 The BRI Zone Model

The BRI zone model was developed by the Building Research Institute of Japan to model fire spread in small, residential scale buildings, see Tanaka, (1983). The BRI zone model uses the same method and form of equations for estimating the mass

transfer in vent flows as the CFAST zone model uses, (a re-arrangement of McCaffrey's plume correlations), however, the BRI model uses a different entrainment length, Z_{TP}.

$$Z_{TP} = Z_{D1} - \frac{\left[\min\left(Z_{Soffit}, Z_{D1}\right) + \max\left(Z_N, Z_{Sill}, Z_{D3}\right)\right]}{2 + Z_{vs}} \tag{4.50}$$

No explanation is given for the form of this relationship or how it has been obtained.

4.6 Conclusion

It is apparent from the presentation above that there is no established method for quantifying the mass exchange that occurs in vent flow mixing. A relationship of the same form as a plume correlation seems to be the favourable means adopted by zone model packages for estimating the mass transfer; the accuracy of this assumption has not been verified. Zukoski and Kubota, (1980), proposed that this form of relationship, (a plume correlation), could be used to estimate the entrainment into the upper door jet and into the lower door jet. The applicability of their relationship to the lower door jet entrainment, however, is dependent upon the presence of a sill in the vent. For doorways this is obviously not the case and the suitability of this form of relationship for estimating the entrainment into the lower layer door jet should be questioned.

Chapter 5
SALT WATER MODELLING

Steckler *et al.* (1986), presented the governing theory for salt water modelling of fire induced gas flows. Their paper presents the scaling laws relating salt water flows to heated gas flows and discusses some of the elements and limitations of the modelling technique. This section re-presents some of this work and discusses how it can be used to model fire induced doorway flows.

5.1 Salt Water Modelling Analogy

In a quiescent environment, the movement of smoke and hot gases generated by a fire is driven by the buoyancy force. The force arises as a result of a density difference between the hot gases heated in the combustion zone and the cooler gas of the ambient environment. Salt water modelling utilises the density difference between a saline solution and freshwater to simulate the density difference between the hot gases and the ambient atmosphere. Consequently, the movement of hot smoke in a cool environment can be modelled by studying the movement of salt water in a freshwater environment.

In salt water modelling, the salt water is used to represent the hot smoke while the freshwater is used to represent the cooler ambient gas. This analogy may at first seem backwards in the sense that salt water is denser than freshwater. This technicality is overcome in the modelling process by inverting the geometrical layout of the fire situation. If we orientate ourself with the model, the gravity vector is now acting in the direction from the floor toward the ceiling of the model. Therefore, when a heavier fluid is injected into the model through its floor, it is driven by gravity toward the ceiling. This is exactly the same driving force that acts on hot gases generated in a combustion zone. Gravity drives them from the floor toward the ceiling.

In salt water modelling the mass of salt in the saline solution can be considered analogous to the heat energy in the gases heated by the fire. Just as the heat energy, and consequently the temperature of the gas is responsible for the density difference in the fire situation, the mass of salt, (NaCl), in saline solution is responsible for the density difference in the hydraulic analog. A high concentration of salt in the saline solution can therefore be thought of as a high gas temperature in the fire situation.

5.2 Governing Theory

Tangren, (1978), used salt water modelling to investigate the convective flows associated with room fires. The relationship between the fire situation and the results of salt water modelling experiments was based upon a dimensionless buoyancy flux parameter, q_H^*. The parameter, used to relate the heat input rate and the mass flow rate of the salt, was based upon Zukoski's dimensionless parameter Q^* used in his fire plume work, refer Zukoski *et al.*, (1980 a).

$$q_H^* = \frac{Q}{\rho_\infty \sqrt{gH}\, c_p T_\infty H^2} = \frac{\Delta\rho_o \dot{V}_o}{\rho_\infty \sqrt{gH}\, H^2}$$

Tangren attempted to match the Reynolds number and the Richardson number for the fire and salt water situations; this was assumed to account for viscous effects and the influence of buoyancy relative to inertia.

The salt water modelling theory presented in Steckler *et. al.* ,(1986), is based upon the mathematical work of Howard Baum and Ronald Rehm. Rehm and Baum (1978), derived a set of approximate equations which are applicable to nonadiabatic, nondisspersive, buoyant flows of a perfect gas. The equations of motion describe the large temperature and density variations induced by a volumetric heat addition. Rehm and Baum demonstrated that if the heat addition is sufficiently weak relative to the size of the enclosure, the approximate equations of motion can be reduced to the Boussinesq equations.

Baum and Rehm (1984), went on to extend their earlier work, (Rehm and Baum, (1978), and Baum *et al.*, (1982)), from two dimensions to three dimensions. The authors used a dimensionless formulation, based upon the characteristics of the volumetric heat source, to derive a non-dimensional version of the Boussinesq equations that describe the large scale buoyant convective motion of an invisid thermally nonconducting gas within an enclosure. The source of heat used to represent the fire, is assumed to be sufficiently weak for the Boussinesq approximation to apply outside the combustion zone.

Since the driving phenomena in both the hydraulic analog and the fire situation are the same, (buoyancy), they can be related through the non-dimensional Boussinesq equations when viscous effects and heat transfer effects are small.

Given that the governing equations of motion for both the hydraulic analog and the fire situation are identical, the two situations can be related if the nondimensional variables in both cases have the same value. Therefore, the non-dimensional variables used in the governing equations have been defined in terms of both the fire situation variables and the salt water model variables. A salt water model experiment can be used to calculate the values of the non-dimensional variables for a particular situation; the non-dimensional variables can then be solved, in terms of fire variables, to predict the behaviour of gases in the equivalent fire situation.

The non-dimensional governing equations, taken from Steckler *et. al.* (1986), are displayed below. Equations (5.1)-(5.3) represent the conservation of mass, momentum and energy, respectively.

$$\nabla^* \cdot \bar{u}^* = 0 \tag{5.1}$$

$$\frac{d\bar{u}^*}{dt^*} + \nabla^* \tilde{p}^* - \theta^* \bar{k} = \left(\frac{1}{\mathrm{Re}\, P}\right) \nabla^{*2} \bar{u}^{*2} \tag{5.2}$$

$$\frac{d\theta^*}{dt^*} = GQ^* + \left(\frac{1}{\mathrm{Re}P}\right)\nabla^{*2}\theta^* \tag{5.3}$$

The non-dimensional variables used in Equations (5.1)-(5.3), (variables with a * superscript), have been expressed as a function of a length scale H, (the enclosure height); a length scale L, (the spatial extent of the source); a velocity scale U, and a density (or temperature) perturbation scale ζ.

The variables used in the governing equations are defined below; refer to Figure 5.1.

Hot Gas **Salt Water**

$$H\nabla = \nabla^* = h\nabla \tag{5.4}$$

Non-Dimensional Position

$$\frac{\overline{x_g}}{H} = \overline{x^*} = \frac{\overline{x_s}}{h} \tag{5.5}$$

Non-Dimensional Time

$$\frac{t_g U_g}{H} = t^* = \frac{t_s U_s}{h} \tag{5.6}$$

Non-Dimensional Velocity

$$\frac{\bar{u}}{U_g} = \overline{u^*} = \frac{\bar{u}}{U_s} \tag{5.7}$$

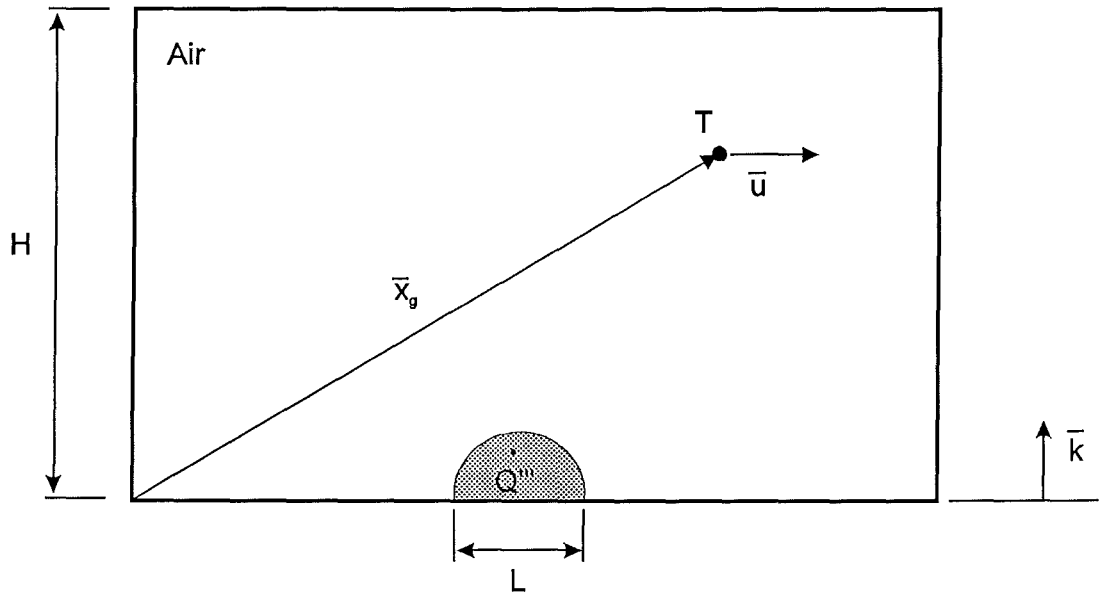

(a) *FIRE*

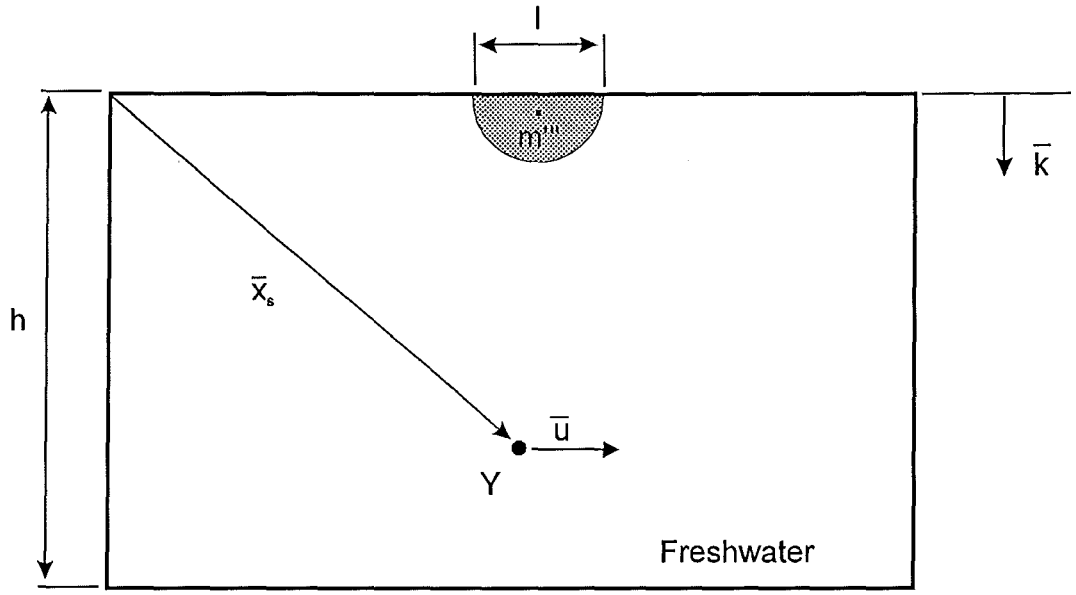

(b) *SALT WATER MODELING*

Figure 5.1[†] *Schematic of the variables used in salt water modelling calculations.*

[†] Figure taken from Steckler *et. al.*, (1986)

Non-Dimensional Pressure Perturbation

$$\frac{\tilde{p}}{\rho_0 U_g^2} = \tilde{p}^* = \frac{\tilde{p}}{\rho_0 U_s^2} \tag{5.8}$$

Non-Dimensional Temperature

$$\frac{(T - T_0)}{T_0 \zeta} = \theta^* = \frac{Y}{\zeta} \tag{5.9}$$

Non-Dimensional Heat Input

$$\frac{Q'''}{\left(\frac{\dot{Q}_o}{L^3}\right)} = 1 = Q^* = 1 = \frac{\dot{m}'''}{\left(\frac{\dot{m}_0}{l^3}\right)} \tag{5.10}$$

Velocity Scale

$$\left(\frac{\dot{Q}_0 g}{\rho_0 c_p T_0 H}\right)^{\frac{1}{3}} = U = \left(\frac{\dot{m}_0 g}{\rho_0 h}\right)^{\frac{1}{3}} \tag{5.11}$$

Density (or Temperature) Perturbation Scale

$$\frac{U_g^2}{g H} = \zeta = \frac{U_s^2}{g h} \tag{5.12}$$

Since the non-dimensional form of the governing equations for both the fire and salt water modelling situations are identical, their solutions in terms of non dimensional variables are identical when the value of following variables are preserved in both situations.

Viscous and Heat Conduction Effects

$$\frac{\mu c_p}{k} = \mathrm{Pr} = \mathsf{P} = Sc = \frac{\mu}{\rho_0 D} \tag{5.13}$$

Reynolds Number Matching

$$\frac{\rho_0 U_g H}{\mu} = \mathrm{Re} = \frac{\rho_0 U_s h}{\mu} \tag{5.14}$$

Compartment Size Scaling

$$\left(\frac{H}{L}\right)^3 = G = \left(\frac{h}{l}\right)^3 \tag{5.15}$$

5.3 Limitations of Salt Water Modelling

5.3.1 Boussinesq Approximation

In the derivation of the non-dimensional governing equations by Baum and Rehm, (1984), the following assumptions have been made.

1. The length scale, time scale and the temperature scale associated with the volumetric heat source are such that the heat addition is slow. This assumption implies that the pressure over a large region surrounding the source is almost uniform in space (while it may vary in time) during heating. However, it does not imply any restriction upon the magnitude of the density (or temperature) variation during heating.

2. The flow velocities are induced by buoyancy effects. This assumption relates the magnitude of the temperature variation, the density variation and the flow velocities induced by the heat source.

3. The vertical height associated with the static density variation is much larger then the vertical length scale of interest. This assumption implies that the static density variation from its mean value is small.

4. The density variations produced by the heat source are small.

5.3.2 Heat Transfer Deficiency

In any real enclosure fire, there are heat losses to the enclosures bounding surfaces. These heat losses result in a thermal boundary layer adjacent to the walls and ceiling in which the temperature of the gases is lower than the temperature of the general ceiling layer. Salt water modeling cannot simulate this phenomenon as it would involve the mass transfer of salt into the model surfaces.

5.3.3 Initial Plume Momentum

The buoyant plume generated by a fire originates with no initial momentum; the flow is driven solely by a density difference due to the elevated temperature of the gases in the combustion zone. In salt water modelling, the heat release rate of a fire is simulated with the mass flux of salt leaving the source. To have a mass flux, the saline solution must be injected with some initial momentum. The magnitude of the initial momentum can be reduced by introducing the saline solution at a low velocity, however, this may jeopardise the critical requirement of producing a turbulent plume. Steckler *et al.*, (1986), proposed a compromise; consider the ratio F of the initial momentum flux to the buoyancy flux at some distance z above the source.

$$F = \frac{\rho U_0^2}{2(\rho - \rho_0) g z} \tag{5.16}$$

At some distance z = z' above the source, the initial momentum effects becomes small and the buoyancy force dominates (F < 1). Above the height z = z' the plume can be assumed to be purely buoyancy driven.

5.3.4 Exact Reynolds Number Matching

It is not always possible to exactly match the Reynolds number in the salt water modelling of a turbulent fire plume. A turbulent fire plume has a Reynolds number of the order of 10^5. In salt water modeling, the reduced length scale and the problem of initial momentum, (as discussed above), means that a Reynolds number this large is not always possible to achieve. However, turbulent plumes do exist with a Reynolds number as low as 10^4. At a Reynolds number of this order, the molecular transport terms in the governing equations are assumed to become negligible in relation to the other terms, and the inconsistencies between the Prandtl number for air and the Schmidt number for salt water in freshwater, become unimportant.

5.3.5 Salt Water Source Geometry

In Baum and Rehm's derivation of the governing equations of motion, the combustion zone is replaced by a volumetric heat source that has a prescribed rate of heat and mass release. Fire can be considered as a volumetric heat source, its volumetric extent, however, is constantly changing and is extremely difficult to define. The derivation of the governing equations assumes that the spatial extent of the fire source can be characterised by the spatial dimension L. In salt water modelling it would be impossible to release the salt mass in a precisely scaled volume corresponding to the real fires volumetric extent. Therefore, the salt water source geometry characteristic dimension, l, is assumed to be the diameter of the planer source.

5.3.6 Plume Mass Flux

The mass flux entering the hot ceiling layer in a fire plume is large when compared to the initial mass flux issuing from the combustion zone. Therefore, in salt water modeling, care must be taken to ensure that the same relative size of mass flux ratio is conserved.

5.4 Correct Modelling of the Volumetric Flux

The entrainment rate of a fluid is dependent on the velocity scale of the fluid. Therefore, when salt water models are being used to investigate entrainment characteristics, it is imperative that the volumetric flux, and consequently the velocities, are scaled correctly.

Consider a small steady state fire in a compartment with a single doorway as a vent. The atmosphere in the compartment will be sharply stratified and can be approximated by two homogeneous gaseous layers. The cool air entering the compartment is entrained into the fire plume, heated, and then driven by a buoyancy force into the hot upper layer. The buoyancy force arises because the cooler air expands and becomes less dense as it is heated in the fire plume.

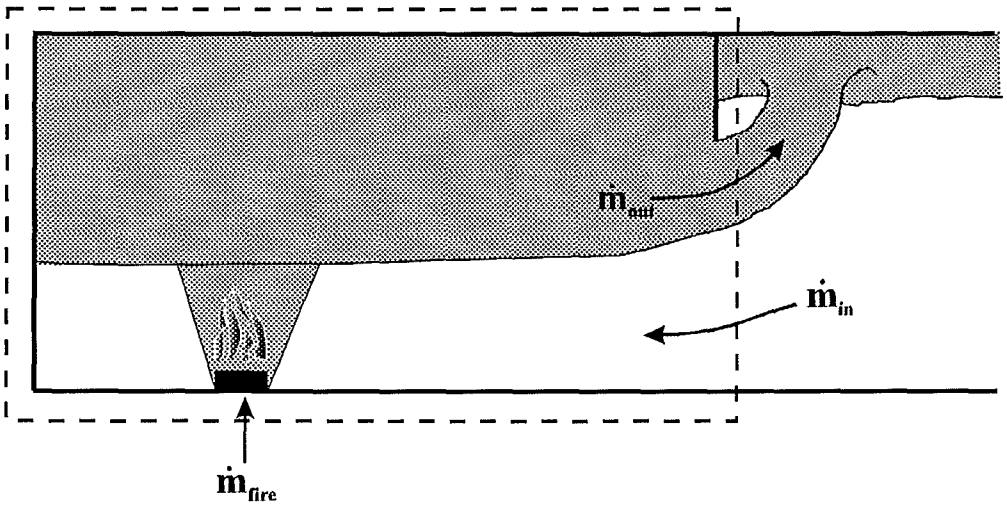

Figure 5.2 ***Schematic showing the mass flux notation for a simple compartment fire situation.***

Consider the compartment as a control volume, and look at the mass flux across its boundaries. Since mass is neither accumulated or destroyed in the compartment at steady state,

$$\dot{m}_{out} = \dot{m}_{in} + \dot{m}_{fire} \tag{5.17}$$

Generally the mass flux generated by a fire source is small enough compared to the mass flux entrained into the plume that it can be neglected. Therefore,

$$\dot{m}_{in} \approx \dot{m}_{out} \tag{5.18}$$

which can be rewritten as

$$\rho_{LL}\dot{V}_{in} \approx \rho_{UL}\dot{V}_{out} \tag{5.19}$$

or, using the Ideal Gas law, this can be rewritten as

$$\dot{V}_{out} = \dot{V}_{in}\left(\frac{T_{UL}}{T_{LL}}\right) \tag{5.20}$$

To properly model fire induced gaseous flows through a doorway with a salt water/freshwater analog, this volumetric relationship needs to be maintained. Consider now a salt water model of the same situation.

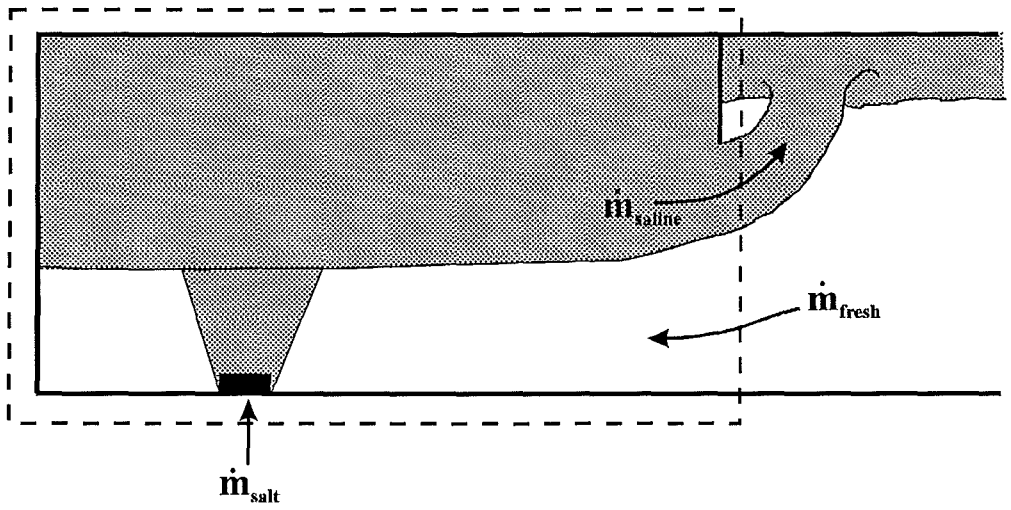

Figure 5.3 ***Schematic showing the mass flux notation for the salt water modelling situation.***

$$\dot{m}_{saline} = \dot{m}_{fresh} + \dot{m}_{salt} \tag{5.21}$$

In salt water modelling situations where the length of entrainment for the plume is small, the volume flux of the of the buoyancy source cannot be neglected as it was in the fire situation. That is, when the volumetric flow rate of fresh water entrained into the salt water plume, is of the same order as the initial volumetric flow rate of salt water injected at the source, $\dot{V}_{salt}$, must be considered.

Because there is no heating involved in salt water modelling there is no volumetric expansion and therefore,

$$\dot{V}_{saline} = \dot{V}_{fresh} + \dot{V}_{salt} \tag{5.22}$$

From the fire situation, we know that

$$\frac{\dot{V}_{out}}{\dot{V}_{in}} = \left(\frac{\rho_{LL}}{\rho_{UL}}\right) \tag{5.23}$$

To satisfy the relationship presented in Equation (5.23) for the fire situation, the salt water injected into the model at the plume source, must be added at a volumetric flow rate such that,

$$\frac{\dot{V}_{fresh} + \dot{V}_{salt}}{\dot{V}_{fresh}} = \left(\frac{\rho_{LL}}{\rho_{UL}}\right)_{fire} \tag{5.24}$$

or alternatively, this can be rewritten as

$$\frac{\dot{V}_{salt}}{\dot{V}_{fresh}} = \left(\frac{\rho_{salt}}{\rho_{fresh}}\right) - 1 \tag{5.25}$$

This relationship is not simple to satisfy. The volumetric flow rate of the freshwater entering the compartment, $\dot{V}_{fresh}$, is the entrainment rate of the salt water plume. The entrainment into the plume is dependent upon the initial buoyancy flux at the source

as well as the height to the interface between the layers. The interface height is a function of the buoyancy source and the volumetric flow rates of fluid entering and exiting the compartment through the doorway. The conditions required to satisfy Equation (5.25) with a salt water plume in a compartment, are extremely difficult to predict and to achieve while providing consideration to the salt water modelling aspects presented earlier in Section 5.3.

5.5 Conclusion

Salt water modelling is a useful technique for simulating fire induced gas flows. As with all models there are limitations to the simulation accuracy. Salt water modelling involves making compromises between the accuracy with which certain phenomenon are replicated. Consider the Reynolds number of the fire plume. Ideally, a Reynolds number of the order of 10^5 is desired, however, due to the lack of initial momentum in a fire plume, a Reynolds number of this order is difficult to achieve in a salt water model and compromises need to be made.

If salt water modelling is being used to model a certain phenomenon associated with fire induced gas flow, it is important that the processes crucial to the phenomena are simulated as accurately as possible. Consider the mixing that occurs in doorway flows, the velocities of the gas streams, and consequently the shear across the density interface, is the driving force behind the mixing. To simulate the velocities correctly, the volumetric flow rate of each gas stream through the doorway must be scaled correctly in the salt water model, refer Section 5.4. This may require making compromises on the accuracy with which the fire plume and other fire phenomenon are simulated in the downstream burn room.

Chapter 6
CONCLUSIONS & FUTURE RESEARCH

6.1 Conclusion

Currently, very little is known about the mixing that occurs in fire induced doorway flows. This review has shown that the mass exchange associated with the mixing in doorway flows is highly dependent on the geometry of the connected compartments relative to the doorway. Zone models presently lack the ability to account for this geometrical dependence. The exchange of mass between the two gas streams in a doorway is dependent on the flow structures that exist. The lower layer door jet is therefore simpler to consider than the upper door jet, as the flow structures within it do not change with time.

Reviewing our present understanding of the mixing that occurs in fire induced doorway flows has highlighted certain topics about which very little is known. The next section pin-points a number of these areas that require further research.

6.2 Areas Requiring Research

The most obvious point to come out of this investigation is that the mixing that occurs in doorway flows, or that is associated with doorway flows, is highly dependent upon the geometrical layout of the doorway and connected compartments. The flow structures that develop in a doorway flow will be strongly dependent on the doorway and compartment geometry. Different flow structures will contribute varying amounts toward the mixing that occurs in different geometrical layouts. Consider, on a residential scale, a burn room venting through a single doorway into a relatively thin corridor that is orientated in-line with the direction of flow through the vent. As described in Section 4.3, a density jump forms on the ceiling, which is latter drowned out by a reflected ceiling jet wave. The majority of the entrainment into the hot smoke door jet is assumed to occur, in a plume like manner, over a length equal to the

difference in elevation between the neutral layer height and the effective interface in the corridor. Now consider the burn room venting into a corridor of the same size that is orientated perpendicular to the direction of the vent flow. If we neglect the possible channelling effect of a partially open doorway, the flow will impinge upon the opposite wall of the corridor and be forced to split into two separate streams. If the corridor is thin, the jump structure on the ceiling and the area where the gas stream impinges on the opposite wall will cause a great deal of turbulent mixing. The entrainment that occurs, in a plume like manner, may in this second case, be negligible when compared to the entrainment that occurs in the impingement region. Further experimental research is needed on the different flow structures that will develop in different geometrical layouts. Quantifying the contribution of each flow structure is perhaps a long term goal, in the short term, there is a definite need for experimental observations that focus on the mixing that occurs in the flow associated with doorways.

Zukoski and Kubota, (1980) observed that the upper door jet of hot smoky gases would not always separate from the soffit of the doorway. In fact, the door jet would initially remain attached to the door soffit and then separate from it as the depth of the layer interface in the burn room deepened with respect to the height of the neutral plane in the doorway. The vent flow mass flux equations used in zone models, (see Rockett, 1976), assume that the door jet is separated and that the pressure at the vena contracta of the door jet is equal to the atmospheric pressure. Obviously, if the door jet does not always separate from the soffit, then this assumption is incorrect. The impact of the inaccuracy in this assumption is unknown. The CFAST verification section, (Peacock *et. al*, 1993), and Quintiere and DenBraven's, (1978), comparison of the measured vent flow with the vent flow predicted by zone model theory shows that the mass flux through a vent is generally underestimated by zone model theory. Further research is required into assessing the accuracy of the vent flow theory with particular focus on the impact of the attached flow case. In the separated flow case, if the air above the nappe of the separated door jet is trapped and being entrained into the door flow, then the pressure in this region may be reduced, this could explain the underestimation of the mass flux through a vent or the reattachment of the door

plume to the soffit or wall at a higher elevation. Further investigation is required in this area. Zukoski and Kubota, (1980), stated that the exact point of transition between the separated and attached flow cases is unknown, further research is also required to quantify this point.

Zone models approximate the mixing that occurs in vent flows. The same mixing algorithm is used for all vents to calculate the mass exchange between zones. No differentiation is made between the mixing that occurs in a doorway and the mixing that occurs in a vent with a sill. The movement of gases from one compartment to another within a building on one level, generally occurs through an internal doorway. Research is needed into the effect that a sill has on the mixing that occurs in vent flows.

Lim, (1984), observed that a decrease in the temperature of the upper layer did not alter the temperature of the lower layer significantly. He observed similar behaviour in the carbon dioxide concentration profiles. Lim proposed that the increase in the mixing, due to the decrease in buoyancy energy in the upper layer, was just sufficient to maintain the properties of the lower layer. This theory requires further research to see if there is some form of equilibrium state for the lower layer that is resistant to change.

Lim also proposed a form of equation for modelling the entrainment of upper layer mass into the lower layer. He determined a mean value of 11.7 $\pm$ 5.3 for the empirical constant A in his model equation. Lim's experimental investigation used a pump and furnace to simulate the action of the fire plume; a series of full scale fire tests are required to gather data for comparison with his model and to confirm the value of the empirical constant.

As an aside to the present topic, the author has noted that experimental fire research data is often compared with zone model theory. There does not, however, seem to be any universally accepted means for reducing the experimental data to define zone properties such as temperature, interface elevation, etc. It would seem that for

consistency and for comparison of different researchers work, a specific method needs to be developed, accepted and defined for this purpose.

6.3 Useful Techniques for Researching Mixing in Doorway Flows

6.3.1 Species Concentration Profiles

The two most common and probably cheapest variables that are recorded in compartment fire experiments when considering vent flows are the temperature and gas velocities. With respect to the mixing that occurs in vent flows, the temperature profiles are better replaced with species concentration profiles. As Lim (1984) noted, mass exchange and heat exchange do not occur by the same mechanisms. The temperature of a layer is influenced by heat transfer through conduction, convection and radiation from other surfaces; the contribution of each of these mechanisms is difficult to accurately quantify. Species concentration profiles better reflect the mass transfer and therefore the mixing that is occurring.

The equipment required to collect and analysis gas samples for species concentrations is expensive. It is therefore unlikely that resources will allow a researcher the luxury of having multiple sampling points such as can be achieved with a thermocouple tree. If temperature profiles are to be used in the analysis of the mixing that occurs in vent flows, the data should be collected using aspirating thermocouples. These thermocouples more accurately reflect the temperature of the gas atmosphere by eliminating the influence of radiation.

6.3.2 Salt Water Modelling

Fire induced gas flows can be modelled using a salt water-freshwater analog. The flow of hot gases generated by a fire is driven by a density difference between the hot gas and the ambient environment. Salt water modeling utilises the density difference

between a saline solution and freshwater to simulate, on a reduced scale, the buoyancy driven motion of smoke in a cooler ambient atmosphere. Salt water modelling does not account for heat transfer effects, however it does provide a relatively cheap and simple way to study the motion of buoyancy driven fluids and the mass transfer associated with their flow structures.

6.4 Outline for Further Research

The objective of this section is to develop and outline a research plan. The research will be carried out as an initial part of the authors doctoral research program addressing the mixing that occurs in fire induced doorway flows. Salt water modelling is to be used to study the behaviour of the buoyant flows in a doorway between a burn room and corridor.

The aim of the research will be to quantify the entrainment of mass into the upper buoyant door jet for a residential scale two-dimensional doorway. By two dimensional doorway, it is meant that the width of the doorway will be equal to the width of the corridor and burn room. This will eliminate the development of recirculation regions adjacent to the doorway that may indirectly transfer mass between the upper and lower door jets. The term residential scale implies that the height of the doorway is equal to $0.813H$, where H is the height of the compartment.

Steckler *et. al.* (1986), presented the theory for scaling salt water models and for relating the results of salt water modelling experiments too an equivalent fire situation, (refer Chapter 5). From Chapter 4, the likely application of the results from this research plan is that they will be incorporated into zone model packages. It is therefore desirable to classify the results in terms of the fundamental properties of each layer rather than the specific properties of the equivalent fire situation.

In the salt water modelling experiments, the objective is to replicate the fire induced flow of gases in a doorway with a salt water - freshwater analog. Since the shear between the two gas steams in the doorway is the destabilising mechanism responsible

for the mixing, it is important that the relative velocities of the gas streams, (with respect to the densities), are modelled correctly. Section 5.4 derives a relationship for the correct salt water modelling of the volumetric flow rate of fire induced gases through a single compartment vent. In order for the velocities of the gas streams to be modelled correctly, the following relationship must be satisfied.

$$\frac{\dot{V}_{out}}{\dot{V}_{in}} = \left(\frac{T_{UL}}{T_{LL}}\right)_{fire} = \left(\frac{\rho_{LL}}{\rho_{UL}}\right)_{fire} \tag{6.1}$$

6.4.1 The Salt Water Model

The salt water scaling theory presented by Steckler *et. al.*, (1986), has been applied in sizing a salt water model from a full scale facility at the University of Canterbury, New Zealand, (see Miller, 1995, and Bolliger 1995). The dimensions of the full size facility and the equivalent salt water model are presented in Table 6.1.

	Full Scale Size	Salt Water Model
Burn Room	$2.2m \times 2.2m \times 5.4m$	$0.3m \times 0.3m \times 0.736m$
Corridor	$2.2m \times 2.2m \times 6.0m$	$0.3m \times 0.3m \times 0.818m$

Table 6.1 ***Full scale and salt water model dimensions for room size, Height × Width × Length***

An oblique sketch of the salt water model to be used in these experiments is presented in Figure 6.1. The model is constructed of clear 6mm perspex. The plate between the burn room section of the model and the corridor section of the model, is removable. This enables the size and aspect ratio of the burn room doorway to be varied in the experimental investigation. The plate at the end of the corridor section of the model is also removable for the same purpose.

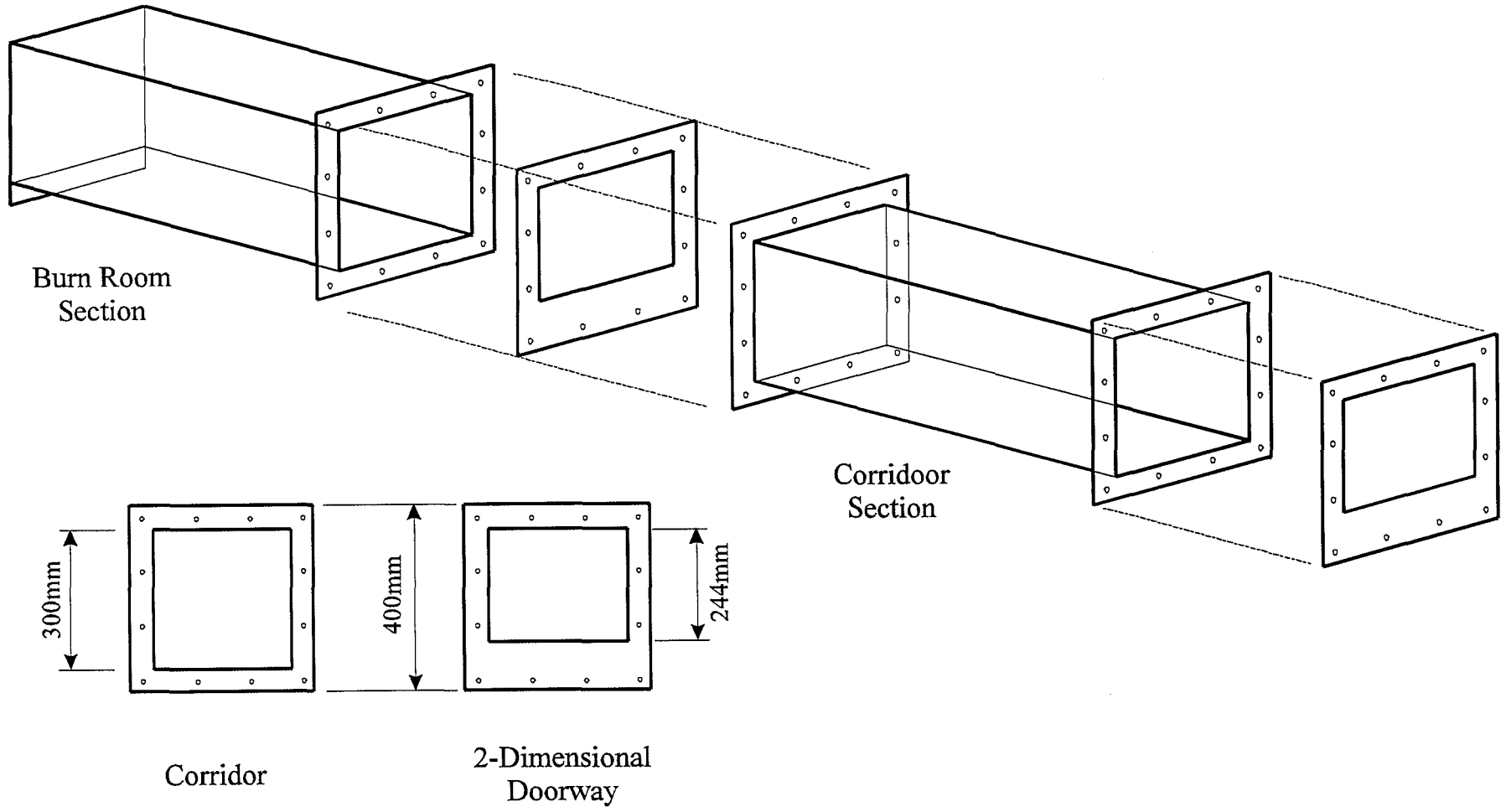

Figure 6.1 Diagram of the salt water model to be used in future research of the mixing that occurs in fire induced doorway flows.

6.4.2 Experimental Technique

Section 5.4 showed that the ratio of the volumetric flow rate entering a compartment to the flow rate exiting a compartment, is equal to the ratio of the densities in the upper and lower layers. This requirement can be satisfied in a salt water model by using pumps to simulate the action of the plume, see Figure 6.2. The pumps can be set to draw freshwater into the compartment and to inject salt water into the ceiling layer of the compartment in the correct volumetric ratios. This method offers more control on the flow rates through the door than using a salt water plume. The problem with this method, is that the pumps impose pressure gradients on the system that would not be there in a fire situation. Flow through a doorway in the fire situation is induced by the density differences between the gases in the compartment and the gases in the outside atmosphere. Flows achieved by imposing an artificial pressure gradient on the system with pumps, may not be physically achievable in a natural fire situation.

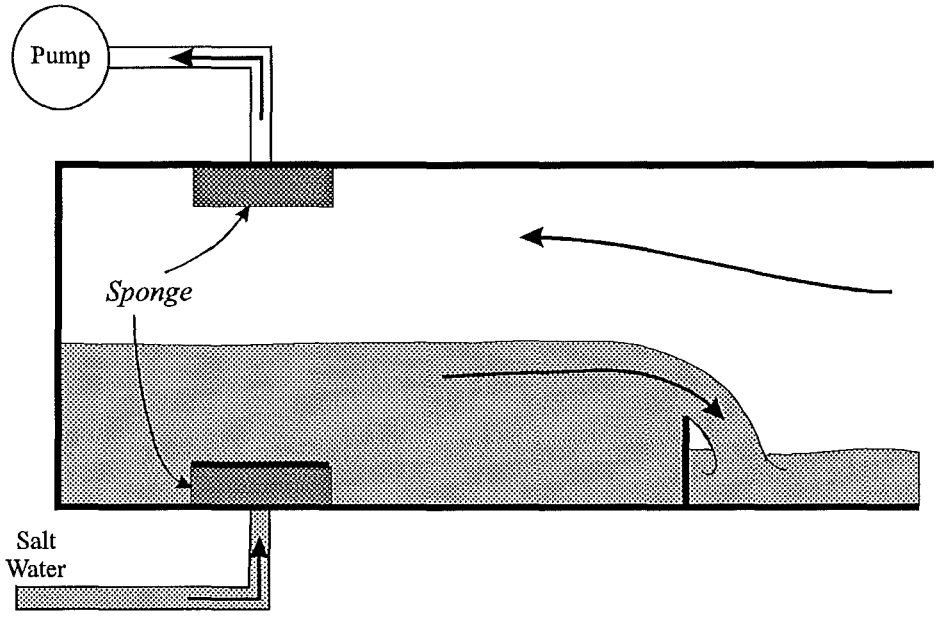

Figure 6.2 Schematic of the pump system to be used in the salt water modelling

To determine which of the flow regimes induced by the action of the pumps are physically achievable in a fire situation, the fractional height of the interface in the

compartment, (Z_D/H_d), at steady state, will be plotted against the ratio of the volumetric flow rates in the pumps, (V_{out}/V_{in}); refer Figure 6.3. The flow rates used in the pumps will be compared with the flow rates predicted by Rockett's two zone vent flow theory for the same factional interface height. If the agreement between the flow rates predicted by Rockett's theory and the flow rates used in the pumps is good, the flow regime will be assumed to be physically achievable for a buoyancy driven flow.

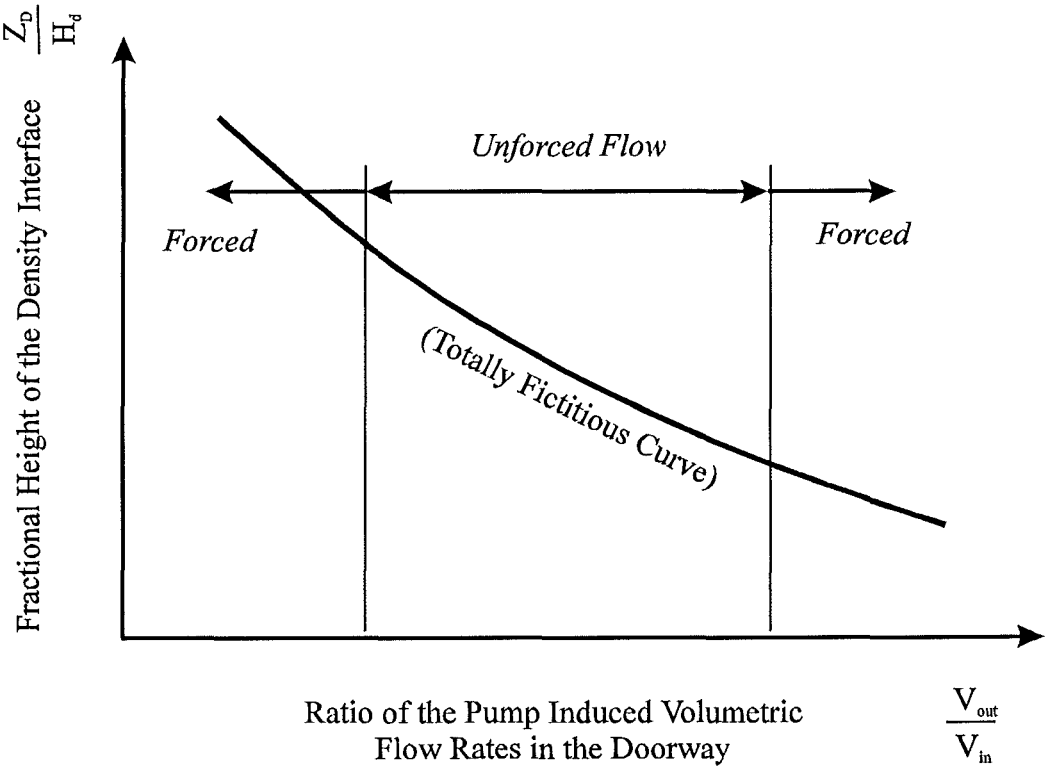

Figure 6.3 ***Fictitious plot of the fraction interface height versus the ratio of flow rates through the compartment doorway.***

For a given density ratio, Equation (6.1) stipulates the ratio of the volumetric flow rates entering and exiting the compartment. The value of the volumetric flow ratio can be achieved using an infinite range of volumetric flow rates. An additional relationship is therefore required to determine the actual flow rate of an individual flow stream entering or exiting the compartment through the doorway. The relationship used for this purpose is given by Equation (6.2). It assumes that the doorway is the control on the flow system . The derivation of Equation (6.2) is presented in Appendix 3.

$$Fr_{saline}^2 + Fr_{fresh}^2 = 1 \tag{6.2}$$

where

$$Fr_i^2 = \frac{\rho}{l_i^3 \Delta\rho g}\left(\frac{\dot{V}_i}{W_d}\right)^2 \tag{6.3}$$

and

l_i = the depth of layer i in the plane of the doorway.

Substituting Equation (6.1) into Equation (6.2) results in the following relationship,

$$\left(\frac{\dot{V}_{fresh}}{W_d}\right) = \sqrt{\frac{g\Delta\rho}{\rho}}\left[\left(\frac{\rho_{salt}}{\rho_{fresh}}\right)\frac{1}{l_{saline}^3} + \frac{1}{l_{fresh}^3}\right]^{-\frac{1}{2}} \tag{6..4}$$

Assuming

$$l_{fresh} \approx \frac{2}{3}H_d \tag{6.5}$$

such that

$$l_{salt} \approx \frac{1}{3}H_d \tag{6.6}$$

Equation (6.4) can be solved to find the volumetric flow rate entering the compartment. This result can then be used to set the volumetric flow rates in the pumps according to the density ratio of fluids in the upper and lower layer, refer Equation (6.1).

Once a range of flow rates have been determined that are physically achievable for a fire situation, the mixing that occurs between the flow streams in the doorway can be investigated with the pump system. Investigation into the entrainment characteristics of the upper buoyant door jet will be carried out using laser induced fluorescence

techniques. A planer sheet of laser light will be used excite a fluorescent dye or fluorescent particles in the fluid so as to view a cross section of the flow. The fluorescent image will be recorded by digital camera and then latter analysed by computer to provide velocity and concentration measurements. For further details on the laser induced fluorescence techniques described simplistically above, see Papps, (1995) and Gaskin (1995).

Velocity measurements of the flow are recorded using Particle Image Velocimetry, (PIV), where the fluid is seeded with small particles that are excited by the laser. Concentration measurements are recorded using Laser Induced Dye Fluorescence, (LDF), where a dye in the fluid is excited by the laser. To establish the consistency of the experimental technique and resulting data, three experiments will be run with exactly the same experimental configuration and initial conditions; the PIV and LDF results for each experiment will be compared.

The likely application of the results from this experimental work is in zone modelling; the mass entrainment into each layer, therefore, must be quantifiable. In order to quantify the mass entrainment, it is necessary that the interface between the two layers is distinctly defined. The fluid environment in the salt water model will be divided into two distinct layers, (or zones), according to the concentration and velocity profiles. The exact method to be used for determination of the interface height is not yet known; further research will be needed to determine if there is a universally accepted method for this purpose.

6.4.3 Research Methodology

The salt water experiments will investigate the accuracy of the formula proposed by Zukoski and Kubota, (1980), to quantify the mass entrained into the upper door jet. Additionally, attention will also be given to locating the point of transition between the attached and separated flow cases for the upper door jet, refer Figure 2.10. The separation of the upper door jet from the soffit of the doorway is likely to depend upon the momentum of the flow at the doorway and the entrainment demand of the

jet relative to the depth of fluid above the door soffit; refer Section 3.9. For this purpose, the volumetric flow rate and the initial density of the salt water solution injected into the ceiling layer of the burn room will be varied during the experiments. The flow rate of freshwater drawn into the compartment will be changed according to the requirement stipulated by Equation (6.1), however, all other variables will remain unchanged. It should be noted that in the investigation of the transition point between the attached and separated door jet door cases, the two dimensional doorway makes the jet more prone to wall attachment than a three dimensional doorway would; refer Section 3.9.

Zukoski and Kubota's proposed formula for estimating the mass entrained into the upper door jet, (Equation 6.7), is similar in form to a plume correlation. The entrainment length used in the equation is equal to the difference in elevation between the neutral layer height in the doorway, and the height of the layer interface in the adjacent room, (Z_{D3} - Z_N). To investigate the accuracy of this formula, the height of the layer interface in the corridor will be varied in the salt water experiments while the source conditions of the flow remain unchanged. The height of the layer interface in the corridor will be changed by adjusting the depth of the soffit of the two dimensional doorway at the corridor exit. The proposed soffit depths for the corridor exit doorway are listed in Table 6.2. The maximum soffit depth to be used at the corridor exit doorway is equal to $0.187H$; this is the expected soffit depth for a residential scale doorway.

$$\dot{m}_e = (C_J)\rho_{LL}\sqrt{g Z_d}\, Z_d^2 \left(Q_d^*\right)^{\frac{1}{3}} \tag{6.7}$$

Experimental Series	Soffit Height
A1	0mm
A2	14mm
A3	28mm
A4	42mm
A5	56mm

Table 6.2 - The range of soffit depths for the corridor exit doorway

The next phase of the experimental investigation will be move from a two dimensional doorway between the burn room and corridor, too a three dimensional doorway. It is hoped that the two dimensional work will result in an estimate of the entrainment rate per unit width for both the upper and lower door jets. Given a three dimensional doorway of a specified width, it should therefore be possible to estimate the contribution of the three dimensional effects to the entrainment rate in each layer.

References

Abramovich, G.N., (1963), Theory of Turbulent Jets, M.I..T. Press, Massachusetts Institute of Technology, Cambridge, Massachusetts.

Baum, H.R. and Rehm, R.G., (1984), Calculations of Three Dimensional Buoyant Plumes in Enclosures, *Combustion Science and Technology*, Vol. 40, pp. 55-77.

Baum, H.R., Rehm, R.G. and Mulholland, G.W., (1982), Computation of Fire Induced Flow and Smoke Coagulation, Nineteenth Symposium (International) on Combustion/The Combustion Institute, pp. 921-931.

Benjamin, T.B, (1963), The Threefold Classification of Unstable Disturbances in Flexible Surfaces Bounding Inviscid Flows, *Journal of Fluid Mechanics*, Vol. 16, pp. 436-450.

Berl, W.G., and Halpin, BM., (1980), Human Fatalities from Unwanted Fires, Johns Hopkins APL Technical Digest, Vol 1., No. 2, pp. 129-134.

Bolliger, I., (1995), Full Residential Scale Backdraft, Masters Thesis, Department of Civil Engineering, University of Canterbury, Christchurch, New Zealand.

Cetegen, B.M., Zukoski, E.E. and Kubota, T., (1984), Entrainment in the Near and Far Field of Fire Plumes, *Combustion Science and Technology*, Vol. 39, pp. 305-331

Chu, V. and Vanvari, M.R., (1976), Experimental Study of Turbulent Stratified Shearing Flow, *Journal of the Hydraulics Division*, ASCE, Vol 102, No. HY6, pp. 691-705.

Cooper, L.Y. and Forney, G.P., (1990), The Consolidated Compartment Fire Model (CCFM) Computer Code Application CCFM.VENTS - Part 1: Physical Basis, NISTIR 4342, National Institute of Standards and Technology, Gaithersburg, MD 20899.

Ellision, T.H and Turner, J.S., (1959), Turbulent Entrainment in Stratified Flows, *Journal of Fluid Mechanics*, Vol. 6, pp. 423-448.

Fischer, H.B., List, J.E., Koh, R.C.Y., Imberger, J. and Brooks, N.H.,(1979), Mixing in Inland and Coastal Waters, Academic Press, Inc., (London) Ltd.

Fisher, T., (1995), Dilution of Axisymmetric Buoyant Jets and Surface Spreading Fields, Masters Thesis, Department of Civil Engineering, University of Canterbury, Christchurch, New Zealand.

Forney, G.P., Cooper, L.Y. and William, M.F., (1990), The Consolidated Compartment Fire Model (CCFM) Computer Code Application CCFM: Vents - Part IV: User Reference Guide, NISTIR 4345, National Institute of Standards and Technology, Gaithersburg, MD 20899.

Gaskin, S., (1995), Draft Ph.D. Thesis, Fluid Laboratory, Department of Civil Engineering, University of Canterbury, Christchurch, New Zealand.

Henderson, F.M, (1966), Open Channel Flow, Macmillan Publishing Co., Inc., New York, USA.

Jones, W.W., (1984), A Model for the Transport of Fire, Smoke and Toxic Gases (FAST), NBSIR 84-2934, U.S. Department of Commerce, National Bureau of Standards, Gaithersburg, MD 20899.

Jones, W. and Peacock, R., (1989), Technical Reference Guide to FAST 18, NIST Technical Note 1262, National Institute of Standards and Technology, Gaithersburg, MD.

Kawagoe, K., (1958), Fire Behaviour in Rooms, Building Research Institute, Ministry of Construction, Tokyo, Japan.

Lim, C.S., (1984), Mixing in Doorway Flows and Entrainment in Fire Plumes, California Institute of Technology, Pasadena, California

McCaffrey, B.J., (1983), Momentum Implications for Buoyant Diffusion Flames, *Combustion and Flame*, Vol. 52, pp. 149-167

McCaffrey, B.J. and Quintiere, J.G., (1975), Fire Induced Corridor Flow in a Scale Model, in CIB Symposium on the Control of Smoke Movement in Building Fires, Vol. 1, pp. 33-47. Borehamwood, UK.

McCaffrey, B.J. and Quintiere, J.G., (1976), Buoyancy Driven Countercurrent Flows Generated by a Fire Source, Turbulent Buoyant Convection, Hemisphere Publishing Corp., pp. 457-472.

Millar, D.J., (1995), Full Scale Limited Ventilation Fire Experiments, Masters Thesis, Department of Civil Engineering, University of Canterbury, Christchurch, New Zealand.

Mitler, H.E., (1978), The Physical Basis for the Harvard Computer Fire Code, Division of Applied Sciences, Harvard University, Home Fire Project Technical Report No. 34.

Mitler, H.E. and Emmons, H.W., (1981), Documentation for CFC V, The Fifth Harvard Computer Fire Code, Division of Applied Sciences, Harvard University, Home Fire Project Technical Report No. 45.

Mitler, H.E., (1984), Zone Modeling of Forced Ventilation Fires, *Combustion Science and Technology*, Vol. 39, pp. 83-106.

Mitler, H.E., (1985), The Harvard Fire Model, *Fire Safety Journal*, Vol. 9, pp. 7-16.

Mitler, H.E., (1991), Mathematical Modeling of Enclosure Fires, NISTIR 90-4294, U.S. Department of Commerce, National Institute of Standards and Technology, Gaithersburg, MD 20899.

Moore, WL., (1943), Energy Loss at the Base of a Free Overfall, *Transactions American Society of Civil Engineers*, Vol. 108, pp. 1343-1360, with Discussion by White, M.P., pp.1361-1364, and others.

Morton, B.R., Taylor, G. and Turner, J.S., (1956), Turbulent Gravitational Convection from Maintained and Instantaneous Sources, *Proceedings. Royal Society*, London, Series A, Vol. 234, pp. 1-23.

Papps, D., (1995), Draft Ph.D. Thesis, Fluid Laboratory, Department of Civil Engineering, University of Canterbury, Christchurch, New Zealand.

Peacock, R.D., Forney, G.P., Reneke, P., Portier, R. and Jones, W.W., (1993), CFAST, the Consolidated Model of Fire Growth and Smoke Transport, NIST Technical Note 1299, National Institute of Standards and Technology, Gaithersburg, MD.

Prahl, J and Emmons, H.W., (1975), Fire Induced Flow Through an Opening, *Combustion and Flame*, Vol. 25, pp. 369-385

Quintiere, J.G. and DenBraven, K., (1978), Some Theoretical Aspects of Fire Induced Flows Through Doorways in a Room-Corridor Scale Model, U.S. Department of Commerce, National Bureau of Standards, Washington, D.C.

Quintiere,J.G. and McCaffrey, B.J., (1980), The Burning of Wood and Plastic Cribs in an Enclosure: Volume 1., NBSIR 80-2054, National Bureau of Standards, U.S. Department of Commerce, Washington DC 20234.

Quintiere, J.G., McCaffrey, B.J and Rinkinen, W., (1978), ??, *Fire and Materials*, Vol. 2, No. 1, pp. 18-24.

Quintiere,J., Steckler, K. and McCaffrey, B., (1981), A Model to Predict the Conditions in a Room Subject to Crib Fires, Presented at the First Specialists Meeting (International) of the Combustion Institute, University of Bordeaux, Talance, France, July 20-24, 1981.

Quintiere, J.G. ,(1989), Fundamentals of Enclosure Fire 'Zone" Models, Reprint from *Journal of Fire Protection Engineering*, Vol. 1, No. 3, pp. 99-119.

Quintiere, J.G., (1993) Compartment Fire Modeling, Section 3/Chapter 5 SFPE Handbook of Fire Protection Engineering, Society of Fire Protection Engineers. Quincy, MA.

Rehm, R.G. and Baum, H.R., (1978), The Equations of Motion for Thermally Driven, Buoyant Flows, *Journal of Research of the National Bureau of Standards*, Vol. 83, No 3. May-June 1978.

Rocket, J.A., (1976), Fire Induced Gas Flow in an Enclosure, *Combustion Science and Technology*, Vol. 12, pp. 165-175

Rockett, J.A., (1982), Modeling of NBS Mattress Tests with the Harvard Mark V Fire Simulation, *Fire and Materials*, Vol. 6, No. 2, pp. 80-95.

Rockett, J.A. and Morita, M., (1986), The NBS/Harvard Mark VI Multi-Room Fire Simulation, NBSIR 85-3281, US Department of Commerce, National Bureau of Standards, Gaithersburg, MD 20899.

Rockett, J.A., Morita, M. and Cooper, L.Y., (1987), Comparisons of NBS/Harvard VI Simulations and Full-Scale, Multi-Room Fire Test Data, NBSIR 87-3567, US Department of Commerce, National Bureau of Standards, Gaithersburg, MD 20899.

Rockett, J.A., (1990), Using the Harvard/NIST Mark VI Fire Simulation, NISTIR 4464, National Institute of Standards and Technology, Gaithersburg, MD 20899.

Scotti, R.S. and Corcos, G.M., (1972), An Experiment on the Stability of Small Disturbances in a Stratified Free Layer Shear Flow, *Journal of Fluid Mechanics*, Vol 52, pp. 499-528.

Sharp, J. J. and Vyas, B. D., (1977), The Buoyant Wall Jet, *Proceedings Institution of Civil Engineers*, Part 2, Vol. 63, Sept., pp. 593-611.

Steckler, K.D., (1989), Fire Induced Flows in Corridors - A Review of Efforts to Model Key Features, US Department of Commerce, National Institute of Standards and Technology, Gaithersburg, MD 20899.

Steckler, K.D., Baum, H.R. and Quintiere, J.G., (1984), Fire Induced Flows Through Room Openings - Flow Coefficients, Twentieth Symposium (International) on Combustion, The Combustion Institute, pp. 1591-1600.

Steckler, K.D. Baum, H.R. and Quintiere, J.G, (1986), Salt Water Modeling of Fire induced Flows in Multicompartment Enclosures, NBSIR 86-3327, US Department of Commerce, National Bureau of Standards, Gaithersburg, MD 20899.

Steckler, K.D., Quintiere, J.G. and Rinkinen, W.J., (1982), Flow Induced by Fire in a Compartment, Nineteenth Symposium (International) on Combustion / Combustion Institute, pp. 913-920.

Tanaka, T., (1983), A Model of Multiroom Fire Spread, NBSIR 83-2718, US Department of Commerce, National Bureau of Standards, Washington, DC 20234

Tangren, E.N., (1978), An Experimental Investigation of Convective Flows Associated with Room Fires, AE Thesis, Graduate Aeronautical Laboratories, California Institute of Technology, Pasadena, California.

Thomas, P.H., Heselden, A.J.M. and Law, M., (1967), Fully-Developed Compartment Fires - Two Kinds of Behaviour, F.R.Technical Paper No. 18, Fire Research Station, Borehamwood, England.

Thorp, S.A., (1973), Experiments on Instability and Turbulence in a Stratified Shear Flow, *Journal of Fluid Mechanics*, Vol. 61, Part 4, pp. 731-751.

Tritton, D.J., (1977), Physical Fluid Dynamics, Published by Van Nostrand Reinhold Limited, Ontario, Canada.

Turner, J.S., (1973), Buoyancy Effects in Fluids, Cambridge University Press, London.

Wood, I.R., Bell, R.G. and Wilkinson, D.L., (1993), Ocean Disposal of Wastewater, Advanced Series on Ocean Engineering - Volume 8, World Scientific, Singapore.

Wood, I.R. and Knudsen, M., (1990), The Interaction between a Boundary and a Horizontal Buoyant Jet, *Journal of Hydraulic Research*, Vol. 28, No. 3.

Wood, I.R. and Wilkinson, D.L., (1971), A Rapidly Varied Flow Phenomenon in a Two-Layer Flow, *Journal of Fluid Mechanics*, Vol. 47, Part 2, pp. 241-246.

Zukoski, E.E. and Peterka, D.L., (1979), Measurements of Entrainment in a Doorway Flow, California Institute of Technology, Pasadena, California

Zukoski, E.E. and Kubota, T., (1980), Two-layer Modeling of Smoke Movement in Building Fires, *Fire and Materials*, Vol. 4, No. 1, pp. 17-27

Zukoski, E.E., Kubota, T. and Cetegen, B., (1980 a), Entrainment in Fire Plumes, U.S. Department of Commerce, National Bureau of Standards, Washington DC 20234.

Zukoski, E.E., (1985), Fluid Dynamic Aspects of Room Fires, Fire Safety Science - Proceedings of the First International Symposium, pp. 1-30.

Bibliography

Buchanan, A.H., (Editor), (1994), Fire Engineering Design Guide, Centre for Advanced Engineering, University of Canterbury, Christchurch, New Zealand.

Drysdale, D., (1985), An Introduction to Fire Dynamics, A Wiley-Interscience Publication, John Wiley & Sons Ltd.

Rodi, W., (1982), Turbulent Buoyant Jets and Plumes, HMT - The Science & Applications of Heat and Mass Transfer, Reports, Reviews and Computer Programs, Volume 6., Pergamon Press Ltd. Oxford, England.

Wilkinson, D., Personal Communication, Civil Engineering Department, University of Canterbury, Christchurch, New Zealand.

Wood, I.R. and Wilkinson, D.L., (1968), The Entraining Hydraulic Jump, The Institution of Engineers Third Australasian Conference on Hydraulics and Fluid Mechanics, pp. 5-9.

Appendix 1

The following derivation is represented from Lim, (1984).

Lim assumed that the cool, lower layer of fresh air, enters the room like a turbulent wall jet with a mixing layer separating it from the hot, upper layer. The mixing layer grows with distance from the doorway until it reaches a stable thickness at a critical local Richardson number. Beyond this critical point, there is assumed to be no mixing between the layers.

The lower door jet of cool gases entering a compartment is required to contract as it passes through the width restriction of the doorway frame. After the door jet has passed through the doorway it is able to expand out laterally again to the bounding walls of the compartment. Lim replaced this three dimensional door jet with a two dimensional approximation. He approximated that the door jet expanded instantaneously upon entering the compartment and therefore had a velocity of $(W_d/W_c)U_{in}$ rather than the actual velocity U_{ic} in doorway.

where

$$U_{in} = \frac{\dot{m}_{in}}{\rho_\infty W_d Z_D} \qquad \text{(A1.1)}$$

Lim assumed that the cool, lower layer wall jet could be divided into three regions: a "supercritical" region where the flow is independent of downstream conditions and has entrainment characteristics similar to a neutral wall jet; a "subcritical" region where gravitational forces suppress mixing between the hot and cold layers; and a hydraulic jump, (or density jump), region which separates the supercritical and subcritical regions.

Lim used Taylor's entrainment hypothesis that assumes that the entrainment rate is proportional to the local maximum velocity, U_{max}, and the local entrainment coefficient, E, (Morton, Taylor and Turner,. 1956).

$$\frac{\partial \dot{m}_{e-LL}}{\partial x} = \rho_{UL} E(Ri_x) U_{\max}(x) W_c \qquad \text{(A1.2)}$$

The entrainment coefficient, E, is a function of the local Richardson number and therefore a function of the distance downstream x from the doorway; ($Ri_x = Ri_x(x)$, see Ellison and Turner, 1959). Lim used a power law to approximate this relationship.

$$E(x) = E_0\left[1 - \frac{x}{x_{cr}}\right]^n \qquad \text{(A1.3)}$$

where

x_{cr} is defined as the position of the critical local Richardson number, ($Ri_o \approx$ 0.25), and

E_o and n are constants to be determined experimentally.

Lim found from the experimental data of Chu and Vanvari, (1976), the following relationship between the entrainment coefficient and the local Richardson number.

$$E(Ri_x) = 0.036\left[1 - \frac{Ri_x}{(Ri_x)_{cr}}\right]^2 \qquad \text{(A1.4)}$$

For a neutral (constant density) wall jet, the entrainment coefficient, E, has a constant value; by assuming that $Ri_x(x) \propto x$, (Scotti and Corcos, 1972), the constants E_o and n used in Equation (A1.3) were therefore approximated for Equation (A1.4) as 0.036 and 2 respectively.

Taylor's entrainment hypothesis assumes that the entrainment rate is proportional to the maximum velocity, U_{max}, of the layer. No velocity measurements were taken in Lim's experimental work; to further complicate the matter, each of the three regions of the wall jet has a different relationship between U_{max} and x, (see Abramovich, 1963). In the near field, (potential core) region, U_{max} is constant. In the far field,

(self-preserving), region $U_{\max} \propto x^{-n}$, $n>0$. Lim found that with few exceptions, that the entrainment data fell within the transition region that separates the near and far field regions. To avoid the problems associated with using a U_{max} for each different region, Lim introduced a velocity scale for use in the entrainment relationship based upon the momentum of the jet. Lim defined the velocity scale, U^*, as

$$U^*(x) = \frac{\int_0^\infty \rho U^2 \, dz}{\int_0^\infty \rho U \, dz} \tag{A1.5}$$

The denominator of the relationship above was evaluated by considering a mass balance for the cold layer.

$$\int_0^\infty \rho U \, dz \equiv \dot{m}(x) = \dot{m}_{in} + \dot{m}_{e-LL} \tag{A1.6}$$

The numerator in Equation (A1.5) was evaluated by considering the momentum balance for the lower layer.

$$\int_0^\infty \rho U^2 \, dz \equiv \dot{m}_{in} U_{in} \left(\frac{W_d}{W_c}\right) - C_F(x) - C_P(x) \tag{A1.7}$$

where

$C_f(x)$ represents the frictional drag of the walls; and

$C_P(x)$ represents the pressure force on the layer due to it's changing depth and density, (see Ellison and Turner 1959).

Assuming that the total momentum of the jet does not vary significantly in the supercritical region where the entrainment process takes place, ie.; losses due to the presence of pressure gradients and wall friction are negligible in comparison to the jets initial momentum; the velocity scale, U^*, can be given by

$$\dot{m}(x)U^*(x) \approx \dot{m}_{in}U_{1c}\frac{W_d}{W_c} \tag{A1.8}$$

where

$\dot{m}(x)$ is the total mass flow at position x, as given by Equation (A1.6).

Lim then derived a relationship to express U_{max} as a function of the velocity scale U^* for the far field region.

$$U^*(x) = \frac{\int_0^\infty \rho U^2\, dz}{\int_0^\infty \rho U\, dz} \tag{A1.9}$$

Therefore,

$$U^*(x) = \frac{xU_{\max}^2(x)\int_0^\infty \rho\left[\frac{U}{U_{\max}}\right]^2 d\left(\frac{z}{x}\right)}{xU_{\max}(x)\int_0^\infty \rho\left[\frac{U}{U_{\max}}\right] d\left(\frac{z}{x}\right)} \tag{A1.10}$$

For self-preserving jets with small density variations in the streamwise direction, $(\rho \approx \rho_\infty)$, Equation (A1.10) reduced to:

$$U^*(x) = \frac{U_{\max}(x)}{A_1} \tag{A1.11}$$

where A_1 is a constant that must be determined experimentally;

$$A_1 = \frac{\int_0^\infty \rho\left[\frac{U}{U_{\max}}\right] d\left(\frac{z}{x}\right)}{\int_0^\infty \rho\left[\frac{U}{U_{\max}}\right]^2 d\left(\frac{z}{x}\right)} = \text{Constant} \tag{A1.12}$$

By substituting Equations (2.25), (A1.03), (A1.08) and (A1.11) into Equation (A1.12), the following relationship was obtained.

$$\left[\frac{\dot{m}_{e-LL}(x)}{\dot{m}_{in}} + 1\right]\frac{\partial\left(\frac{\dot{m}_{e-LL}(x)}{\dot{m}_{in}}\right)}{\partial\left(\frac{x}{Z_D}\right)} = A_1 E_o \frac{\rho_{UL}}{\rho_\infty}\left[1-\frac{x}{x_{cr}}\right]^n \qquad \text{(A1.13)}$$

Lim stated that this relationship is valid for the self-preserving region of a turbulent, two-dimensional, constant momentum jet.

By assuming that buoyancy prevents mixing for $x > x_{cr}$, the total entrainment rate could be found be integrating the above relation between $x = 0$ and $x = x_{cr}$. This results in the following relationship;

$$\frac{1}{2}\left[\frac{\dot{m}_{e-LL}(x)}{\dot{m}_{in}}\right]^2 + \frac{\dot{m}_{e-LL}}{\dot{m}_{in}} = A_1 \frac{E_o}{n+1}\frac{\rho_{UL}}{\rho_\infty}\left[\frac{x_{cr}}{Z_D}\right] \qquad \text{(A1.14)}$$

The critical length, x_{cr}, is the position downstream from the doorway where the local Richardson number has the critical value 0.25.

$$(Ri_x)_{cr} = Ri_x(x_{cr}) = \left[\frac{\frac{-1}{\rho}\frac{\partial\rho}{\partial z}g}{\left(\frac{\partial U}{\partial z}\right)^2}\right]_{\substack{x=x_{cr}\\ z=Z_D}} \qquad \text{(A1.15)}$$

Lim made the following approximations to evaluate the above definition of the local Richardson number.

$$\left[\frac{-1}{\rho}\frac{\partial\rho}{\partial z}\right]_{z=Z_D} \approx \frac{1}{\delta(x)}\frac{\rho_{LL}-\rho_{UL}}{\rho_{UL}} = \frac{1}{\delta(x)}\frac{\Delta\rho}{\rho_{UL}} \qquad \text{(A1.16)}$$

$$\left[\frac{\partial U}{\partial z}\right]_{z=Z_D} \approx \frac{U_{\max}(x)}{\delta(x)} \tag{A1.17}$$

$$\delta(x) = A_2 x \tag{A1.18}$$

where

$\delta(x)$ is the thickness of the mixing layer, and

A_2 is a constant with a value of approximately 0.23 for two-layer stratified flows with a density ratio of about 1.4, (Abramovich, 1963).

Using Equation (A1.11) to approximate U_{max},, and substituting Equations (A1.16) and (A1.18) into Equation (A1.15), the following relationship was arrived at.

$$\frac{x_{cr}}{Z_D} = \left[\frac{A_1^2}{A_2}(Ri_x)_{cr}\frac{\rho_{UL}}{\rho_\infty}\left(\frac{W_d}{W_c}\right)^2\frac{1}{Ri_o}\right]\left[\frac{\dot{m}_{in}}{\dot{m}_{in}+\dot{m}_{e-LL}(x)}\right]^2 \tag{A1.19}$$

The equation for the entrainment rate into the cold layer is finally obtained by substituting this relationship into Equation (A1.14).

$$\left[\frac{1}{2}\left[\frac{\dot{m}_{e-LL}}{\dot{m}_{in}}\right]^2 + \frac{\dot{m}_{e-LL}}{\dot{m}_{in}}\right]\left[1+\frac{\dot{m}_{e-LL}}{\dot{m}_{in}}\right]^2 = AF^2 \tag{A1.20}$$

where

$$A = \frac{A_1^3}{A_2}\frac{E_o}{n+1}(Ri_x)_{cr} \tag{A1.21}$$

$$F = \frac{\rho_{UL}}{\rho_\infty}\frac{W_d}{W_c}\frac{1}{\sqrt{Ri_o}} \tag{A1.22}$$

Appendix 2

The following derivation is represented from Quintiere and McCaffrey, (1980).

The rate of entrainment into the lower layer is given by

$$\dot{m}_e = \rho_e A_e U_e \qquad \text{(A2.1)}$$

where

ρ_e is the density of the entrained fluid

A_e is the effective surface area of the jet through which entrainment takes place

U_e is the entrainment velocity normal to the jet surface

The entrainment velocity is assumed to be proportional to the mean velocity of the jet in the doorway, (Morton, Taylor and Turner, 1956).

$$U_e = k_m U_d \qquad \text{(A2.2)}$$

where

k_m is the entrainment constant

The effective surface area of the jet is assumed to be

$$A_e = (Z_N - Z_{D1}) W_C \left(\frac{W_C}{W_d}\right)^{n-1} \qquad \text{(A2.3)}$$

where

$\left(\frac{W_C}{W_d}\right)^{n-1}$ is an empirical factor included to account for the change in area as the door jet expands from the doorway to the compartment walls.

when n=0, the width = W_d

when n=1, the width = W_C

Substituting Equations (A2.2) and (A2.3) into Equation (A2.1), results in the following relationship.

$$\dot{m}_e = \rho_e (Z_N - Z_{D1}) W_C \left(\frac{W_C}{W_d}\right)^{n-1} k_m U_d \qquad \text{(A2.4)}$$

The mass flux into the compartment can be written as

$$\dot{m}_{in} = \rho_{in} U_{in} (W_d Z_N) \qquad \text{(A2.5)}$$

Using Equations (A2.4) and (A2.5) the entrainment of the hot gas into the lower layer was modelled with the following relationship

$$\frac{\dot{m}_e}{\dot{m}_{in}} = k_m \left(\frac{T_{in}}{T_e}\right)\left(\frac{Z_N - Z_D}{Z_N}\right)\left(\frac{W_C}{W_d}\right)^n \qquad \text{(A2.6)}$$

Which in terms of the zone model is written as

$$\frac{\dot{m}_{12}}{\dot{m}_{42}} = k_m \left(\frac{T_4}{T_1}\right)\left(\frac{Z_N - Z_D}{Z_N}\right)\left(\frac{W_C}{W_d}\right)^n \qquad \text{(A2.7)}$$

From an energy balance on the system, (ignoring radiative heat transfer), the following upper limit could be obtained for the mass entrainment rate.

$$\dot{m}_{in} C_p T_{in} + \dot{m}_e C_p T_e = (\dot{m}_{in} + \dot{m}_e) C_p T_{out} \qquad \text{(A2.8)}$$

$$\frac{\dot{m}_e}{\dot{m}_{in}} = \frac{(T_{in} - T_{out})}{(T_{out} - T_e)} \qquad \text{(A2.9)}$$

From this energy relation, the mixing ratio could be approximated from experimental data. To determine the value of k_m and n used in the proposed entrainment relationship, (Equation A2.7), a series of small scale model experiments were carried out. From the reduced scale model, the following values were obtained for the relationship constants.

$$k_m = 2.0$$
$$n = 0.25$$

Using these values in the mixing relationship, a series of full scale timber and plastic crib burning experiments were compared with the predictions of an early zone model. The mixing in the zone model was over estimated and therefore the value of the empirical constants was reassessed from the full scale data. The results of this reassessment were k_m=0.5 and n=0.25 such that the final relationship proposed was,

$$\frac{\dot{m}_{12}}{\dot{m}_{42}} = 0.5\left(\frac{T_4}{T_1}\right)\left(\frac{Z_N - Z_D}{Z_N}\right)\left(\frac{W_C}{W_d}\right)^{\frac{1}{4}} \qquad \text{(A2.10)}$$

Appendix 3

Consider the flow depicted in Figure A3.1

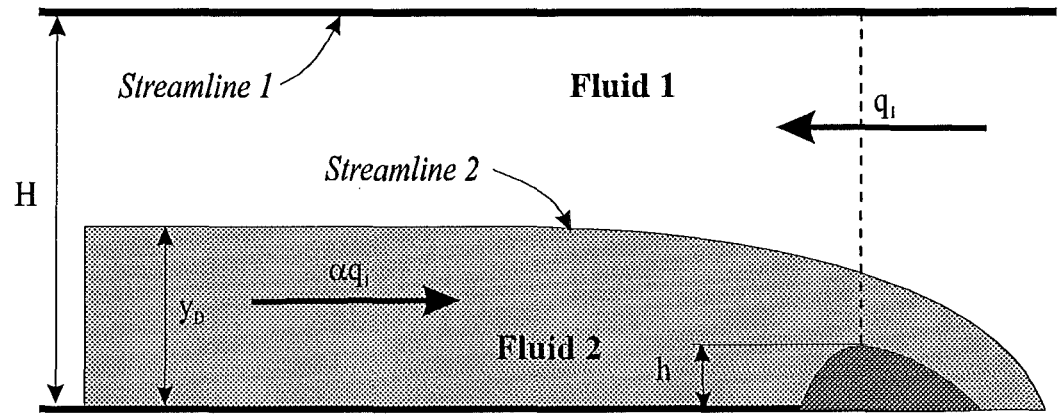

Figure A3.1 Schematic of a two layer flow situation where the flow in the lower layer passes over a smooth hump-like control structure.

The flow situation shown in Figure A3.1 has been used to approximate the flow situation through a doorway in salt water compartment experiments.

Consider the flow above the control structure.

Approximating the depth of fluid 2 over the control as (y_D - h), the total energy for streamline 1, (as given by Bernoulli's equation), can be written as

$$\frac{\rho_1}{2}\left(\frac{q}{H - y_D + h}\right)^2 + P_1 + \rho_1 g H \qquad \text{(A3.1)}$$

where

P_1 is the pressure at height H above the elevation datum.

Similarly, the Total Energy for streamline 2 can be expressed as

$$\frac{\rho_2}{2}\left(\frac{\alpha q}{(y_D - h)}\right)^2 + \left[P_1 + \rho_1 g(H - y_D + h)\right] + \rho_2 g(y_D - h) \qquad \text{(A3.2)}$$

The pressure term P_1 can be eliminated by setting streamline 1 as the total energy datum, ie Equation (A3.1) = 0. The total energy along streamline 2, relative to the datum, is therefore given by Equation (A3.3) = Equation (A3.2) - Equation (A3.1).

$$E_2 = \frac{\rho q^2}{2}\left(\frac{\alpha^2}{(y_D - h)^2} - \frac{1}{(H - y_D + h)^2}\right) + (\rho_2 - \rho_1) g(y_D - h) \qquad \text{(A3.3)}$$

Differentiating Equation (A3.3) with respect to x, and remembering that $y_D = f(x)$ and $h = f(x)$ results in the following relationship.

$$\begin{aligned} 0 = {} & \frac{\rho q^2}{2}\left(\frac{-2\alpha^2}{(y_D - h)^3}\left(\frac{\partial y_D}{\partial x} - \frac{\partial h}{\partial x}\right) - \frac{-2}{(H - y_D + h)^3}\left(-\frac{\partial y_D}{\partial x} + \frac{\partial h}{\partial x}\right)\right) \\ & + (\rho_2 - \rho_1) g\left(\frac{\partial y_D}{\partial x} - \frac{\partial h}{\partial x}\right) \end{aligned} \qquad \text{(A3.4)}$$

This can be re-written as

$$\begin{aligned} & \frac{\partial y_D}{\partial x}\left(\frac{\rho q^2 \alpha^2}{(y_D - h)^3} + \frac{\rho q^2}{(H - y_D + h)^3} - (\rho_2 - \rho_1) g\right) \\ = {} & \frac{\partial h}{\partial x}\left(\frac{\rho q^2 \alpha^2}{(y_D - h)^3} + \frac{\rho q^2}{(H - y_D + h)^3} - (\rho_2 - \rho_1) g\right) \end{aligned} \qquad \text{(A3.5)}$$

Evaluating Equation (A3.5) at the peak of the control structure, ie where $\frac{\partial h}{\partial x} = 0$,

$$\frac{\partial y_D}{\partial x}\left(\frac{\rho q^2 \alpha^2}{(y_D - h)^3} + \frac{\rho q^2}{(H - y_D + h)^3} - (\rho_2 - \rho_1) g\right) = 0 \qquad \text{(A3.6)}$$

The slope of the fluid surface over the control structure is not zero and therefore,

$$\left(\frac{\rho q^2 \alpha^2}{(y_D - h)^3} + \frac{\rho q^2}{(H - y_D + h)^3} - (\rho_2 - \rho_1)g\right) = 0 \qquad \text{(A3.7)}$$

Divide Equation (A3.7) through by through by $(\rho_2 - \rho_1)_1 g = \Delta\rho g$,

$$\left(\frac{\rho q^2 \alpha^2}{\Delta\rho g(y_D - h)^3} + \frac{\rho q^2}{\Delta\rho g(H - y_D + h)^3} - 1\right) = 0$$

which can be re-written as

$$\left(Fr_2^2 + Fr_1^2\right) = 1 \qquad \text{(A3.8)}$$